AD NUMBER

AD377071

CLASSIFICATION CHANGES

TO: unclassified

FROM: confidential

LIMITATION CHANGES

TO:

Approved for public release, distribution unlimited

FROM:

Controlling DoD organization; Air Force Rocket Propulsion Lab., Research and Technology Div., Edwards AFB, CA.

AUTHORITY

OCA; IAW markings on document, 15 Nov 1978; AFRPL ltr 7 May 73

AFRPL-TR-66-278

(Unclassified Title)

ADVANCED PRESSURIZATION SYSTEMS TECHNOLOGY PROGRAM FINAL REPORT

H. E. Barber

Rocketdyne
A Division of North American Aviation, Inc.
Canoga Park, California

Technical Report AFRPL-TR-66-278

15 November 1966

Group 4
Downgraded at 3-Year Intervals
Declassified After 12 Years

In addition to security requirements which must be met, this document is subject to special export controls and each transmittal to foreign governments or foreign nationals may be made only with prior approval of AFRPL, Edwards, California 93523.

Air Force Rocket Propulsion Laboratory
Research and Technology Division
Edwards Air Force Base, California
Air Force Systems Command
United States Air Force

AFRPL-TR-66-278

(Unclassified Title)
ADVANCED PRESSURIZATION SYSTEMS TECHNOLOGY PROGRAM
FINAL REPORT

H. E. Barber

Rocketdyne
A Division of North American Aviation, Inc.
Canoga Park, California

Technical Report AFRPL-TR-66-278

15 November 1966

Group 4
Downgraded at 3-Year Intervals
Declassified After 12 Years

Air Force Rocket Propulsion Laboratory
Research and Technology Division
Edwards, California
Air Force Systems Command
United States Air Force

"When U.S. Government drawings, specifications, or other data are used for any purpose other than a definitely related Government procurement operation, the Government thereby incurs no responsibility nor any obligation whatsoever, and the fact that the Government may have formulated, furnished, or in any way supplied the said drawings, specifications, or other data, is not to be regarded by implication or otherwise, or in any manner licensing the holder or any other person or corporation or conveying any rights or permission to manufacture, use, or sell any patented invention that may in any way be related thereto."

FOREWORD

(U) This Final Report was prepared in compliance with the requirements of DD Form 1423, Line Item 5, of Air Force Contract AF04(611)-11383, under Rocketdyne GO 8782. Mr. Charles H. Allen of the AFRPL, was the Program Technical Monitor. Mr. H. Barber, Small Engine Division, was Program Manager for the subject contract.

(U) This publication was prepared by Rocketdyne, a Division of North American Aviation, Inc., as report R-6745.

(U) This technical report has been reviewed and is approved.

Charles H. Allen
Program Manager
AFRPL

ACKNOWLEDGMENT

(U) Important contributions to the conduct of the program and to the preparation of the technical report were made by the following personnel:

G. L. Falkenstein
G. O. Haroldsen
D. H. Grubman
R. W. Roberts

UNCLASSIFIED ABSTRACT

(U) The results of catalytic reactor experiments using mixtures of oxygen/hydrogen and oxygen/hydrogen/methane in the inert diluents, helium and nitrogen, are reported. Analyses are included showing the basis for the selection of the better gaseous mixtures as pressurants for use in propellant pressurization systems. The experiments include the areas of detonability, elevated temperature storage, catalytic reactor response and performance, and expulsion demonstrations.

CONTENTS

ILLUSTRATIONS

TABLES

SUMMARY

(U) This program defines and experimentally determines the operating characteristics of selected, catalytically reacted, stored-gas, pressurization systems. The experimental pressurant gases consist of a major fraction of an inert constituent, helium or nitrogen, and a minor fraction of reactive gases in stoichiometric proportions, oxygen/hydrogen or oxygen/hydrogen/methane.

(U) Theoretical performance maps of reactive to inert gas mixture ratios for the above four combinations of inert and reactive constituents are presented. The mixtures containing helium result in lower pressurization system weights and were selected for the major experimental efforts. Analytical determinations of the effects of gas flame temperature and moisture condensation effects are shown. These were generated by the Rocketdyne digital computer pressurization program which was further used throughout the program to correlate experimental data.

(U) The ignition sensitivity of each gas mixture is shown as a function of mixture ratio, pressure, and temperature. The reactive specie concentration in helium resulting in ignitions from an exploding wire contained twice the volume percentage of oxygen required to produce 1500 F flame temperatures (considered to be the maximum long-duration operability limit of the catalyst). The reactant concentrations exceeded the comparable limits in nitrogen mixtures by a minimum margin of 50 percent over the range tested.

(U) Catalytic reactor tests evaluating catalytic conversion effectiveness as functions of the reactor length and diameter, catalyst pellet size, and operating conditions were made. Parametric design data are provided to permit comparative system evaluations to be made with conventional expulsion systems. The experiments were made at nominal flowrates of 1000 and 100 standard cubic inches per second (sci/sec), chamber pressure levels of 500 and 40 psia, gas inlet temperatures from -100 to 200 F, and with reactor bed initial temperatures from -300 to 1500 F. While the majority

of the experiments were made with 1-inch-diameter catalyst chambers 3 inches long, data were also obtained on 0.5- and 0.75-inch-diameter chambers. Catalyst pellet diameters of 0.125 and 0.0625 inch were utilized in separate reactor chambers operating simultaneously at different flowrates during each test sequence. Varying compositions of $He/O_2/H_2$ and $He/O_2/H_2/CH_4$ were employed as the catalytically reacted media with mixture ratios selected to produce 1500 F peak temperatures. The tests emphasized the transient response characteristics, pressures, and temperatures of the reactor chambers and extended over nominal 10-second intervals. Supplemental tests to show catalyst durability were made with an accumulated duration of 1300 seconds (sequential runs of 800 and 500 seconds) on one charge of 0.062-inch catalyst pellets with no apparent loss in effectiveness.

(U) Generally, the high mass flow tests produced thermal efficiencies of 95 percent or better with the principal variant being the time interval required to reach equilibrium temperatures. The low mass flow tests, 100 sci/sec, were apparently below the range for satisfactory reactor operation and consequently resulted in data of limited application. The time required for the low-flowrate temperature transients to reach equilibrium conditions exceeded the normal 10-second test periods by substantial amounts. The data from the high flowrate tests are reasonably consistent and provide system design parameters which may be used with a high degree of confidence. The test installation also provided data of interest in the areas of orifice flow coefficients and catalyst bed pressure losses.

(U) The test program was initially designed to provide data in the form of a matrix of test variables. The matrix included gas composition, reactor geometry and temperature, and gas temperature, pressure and flowrate. Changes in efficiency resulting from parametric variations were to be determined by means of a statistical mathematical model. However, the early test data showed that the principal test variant was the time response of the gas mixture and catalysts to achieve thermal equilibrium. The peak catalytic conversion efficiencies approached 100 percent when appropriate gas flowrates were used for a given size reactor. Additionally, it was determined that the flowrate range planned (1000 sci/sec to

(U) 100 sci/sec) over the pressure range of 500 to 25 psig was excessive for the catalytic reactor sizes selected. Consequently, moderate changes in the program test conditions were made to provide a maximum of usable data. Test conditions were selected to provide data in the range of peak performance of the catalytic reactors. The test emphasis was placed on the reactor transient start characteristics, pressure and temperature, and on flow coefficient evaluations.

(U) Propellant expulsion demonstration tests were made in which alcohol, simulating a space storable propellant, and liquid nitrogen, simulating a cryogenic propellant, were expelled from a pressure vessel. Employed as comparative pressurants were ambient helium and a reacted mixture of $He/O_2/H_2$ at above 1500 F. The reacted mixture weight was 55.4 percent of the helium weight for the alcohol tests, and 31.5 percent of the helium weight for the liquid nitrogen tests.

(U) Two propulsion systems were selected by the Air Force for comparative analysis of reacted gas and cold-gas pressurization subsystems. The storable propellant system using nitrogen tetroxide and monomethyl hydrazine, indicated an approximate weight savings of 37 percent through the use of an $He/O_2/H_2$ reacted pressurant in place of ambient temperature helium. A second system, using liquid hydrogen and liquid fluorine as propellants, showed a significant operational advantage through the use of reacted $He/O_2/H_2$ as a prepressurization agent to provide a net positive suction pressure for pump operation.

INTRODUCTION

(U) The pressurization subsystem contributes a significant portion of the total weight of virtually all space rocket propulsion systems. Considerable past effort has been expended in the development and improvement of the various pressurization subsystem components, stressing lightness, simplicity, reliability, and ease of operation. The program described herein complements this improvement effort by providing data on catalytically heated gases as pressurization media to produce higher overall system of efficiencies.

(U) The pressurant gases are stored as a nonhypergolic, nondetonable mixture of reactive and inert constituents in a single container. The gases are admitted, as required, into the propellant tanks through a catalyst bed which promotes an exothermic reaction between the reactive constituents, thus heating the predominantly inert mixture.

(U) A major attraction of the catalytically reactive gas concept is that the heat addition is effected with no external heat source and with virtually no penalty in weight, system complexity, or reliability. It is particularly suitable for systems employing short-duration pressurization intervals where system weight is critical. Heated gas pressurant can also be efficiently used for multiple-cycle operation of pump-fed systems. The heated gas will provide the net positive suction pressure (NPSP) requirements during system operation and will result in a pressure collapse by cooling during coasting. This characteristic permits propellant repressurization without tank venting for the subsequent thrusting operations.

(U) The program presented herein provides experimental data on selected gaseous mixtures over a wide range of compositions, pressures, and temperatures. The specific areas are the detonability, the sensitivity of various reactive specie concentrations, the performance and response characteristics of reactive gases in the catalyst reactors, and the demonstration of expulsion cycles employing catalytically reacted gases.

EXPERIMENTAL INVESTIGATIONS

(U) The experimental investigations were conducted in three separate tasks: gaseous mixture stability evaluations, catalytic reactor evaluations, and propellant expulsion demonstrations. The purposes, experimental facilities and techniques, and results of these tasks are described below.

MIXTURE STABILITY EVALUATIONS

(U) The initial experimental task was to evaluate the stability of the gaseous mixtures under consideration. The major portion of this task was concerned with the ignition sensitivity of the blends, and was accomplished by subjecting selected mixtures to an exploding wire and noting the occurrence of deflagration and/or detonation. These mixtures included oxygen/hydrogen and oxygen/hydrogen/methane in helium and nitrogen diluents. For the O_2/H_2 mixtures the oxidizer-to-fuel ratio was maintained at stoichiometric and the proportion of diluent varied. In the case of the $O_2/H_2/CH_4$ mixtures, the oxygen-to-methane ratio was maintained at stiochiometric based on a complete chemical reaction to the products, carbon dioxide and water. Since methane and oxygen will not catalytically react at temperatures below 400 F, sufficient hydrogen was added so that the O_2/H_2 reaction would raise the temperature to approximately 400 F.

(U) The quantity of diluent was systematically varied so as to define safe concentration limits. The bulk of the experiments was conducted at a pressure of $\sim$ 2000 psia and temperatures of 75 and 200 F. In addition, selected experiments were conducted at $\sim$ 1000 and $\sim$ 3000 psia to evaluate the effect of pressure on the experimentally determined limits.

(U) In addition to the above experiments, a secondary effort was aimed at determining the storability of the blends and, in the event that a slow, long-term reaction was noted, the resulting effects on mixture stability.

Mixture Deflagration/Detonation Stability
Experimental Apparatus and Procedure

(U) Experimental Apparatus. The experimental apparatus used in the detonability investigation is illustrated in Fig. 1 and 2. The apparatus consisted of a stainless-steel, high-pressure gas reservoir provided with propellant inlet ports and adaptors for temperature and pressure measurements, and fitted with an ignition source and a burst diaphragm for pressure relief. The ignition source used in these studies consisted of a 0.001-inch-diameter tungsten-5 percent rhenium wire approximately 1 inch long. This wire was exploded over a time period of less than 100 microseconds by applying a 28-volt potential. During the period of time in which the potential was applied, the wire reached a temperature of at least 3370 C, (~ 6100 F), the melting temperature of tungsten.

(U) Experimental Procedures. The mixture ignition stability experiments were conducted in a two-step operation. The first step was a controlled temperature mixing of the appropriate components and the second, an actuation of the exploding wire.

(U) For the blending operation, the first gas charged to the detonation capsule was oxygen. This gas was first used to thoroughly purge the bomb. Following the purge operation, oxygen was introduced, followed by the diluent, and finally by the hydrogen, in the case of three-component mixtures. In experiments involving the use of four-component mixtures, the sequence consisted of oxygen, followed by methane, inert gas, and hydrogen.

(U) The introduction of the inert gas prior to the introduction of hydrogen served to dilute the oxygen and thereby eliminate the possibility of an explosion because of the accidental ignition of concentrated stoichiometric blends of oxygen and hydrogen. All blends were prepared on the basis of partial pressures, since compressibility effects are negligible.

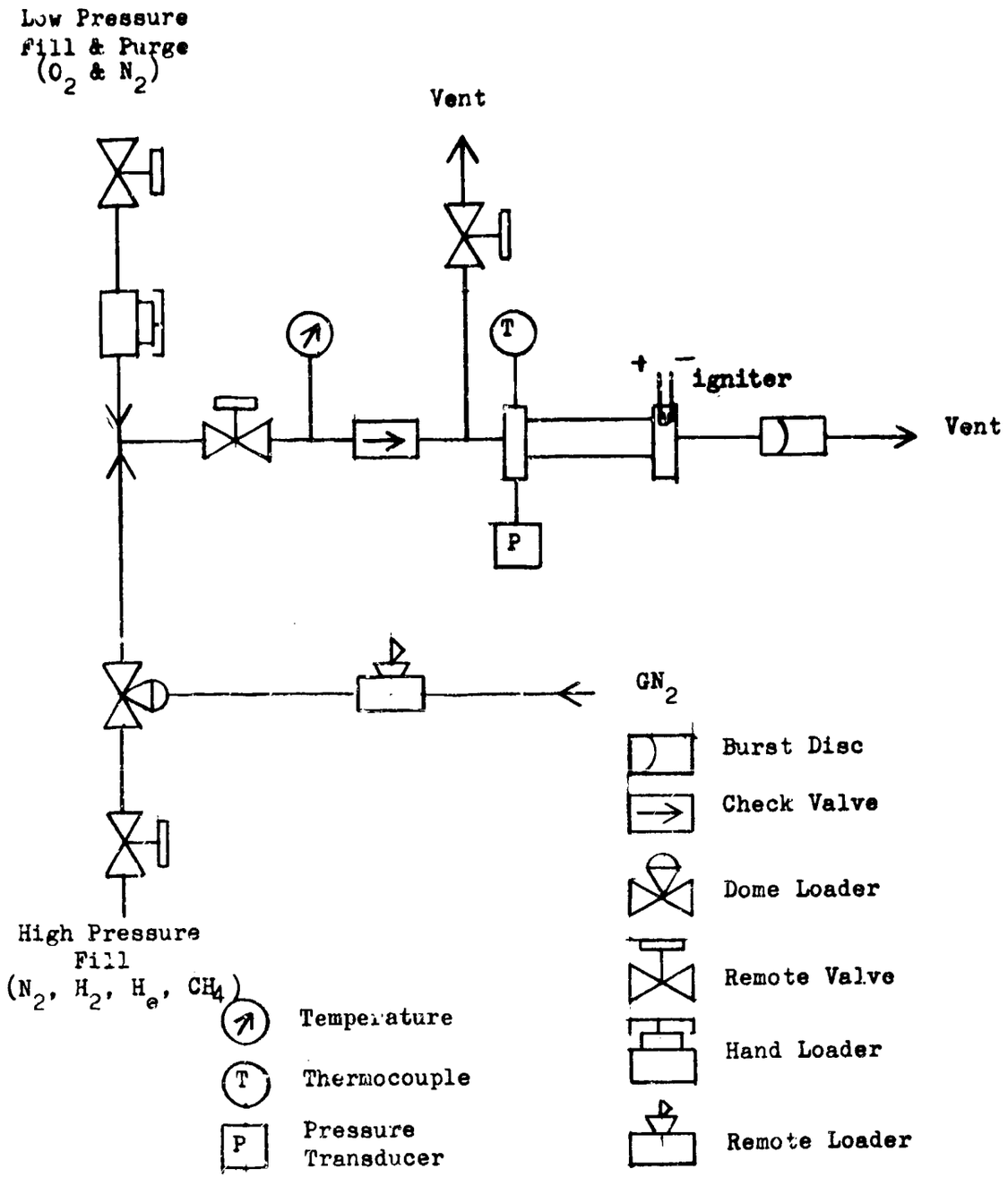

Figure 1. Schematic for Detonability Evaluation

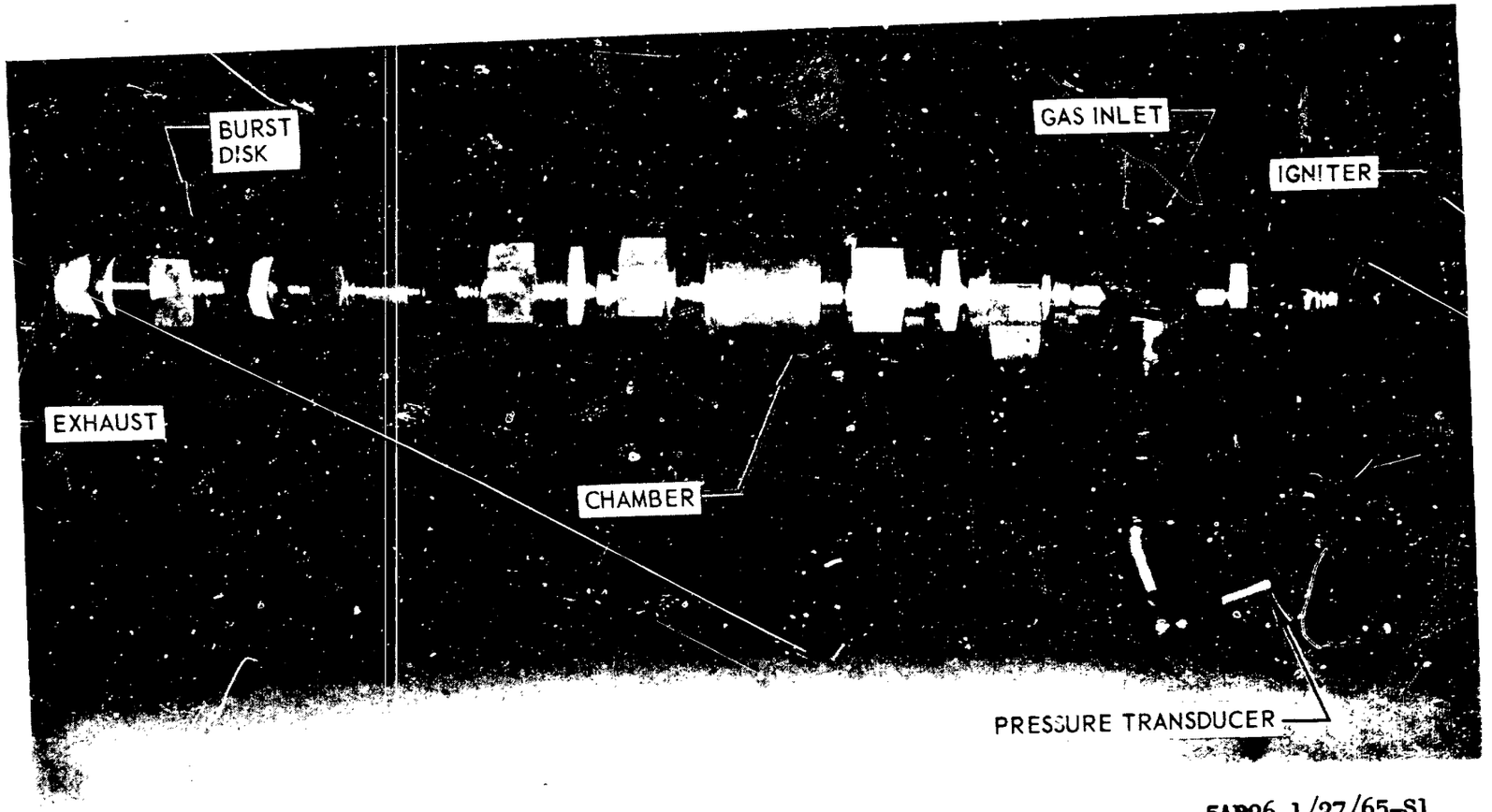

Figure 2. Ignitability Test Chamber

(U) In experiments conducted at an environmental temperature of 200 F, the stainless-steel detonation chamber was heated to a temperature of approximately 225 F. Following introduction of the gaseous propellants, the chamber was allowed to cool to 200 F, and the test was conducted. Experiments conducted at pressures of 1000 and 3000 psia were performed in a manner identical to that employed in experiments at 2000 psia.

Results of the Deflagration/Detonation Stability Experiments

(U) Stability Limits at Constant Pressure. The results of the experimental deflagration/detonation stability study are presented in Table 1 and Fig. 3 through 6. These figures show the stability limits of each mixture at a pressure of 2000 psia in terms of the oxygen concentration. The results for pretest temperatures of both 75 and 200 F are shown. The limits define the highest stable concentration and the lowest deflagrable/detonable concentration tested. Also indicated is the temperature gain, resulting from complete reaction as a function of the oxygen concentration.

(U) The $He/O_2/H_2$ test results at the 2000-psia pressure level are shown in Fig. 3. Although an appreciable effect of storage temperature on the critical stability concentration was noted, the stability region was found to extend to almost double the oxygen concentration of that needed to produce a 1500 F gas.

(U) The $N_2/O_2/H_2$ blend stability characteristics are shown in Fig. 4. The results obtained at the two pretest temperatures of 75 and 200 F were identical, indicating a negligible deflagration/detonation sensitivity to small increases in initial temperature. The critical oxygen concentration for a stable blend was found to be only ~ 50 percent greater than that

TABLE 1

SUMMARY OF DEFLAGRATION/DETONATION TEST RESULTS AT 2000 PSIA

Run	Environmental Temperature, F	Propellant Concentrations, volume percent				Theoretical Incremental Temperature, F	Comments
		O_2	H_2	CH_4	Inert		
1	75	3.6	7.2		89.2 (He)	1473	No ignition
2	75	5.4	10.7		83.9 (He)	2180	No ignition
3	75	7.15	14.3		78.6 (He)	2920	No ignition
4	75	8.93	17.9		73.2 (He)	3650	No ignition
5	75	10.7	21.4		67.9 (He)	4370	Ignition
6	200	5.4	10.7		83.9 (He)	2180	No ignition
7	200	6.25	12.5		81.8 (He)	2550	No ignition
8	200	7.15	14.3		78.6 (He)	2920	Ignited after ~ 2-second delay
9	200	8.93	17.9		73.2 (He)	3659	Ignition
10	75	15.0	30.0		55.0 (N_2)	4275	Ignition
11	75	10.0	20.0		70.0 (N_2)	2850	Ignition
12	75	8.75	17.5		73.75 (N_2)	2500	Ignition
13	75	7.5	15.0		77.5 (N_2)	2130	No ignition
14	75	8.2	16.4		75.4 (N_2)	2320	No ignition
15	200	6.25	12.5		81.25 (N_2)	1440	No ignition
16	200	7.5	15.0		77.5 (N_2)	1720	No ignition
17	200	8.0	16.0		76.0 (N_2)	1850	No ignition
18	200	8.75	17.5		73.75 (N_2)	2500	Ignition

Note: All runs made at 2000 psia.

TABLE 1

(Concluded)

Run	Environmental Temperature, F	Propellant Concentrations, volume percent				Theoretical Incremental Temperature, F	Comments
		O_2	H_2	CH_4	Inert		
19	75	4.4	2.9	2.2	90.5 (He)	1520	No ignition
20	75	5.5	2.9	2.7	88.9 (He)	1900	No ignition
21	75	6.6	2.9	3.3	87.2 (He)	2280	No ignition
22	75	7.7	2.9	3.8	85.6 (He)	2670	No ignition
23	75	8.2	2.9	4.1	84.8 (He)	2830	Ignition
24	75	8.8	2.9	4.4	83.9 (He)	3040	Ignition
25	200	4.4	2.9	2.2	90.5 (He)	1520	No ignition
26	200	6.6	2.9	3.3	87.2 (He)	2280	No ignition
27	200	7.7	2.9	3.8	85.6 (He)	2670	No ignition
28	200	8.8	2.9	4.4	83.9 (He)	3040	Ignition
29	75	6.7	4.4	3.3	85.6 (N_2)	1540	No ignition
30	75	10.1	4.4	5.0	80.5 (N_2)	2320	No ignition
31	75	11.7	4.4	5.8	78.1 (N_2)	2700	No ignition
32	75	13.4	4.4	6.7	75.5 (N_2)	3090	Ignition
33	200	10.1	4.4	5.0	80.5 (N_2)	2320	No ignition
34	200	11.7	4.4	5.8	78.1 (N_2)	2700	Ignition

Note: All runs made at 2000 psia

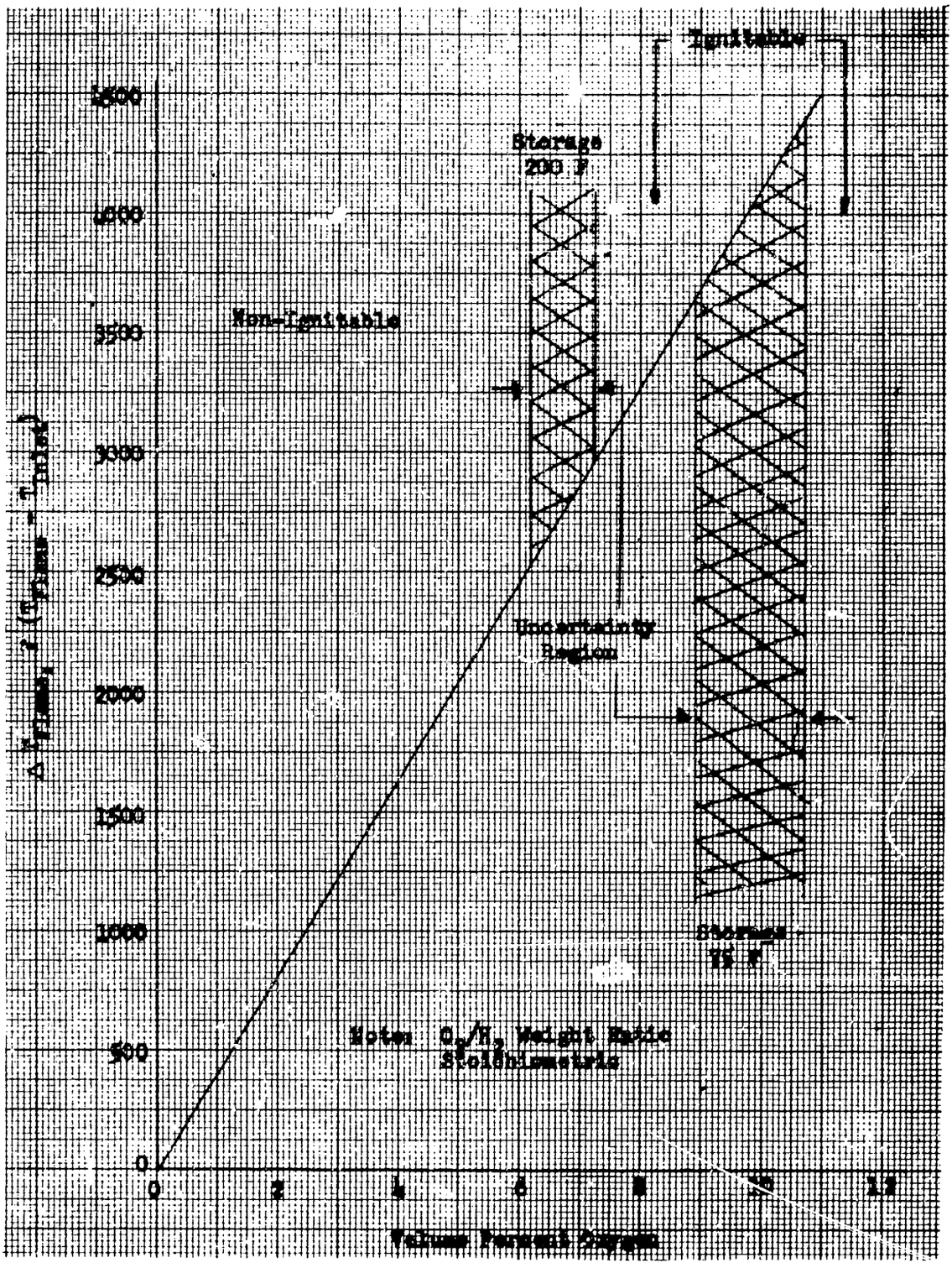

Figure 3. Concentration-Stability Relationship for the $He/O_2/H_2$ System at 2000 psia

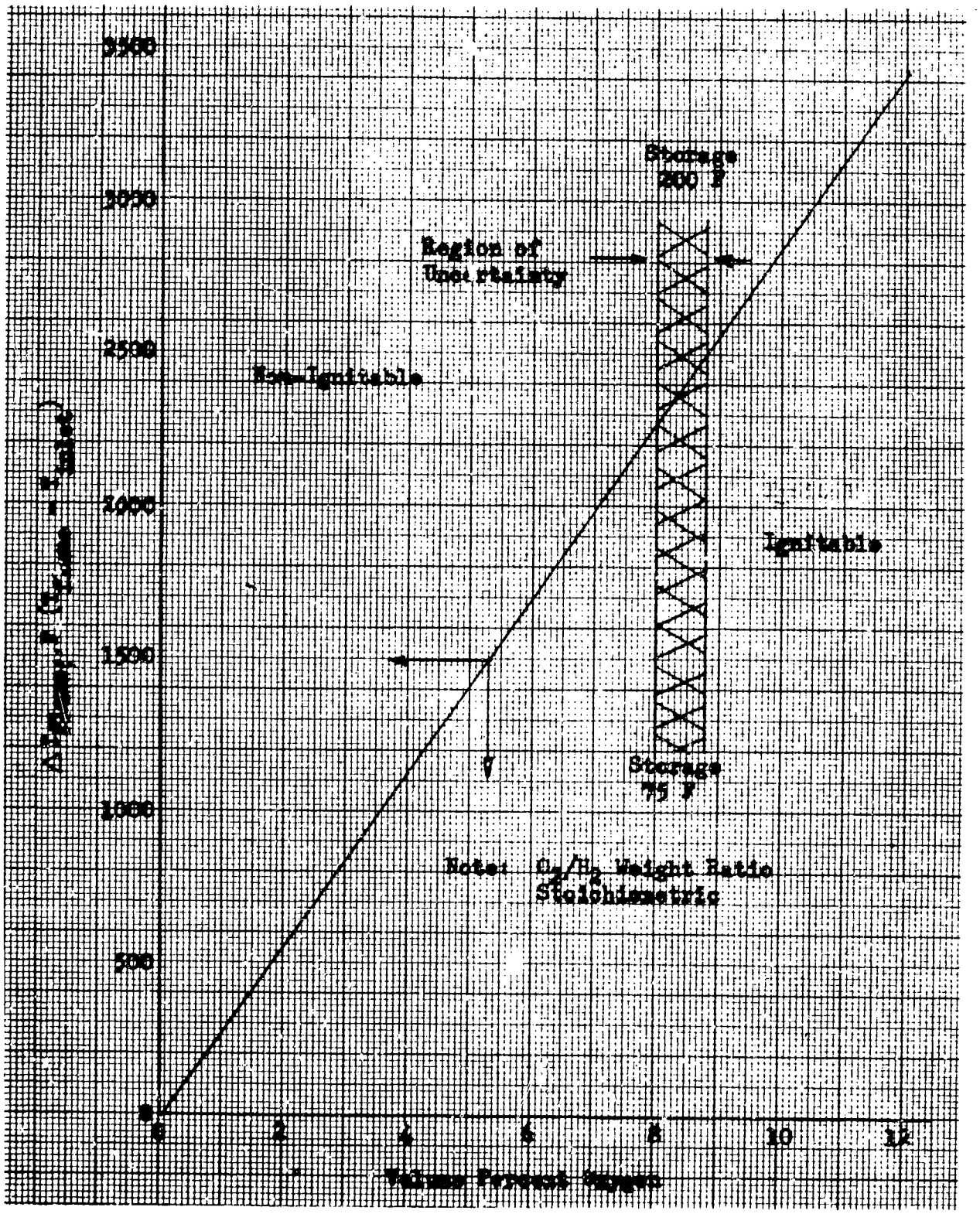

Figure 4. Concentration-Stability Relationship for the $N_2/O_2/H_2$ System at 2000 psia

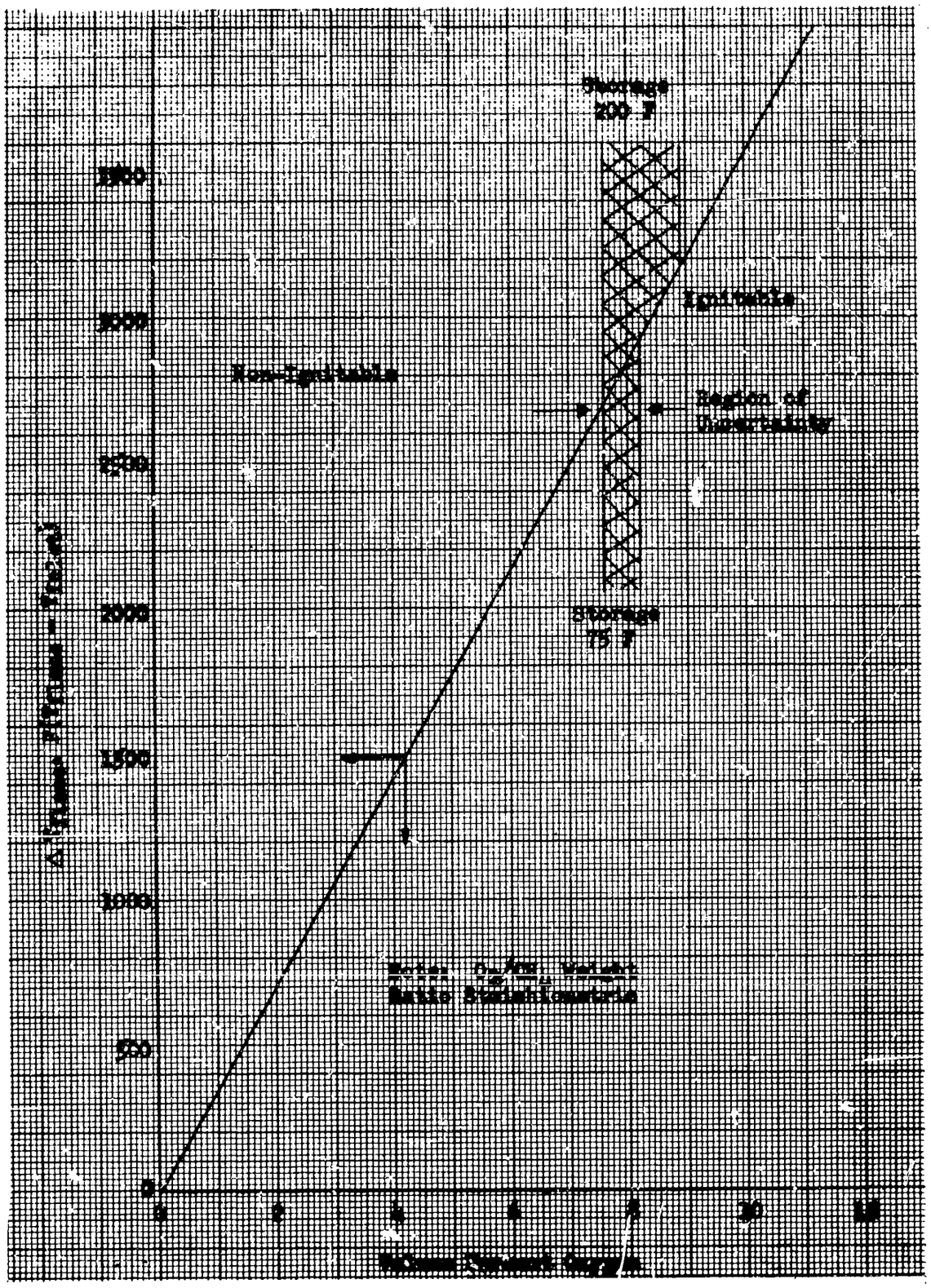

Figure 5. Concentration Stability Relationship for the $He/O_2/H_2/CH_4$ System at 2000 psia

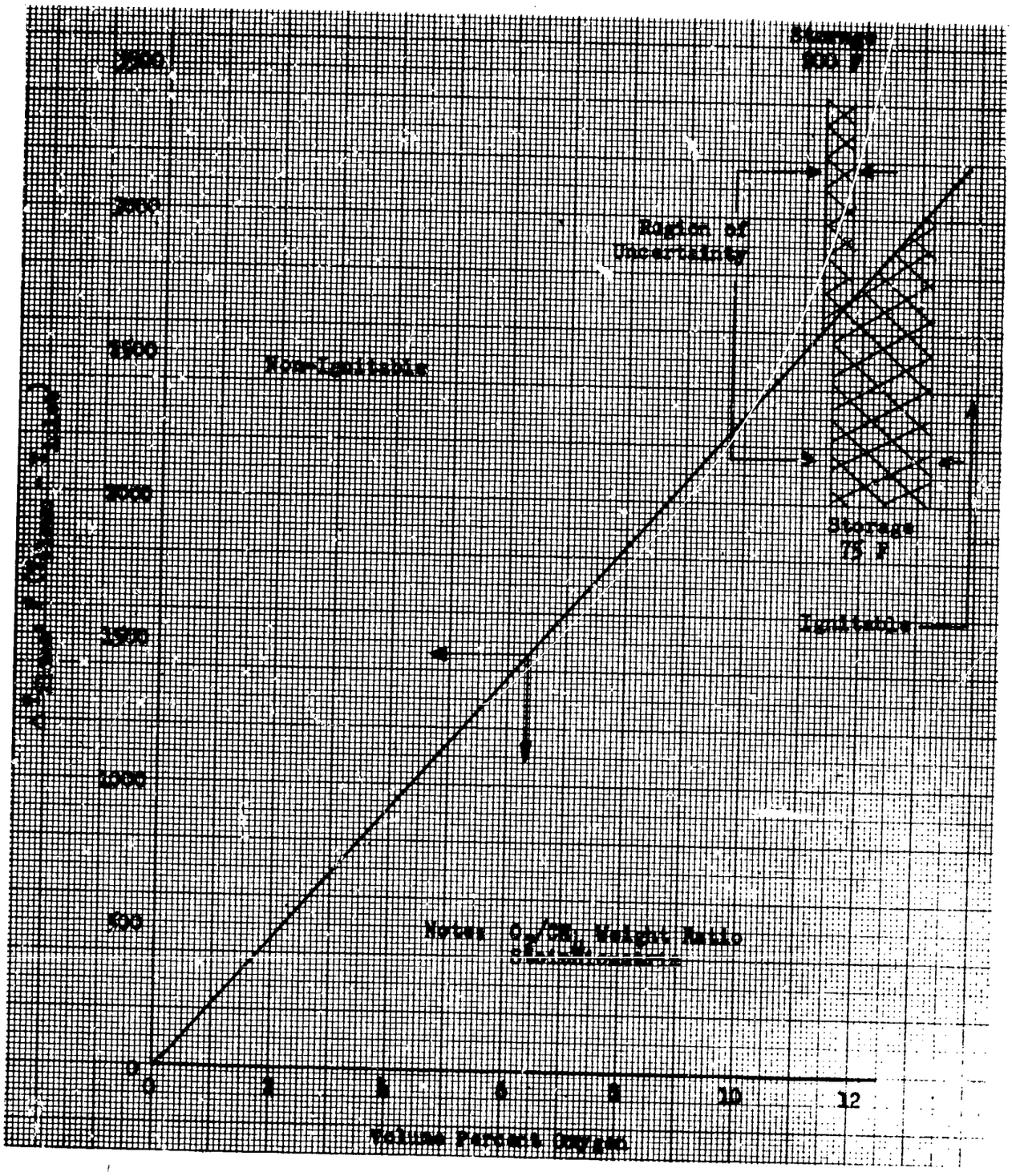

Figure 6. Concentration-Stability Relationship for the $N_2/O_2/H_2/CH_4$ System at 2000 psia

needed to produce a 1500 F gas which uses a substantially smaller margin of safety than with the helium diluent. It is noted, however, that the critical oxygen volume concentrations are approximately the same with the two diluents, the nitrogen results falling between the 75 and 200 F results with helium diluent. The reduced molal (volumetric) heat capacity of the helium as compared to nitrogen results in a higher temperature for the helium blend at a given oxygen concentration, and is responsible for the difference in the margin of safety for the systems.

(U) The similar limit concentrations indicate a branched-chain mechanism of reaction propagation. The inert gases inhibit the propagation of specie activity and terminate chain reactions in the region of the combustion front. The alternative would be a thermal propagation of the combustion front, but in this case the flame temperatures would be similar at the stability limit. It is recognized that such an interpretation is only speculative, and that more definitive experiments are required to achieve precise definitions of the mechanisms.

(U) Figure 5 shows the deflagration/detonation stability limits of the $He/O_2/H_2/CH_4$ mixture. The results obtained at the two storage temperatures are essentially the same. A substantial margin of safety was indicated, since the critical concentration was found to be approximately 70 percent larger in reactants than required for a 1500 F mixture.

(U) The $N_2/O_2/H_2/CH_4$ characteristics are shown in Fig. 6. The critical oxygen concentrations are again almost equal and at a value substantially above that required for a 1500 F gas.

(U) With the $He/O_2/H_2/CH_4$ and $N_2/O_2/H_2/CH_4$ gases, it is noted that the critical stability limit was observed to occur at concentrations giving essentially identical flame temperatures. This is interpreted as indicating a thermal mechanism for reaction propagation.

Effects of Pressure on Deflagration/Detonability

(U) As the helium-base mixtures offer significant weight advantages over nitrogen-base mixtures, further tests of the helium mixtures to evaluate the effects of pressures were made at two additional pressure levels, 1000 and 3000 psia, for comparison with the data obtained at 2000 psia. The experiments were accomplished at 75 F and the results are shown in Table 2 and Fig. 7 and 8.

(U) The figures present the results in the same format as used above. The effects of pressure are not pronounced and substantial margins above the reactant concentration for 1500 F temperatures are shown.

(U) A plot of the same data as a function of pressure (Fig. 9) reveals a high degree of internal consistency in the limits except for one condition. A slight inconsistency is evident in the ignitability limit shown at 2000 psia. The limit for the $He/O_2/H_2$ mixture would be expected to be at or below that shown for the $He/O_2/H_2/CH_4$ to be consistent with the 1000-psia data and to be in agreement with the apparent trend for a slight decrease in allowable oxygen content with increasing pressures. While the effects of pressure on ignitability are not large, the test results obtained do not identify a precise relationship between pressure and ignitability other than to show a substantially safe margin between ignitable concentrations and those which provide flame temperatures in the vicinity of 1500 F.

(U) The experimental data for the $N_2/O_2/H_2/CH_4$ mixture (Fig. 6) showed a substantially higher allowable oxygen volume percentage (40 percent) than for the $N_2/O_2/H_2$ system which is consistent with the general tendency for methane to suppress detonability. In the event that high reactant concentrations are required in future systems, the mixtures containing methane would warrant further evaluation.

TABLE 2

SUMMARY OF DEFLAGRATION/DETONATION TEST RESULTS AT 1000, 2000, and 3000 PSIA

Run	Pressure, psia	Propellant Concentrations, volume percent				Theoretical Incremental Temperature, F	Comments
		O_2	H_2	CH_4	He		
1	1000	10.8	21.6	---	67.6	4400	Ignition
2	1000	9.9	19.8	---	70.3	4040	Ignition
3	1000	8.9	17.7	---	73.4	3800	Ignition
4	1000	7.9	15.8	---	76.3	3300	No ignition
4*	2000	8.9	17.9	---	73.2	3650	No ignition
5*	2000	10.7	21.4	---	67.9	4370	Ignition
5	3000	8.9	17.9	---	73.2	3650	Ignition
6	3000	8.0	16.0	---	76.0	3350	Ignition
7	3000	7.0	14.0	---	79.0	2800	No ignition
8	1000	8.2	2.9	4.1	84.8	2830	No ignition
9	1000	8.9	2.9	4.4	85.8	3100	No ignition
10	1000	10.3	2.9	5.1	81.7	3560	Ignition
22*	2000	7.7	2.9	3.8	85.6	2670	No ignition
23*	2000	8.2	2.9	4.1	84.8	2830	Ignition
11	3000	6.6	2.9	3.3	87.2	2350	No ignition
12	3000	7.7	2.9	3.9	85.5	2700	No ignition
13	3000	8.4	2.9	4.2	84.5	2950	Ignition

*From Table 1

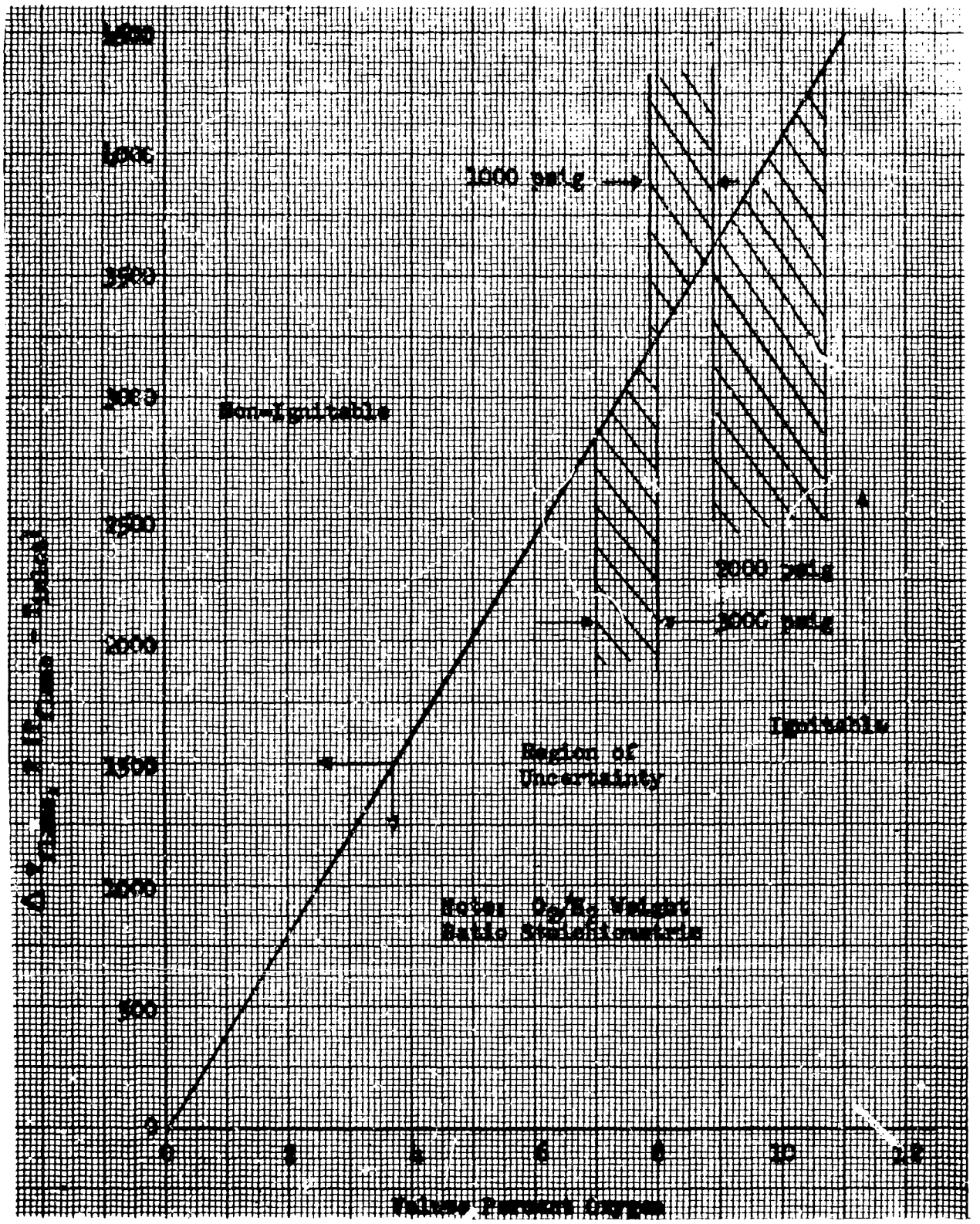

Figure 7. Concentration-Stability Relationship for the $He/O_2/H_2$ System at Pressures of 1000, 2000, and 3000 psia

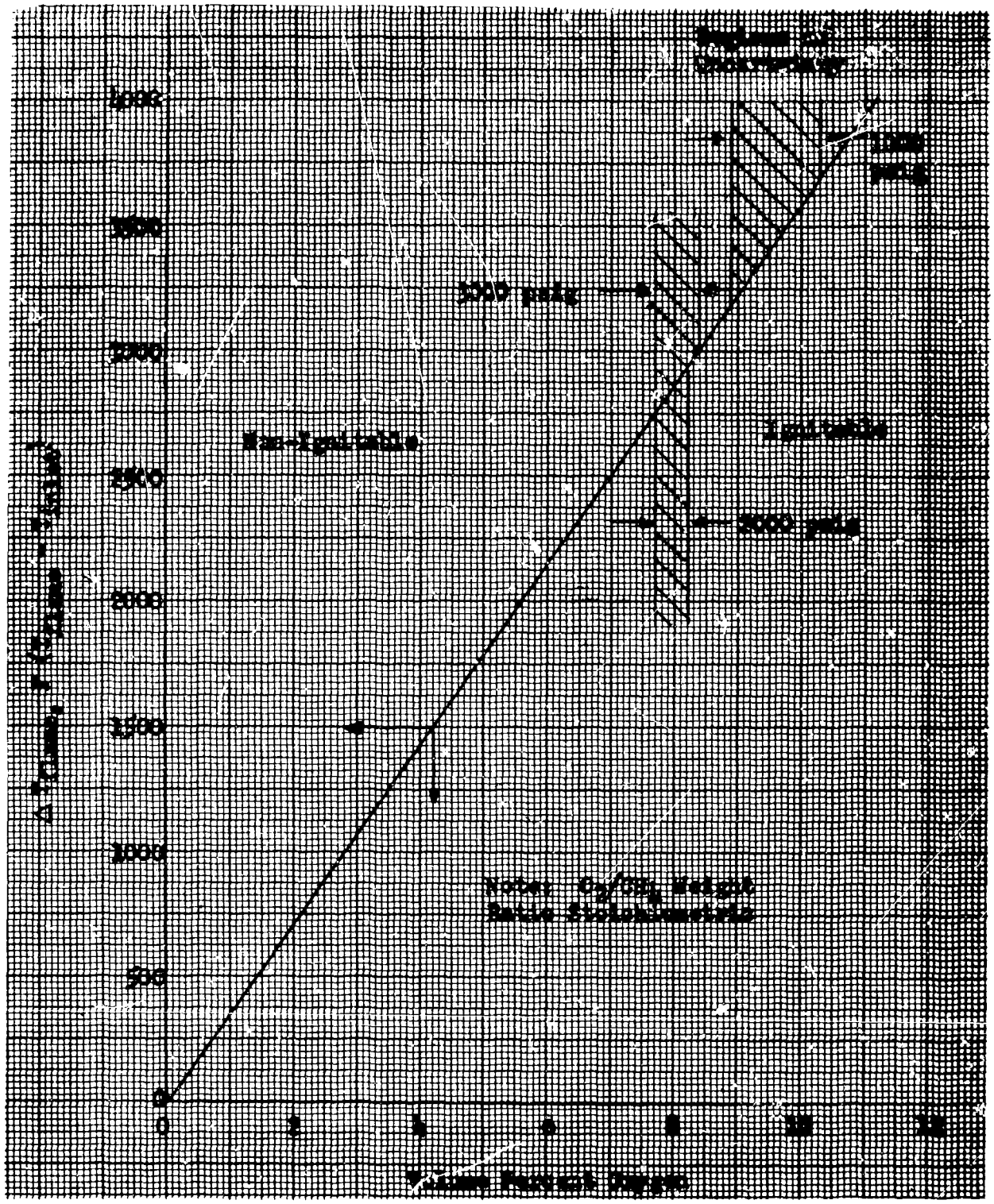

Figure 8. Concentration-Stability Relationship for the $He/O_2/H_2/CH_4$ System at Pressures of 1000, 2000, and 3000 psia

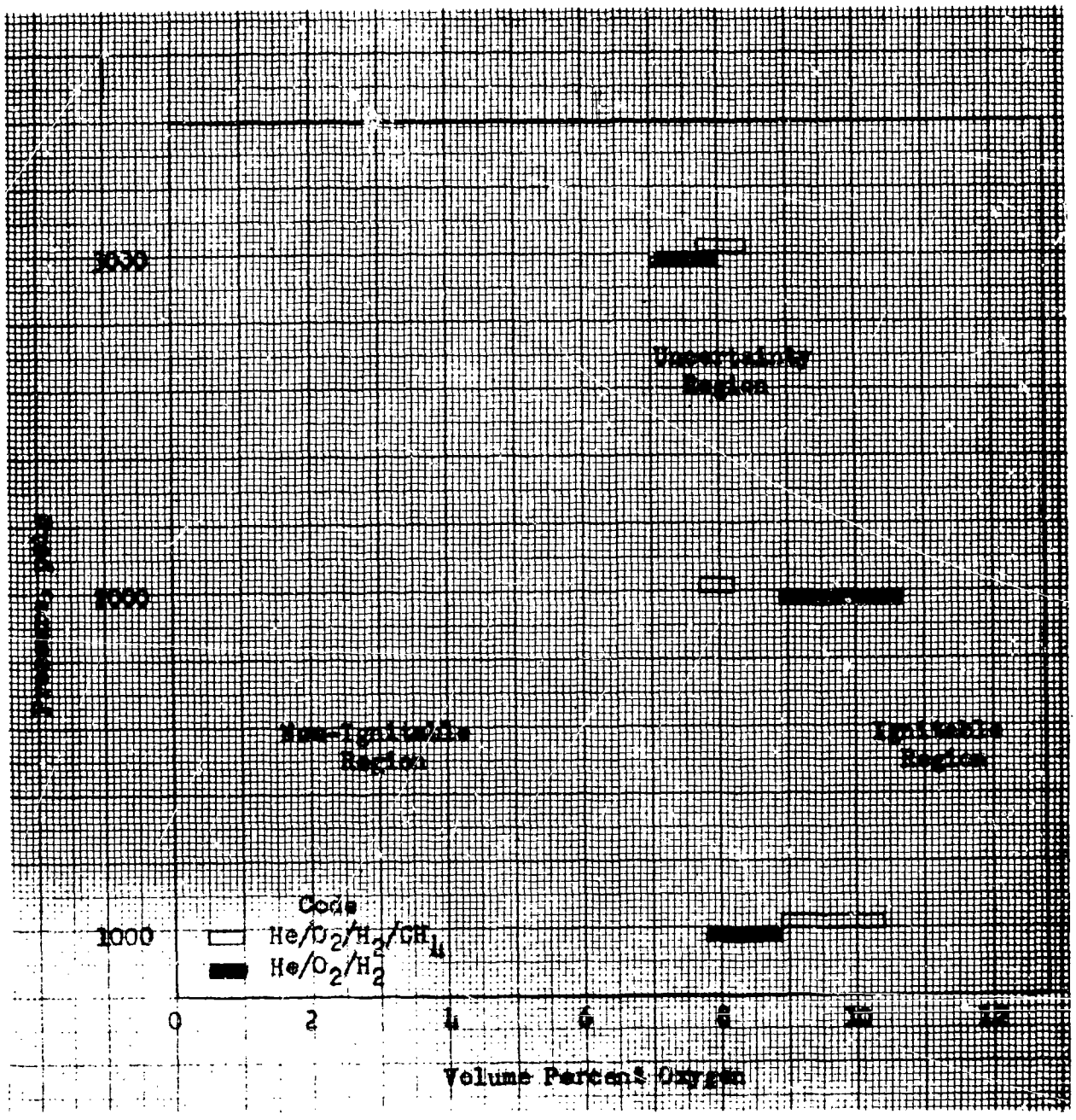

Figure 9. Pressure Effects on Stability for the $He/O_2/H_2$ and $He/O_2/H_2/CH_4$ Systems at 75 F

Comparison of Results With Previous Work

(U) Ignition experiments were conducted by Wilkins and Carros (Ref. 1) on stoichiometric mixtures of oxygen and hydrogen in helium as an inert diluent. Test pressures were varied from 300 to 8000 psia. The test device used for the ignition limit evaluation was very similar in shape and size to the one employed in the subject program (Fig. 2). The ignitor configuration for most of the Wilkins and Carros experiments consisted of exploding manganin wires, 0.0015-inch diameter, energized by 0.5 to 9.3 kilovolts of 7.5-microfarad capacitance. This energy level is substantially above that used for the tests of this report, although a direct comparison of absolute values is difficult to make.

(U) Some effects were noted in the Wilkins and Carros tests from the manner in which the experimental mixtures were loaded into the test device. The results of tests in which oxygen, helium, and hydrogen were introduced separately in the listed order, the same order as used in the subject program, are presented in Fig. 10. Also shown are the ambient temperature $He/O_2/H_2$ ignition limit test results from the present study. Good agreement is shown by the two sets of data.

(U) Additional tests were performed in which premixed helium and hydrogen were introduced into the chamber which contained oxygen. The results of these tests and the data for the subject program are shown in Fig. 11. There is a fairly wide zone in which Wilkins and Carros encountered ignitions below the ignitable region shown by the present study. The disagreement of these data is probably attributable to either the manner of mixing the test gases or to the differences in the ignition energy levels. While the margin of reactant concentrations resulting in no reaction is shown to be substantially lower with the Wilkins and Carros data than with the subject program data, both test series show no reaction with O_2/H_2 concentrations producing temperatures of 1500 F. However, additional work is required to establish a higher degree of confidence in the ignition limit area.

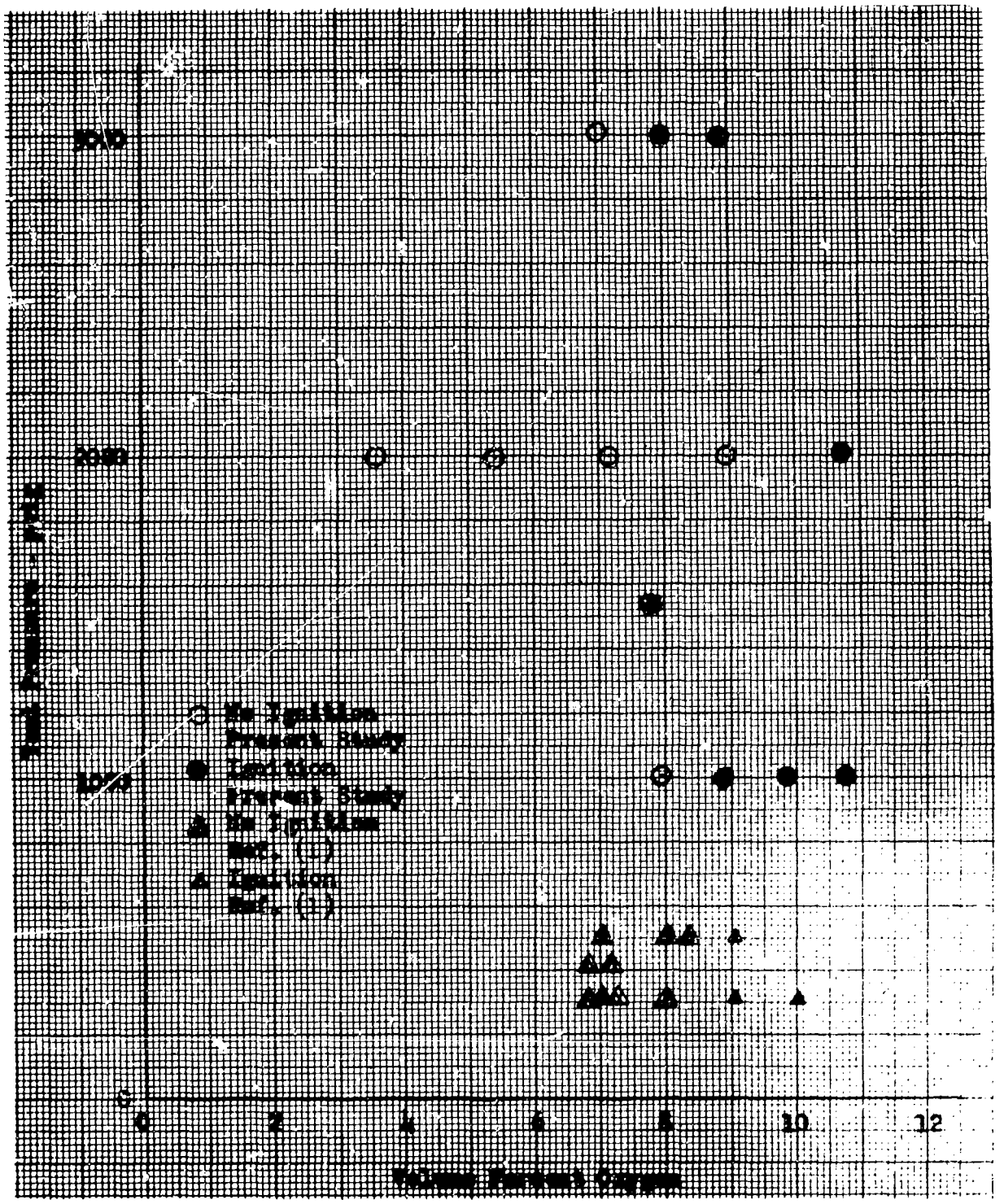

Figure 10. Concentration-Stability Relationship for $He/O_2/H_2$ System at Ambient Temperature (Comparison with Ref. 1)

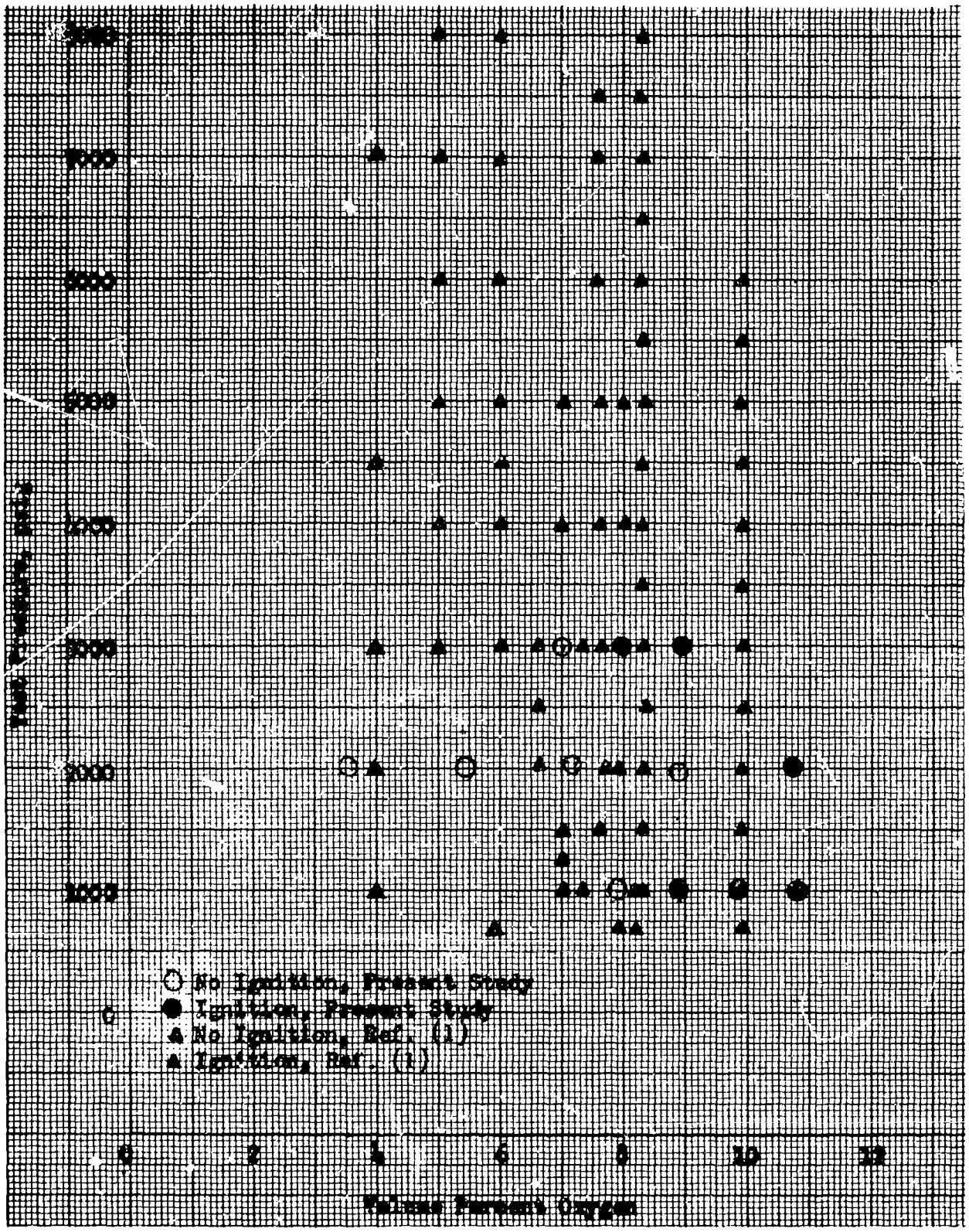

Figure 11. Concentration-Stability Relationship for the $He/O_2/H_2$ System at Ambient Temperatures and at Pressures to 8000 psia (Comparison with Ref. 1)

MIXTURE STABILITY UNDER STORAGE CONDITIONS

(U) The evaluation of storability characteristics of two mixtures, one composed of $He/O_2/H_2$ and the other of $He/O_2/H_2/CH_4$, was conducted to determine the effects of extended storage at 1000 psia and 200 F on blend composition. The two indicated mixtures were selected on the basis of analytical comparisons of pressurization capability. The compositions evaluated are shown in Table 3, and were selected to give flame temperatures of 2250 F. This is approximately a 50-percent increase over the desired reactant concentrations designed for a 1500 F flame temperature.

Experimental Apparatus

(U) The experimental apparatus employed in this investigation was identical to that shown in Fig. 2, with one exception: the gas reservoir was immersed in a constant-temperature bath. The bath consisted of a nominally 25-gallon container filled with water and equipped with a rheostat-controlled electrical heating element which controlled the water temperature at $\sim$ 200 F.

Experimental Procedures

(U) The gaseous blends employed in the storability investigations were mixed in a manner identical with that for the deflagration/detonability tests. After the blends were prepared, the bomb and contents were heated to approximately 200 F in the hot water bath. After approximately 1 week of storage at 1000 psia and 200 F, a sample of gas was withdrawn from the bomb and analyzed to determine the occurrence of any chemical reaction. The mixture was allowed to remain at storage conditions for a second week and was again sampled for analysis. Since chemical reaction would invariably result in the formation of water as a reaction product with the gaseous constituents involved, the gas sample was analyzed for the presence of water.

Results and Discussion

(U) The results of the storage tests are presented in Table 3. Only two successful data points were obtained. The sample from the $He/O_2/H_2$ mixture taken at the end of the first week was contaminated during the analysis procedure, so the water content was not obtained. However, the analysis at the end of the second week showed a water content virtually unchanged from the original content. The $He/O_2/H_2/CH_4$ sample showed no reaction at the end of the first week. However, a leak developed in the storage vessel with the second mixture and essentially all the stored gas escaped prior to the end of the second week. Again, the water content could not be determined. Since the analysis at the end of the first week showed no reaction with $He/O_2/H_2/CH_4$ and at the end of the second week the $He/O_2/H_2$ sample gave no indication of any reaction, the tests were not rerun.

(U) It is apparent that no measurable reaction occurred during the storage period, when it is recognized that conversion of only 1 percent of the oxygen present in the three-component blend would result in the production of water equivalent to nearly 3700 ppm. For the four-component blend, the stoichiometry is not as well defined, but the water production would be of the same order of magnitude.

(U) Since the chemical analyses indicated no chemical reaction had occurred, no further deflagration/detonation or storability studies were conducted.

Summary of Blend Stability Results

(U) The reactant gas stability studies showed the mixtures under consideration for use in advanced pressurization systems (with $\sim$ 1500 F flame temperatures) to be stable to an exploding wire ignition source. Further, with the $N_2/O_2/H_2$ blend, an approximately 50-percent margin of safety was observed; increased margins of safety were measured with the other blends. The storage evaluations indicated the blend to be completely

stable over a 2-week time period at storage conditions of ~ 200 F and 1000 psia. Thus, the blends under consideration for advanced pressurization systems have been shown to be feasible from the safety and storage standpoints defined for this program.

TABLE 3

COMPOSITION AND CHEMICAL ANALYSES
OF STORED GAS SAMPLES

Composition, volume percent					Water Content, ppm		
Blend	Oxygen	Hydrogen	Methane	Helium	Original*	1 Week	2 Weeks
1	5.4	10.8	—	83.8	83	NG 1**	86
2	6.6	2.9	3.3	87.2	82	75	NG 2***

*Calculated on the basis of individual component analyses
**NG 1 sample inadequate for precise analysis
***NG 2 storage bomb leakage precluded sample availability

CATALYTIC REACTOR EVALUATION

(U) The catalytic reactor evaluation program determined the effectiveness of catalytic reactors in combining the reactive constituents and raising the final gas temperatures to the desired values. Performance was evaluated as a function of bed geometry (length, diameter, and catalyst pellet size) and operating conditions (pressure, temperature, and flowrate). This information was generated to provide preliminary design data for a catalytic pressurization system, and to enable comparative performance evaluations to be made with conventional expulsion systems.

(U) The experiments were conducted at two nominal flowrates (1000 and 100 sci/sec) and two nominal chamber pressure levels (500 and 40 psia). The gaseous feed temperatures were varied from -100 to 200 F. These conditions were chosen to include typical operating regimes for both storable, pressure-fed and cryogenic, pump-fed propulsion systems. In addition, the catalyst bed geometry was varied: the diameter from 0.5 to 1.0 inch and the length from 1 to 3 inches.

Apparatus

(U) Experimental System. The experimental system, Fig. 12 and 13, consisted of dual reactor units to expedite execution of the test program. The blend was prepared in a high-pressure, 20-gallon supply tank. Each circuit leading from the tank consisted of a pressure regulator, an orifice meter, a main circuit valve, a heating and/or cooling coil, and the catalytic reactor itself. The orifice meter was used during the first 14 tests only. The coil was used to condition the gas to the desired injection temperature, and for cooling, was immersed in a bath of dry ice and trichloroethylene. For heating, the bath was converted to boiling water. The purge gas used to prechill the catalyst also employed the same coil. The coils were added to the system when other means of heating and cooling proved inadequate. They were removed when running the ambient temperature tests.

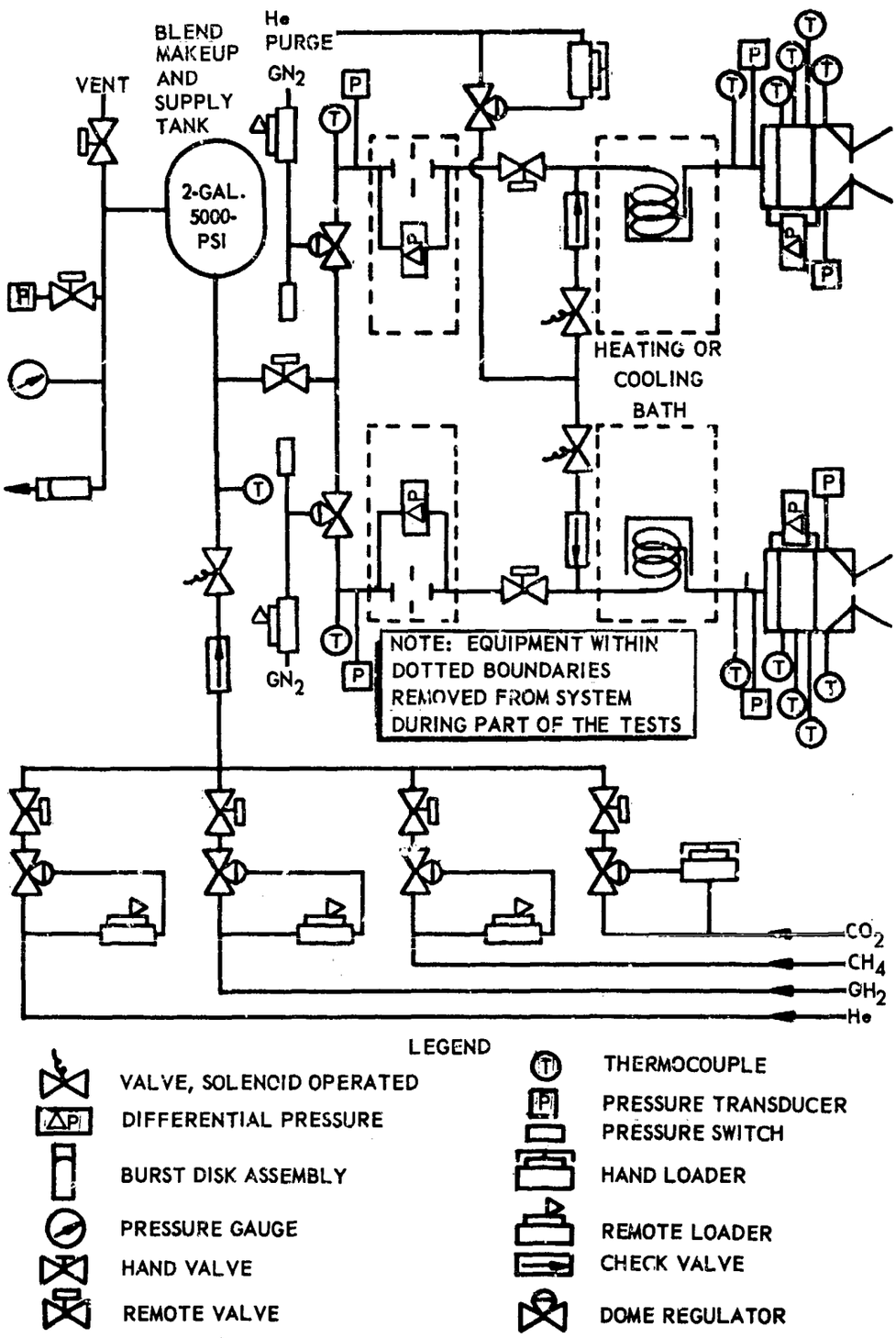

Figure 12. Catalytic Reactor System Schematic

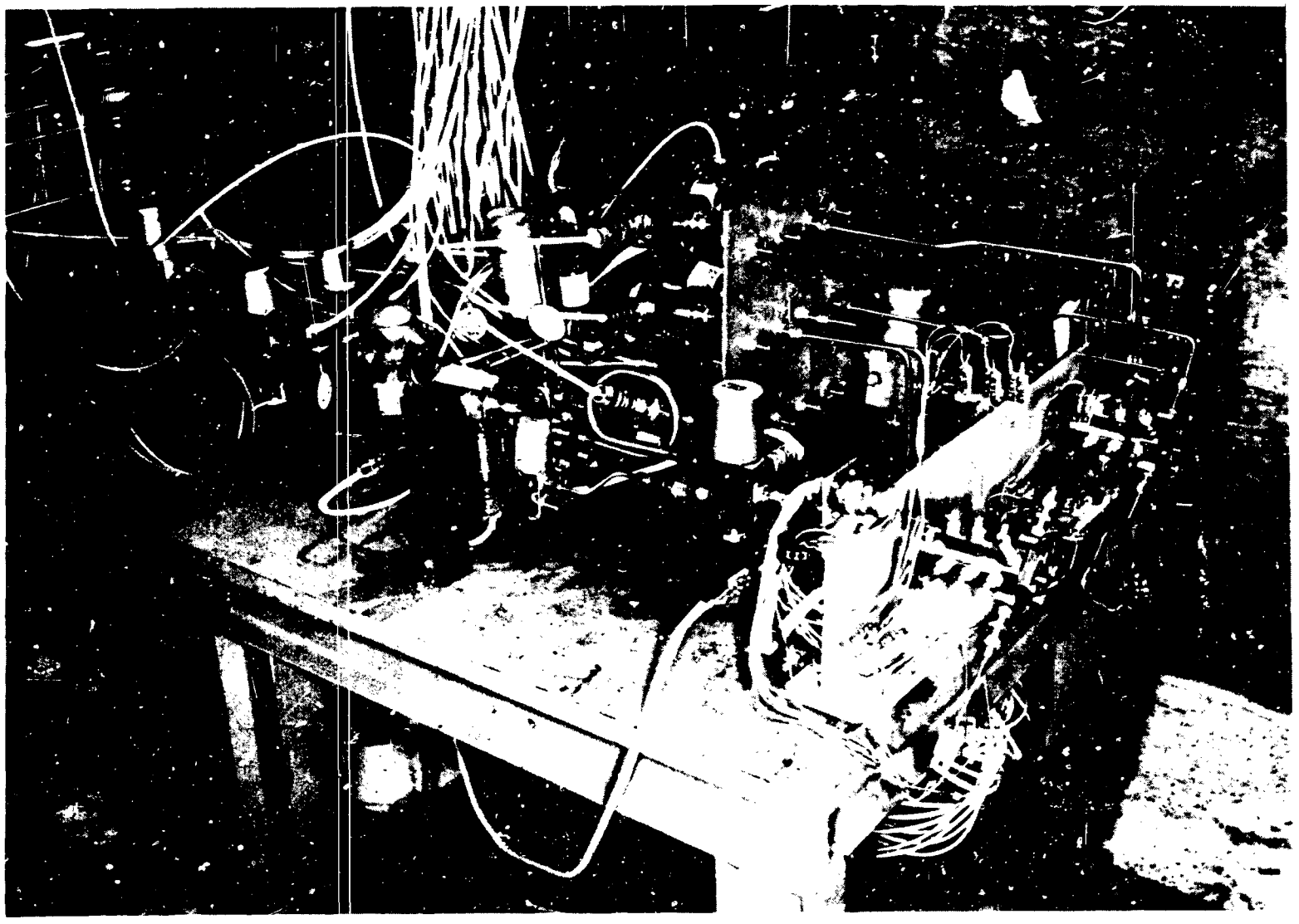

5AA21-6/9/66-S1B

Figure 13. Catalytic Reactor Test Installation

(U) Catalytic Reactors. A schematic drawing of the catalytic reactor is shown in Fig. 14, and the reactor components are shown in Fig. 15. The reactors were of rather heavy construction, having 0.437-inch stainless-steel walls. The entrance and exit flanges were 0.5 and 0.75 inch thick, respectively. The distribution plate, located between the catalyst bed and the injector fitting, consisted of a 0.15-inch-thick disk of Rigimesh. The downstream catalyst retaining screen was a 64-mesh tantalum screen. A 1/4-inch gap was provided between the exit screen and the exit orifice. In this space, the bed exit pressure and temperature were measured, and are referred to as chamber pressure and temperature.

(U) A sleeve liner, with an outside diameter slightly smaller than the inside diameter of the reactor chamber wall, served as a thermal barrier between the catalyst and the chamber wall. Cutting the liner at 1-1/2-inch and 1-inch distances along the length and inserting the downstream retaining screen between the segments was the means of varying bed length. Bed diameter was varied by employing liners of different thicknesses. Eleven thermocouples oriented in a helical pattern had an axial spacing of 1/4 inch along the bed. Holes in the liner at appropriate locations permitted the thermocouples to penetrate into the bed. All 11 thermocouples were located at a 1/4-inch radial distance from the axis of the bed.

(U) Because the reactors were of heavy construction, the chambers themselves provided a relatively large heat sink or heat source, depending upon the circumstances of a particular test. Chilling the bed tended to make the chamber a heat sink while successive tests tended to make it a heat source. As a consequence, the axial temperature pattern was often uneven, and, additionally, the radial temperature distribution was unknown. The heat-source, heat-sink nature of the chambers had a significant effect on test results, as discussed below.

(U) Four interchangeable exit orifices were fabricated. The particular orifice used in a test was dictated by the pressure regulator setting to be used in the particular test and by the desired flowrate range. Two of the orifices were sized to give flowrates of 1000 and 100 sci/sec, respectively, at a chamber pressure of 500 psia, the other two were sized for the same flowrates at a pressure of 40 psia.

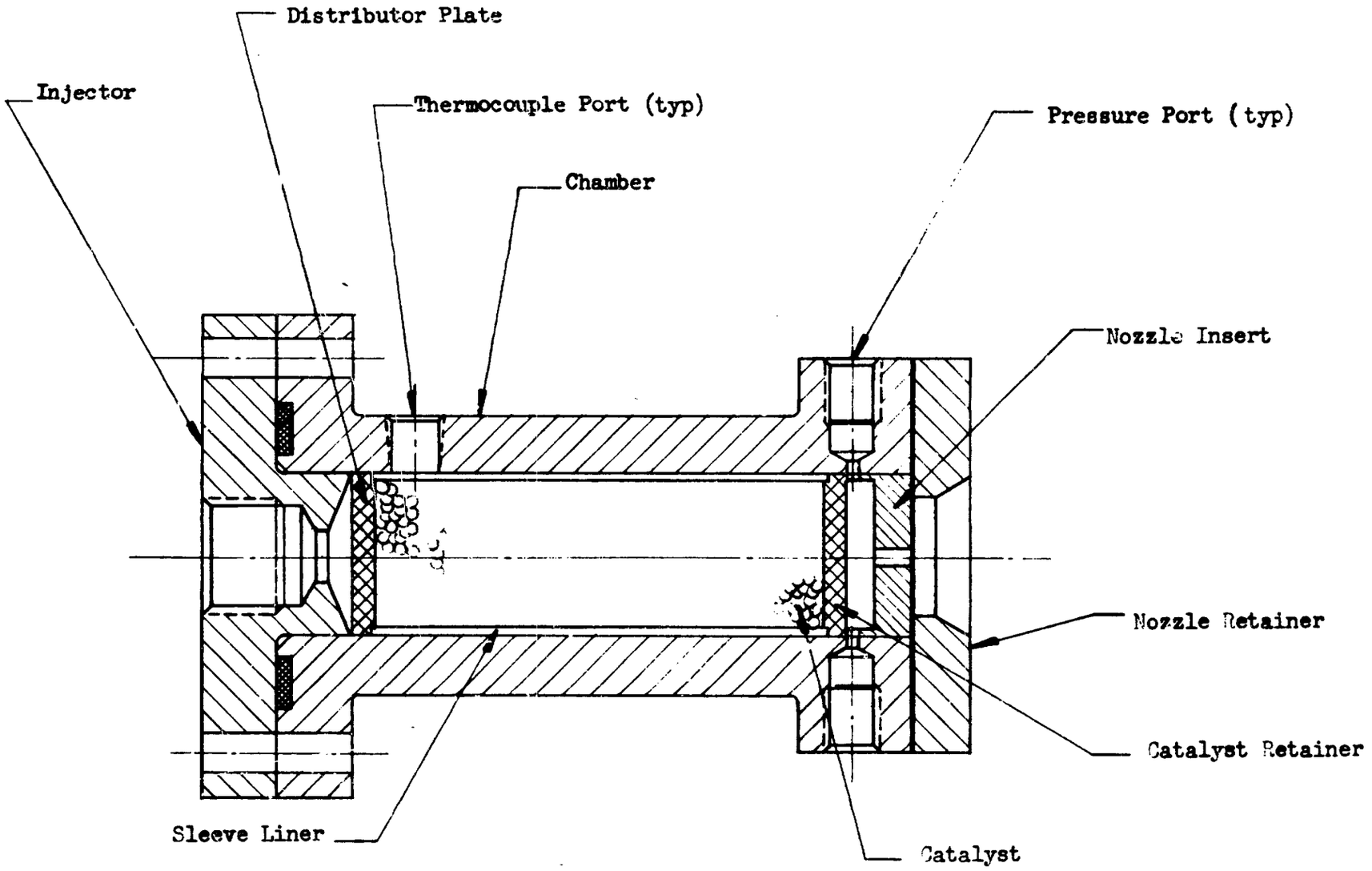

Figure 14. Schematic of the Catalytic Reactor Illustrating Instrumentation Ports and Component Hardware

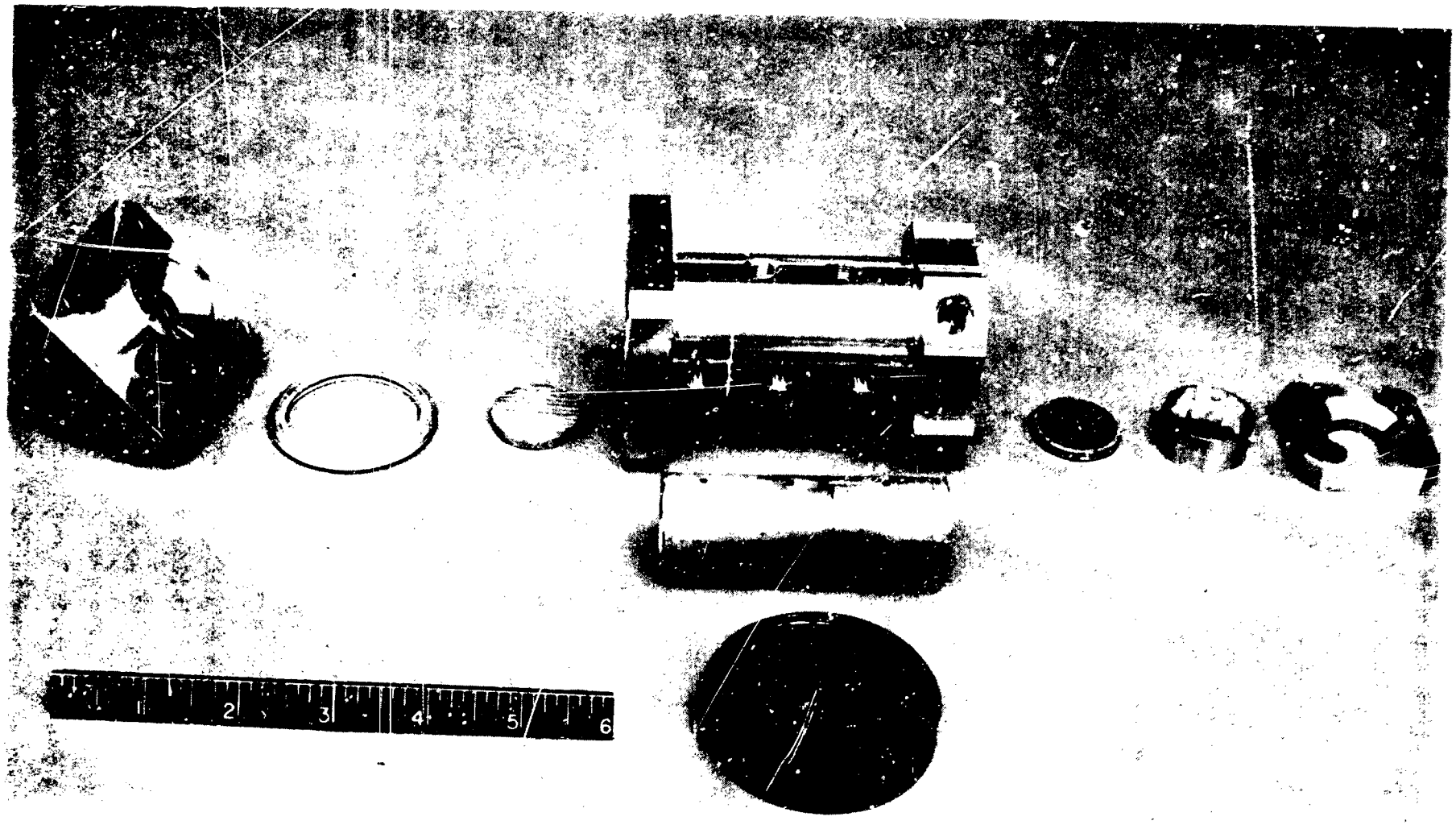

5AA26-9/14/66-S1

Figure 15. Catalytic Reactor Components

(U) Catalyst. The catalyst employed (type MFSA) was supplied by Engelhard Industries, Inc. Two pellet sizes were used: 0.125 and 0.0625 inch. The 3- by 1-inch-diameter beds were charged with 30.7 grams of the 0.125 inch and 32.9 grams of the 0.0625-inch material, respectively. The initial charge of the 0.0625-inch catalyst was employed throughout the entire test program. The 0.125-inch catalyst was replaced with a new charge of 0.0625-inch material at Run No. 80, when bed parameters were being varied. None of the catalyst showed any deterioration from use.

(U) The Engelhard catalysts were selected on the basis of past experience; a number of previous programs had utilized these catalysts (Ref. 2, 3, 4, and 5). A recent study by the Shell Development Corporation, however, has indicated that other catalysts may be superior in related service. A direct experimental comparison is needed if an optimum catalyst is to be used in the future systems.

(U) System Changes Made During the Test Program. During the course of the test program, it became necessary to modify the system to achieve certain objectives and test conditions. The first significant change was the elimination of the orifice meters in favor of the exit orifices as a flow-rate measuring device. The primary reason for making this change was to eliminate the excessive amount of time required to open the flanges and remove and install orifices of the appropriate size for each test. Secondly, the procedure of continually opening and closing the flanges tended to create leaks in a previously tight system, causing further time delays.

(U) A second major modification was necessary to achieve the blend temperature target of -100 and +200 F at the point of injection to the reactors. Originally, it was intended to heat or cool the gas to the desired temperature in the jacketed supply tank and introduce the gas to the reactors through insulated lines. Similarly, it was intended to cool the catalyst bed to -100 F by chilling the purge gas in a dry ice-trichloroethylene bath located upstream of the purge valves. Both proved ineffective. The successful modification that allowed achievement of the target temperatures was the inclusion of the cooling coils as described in the preceding section.

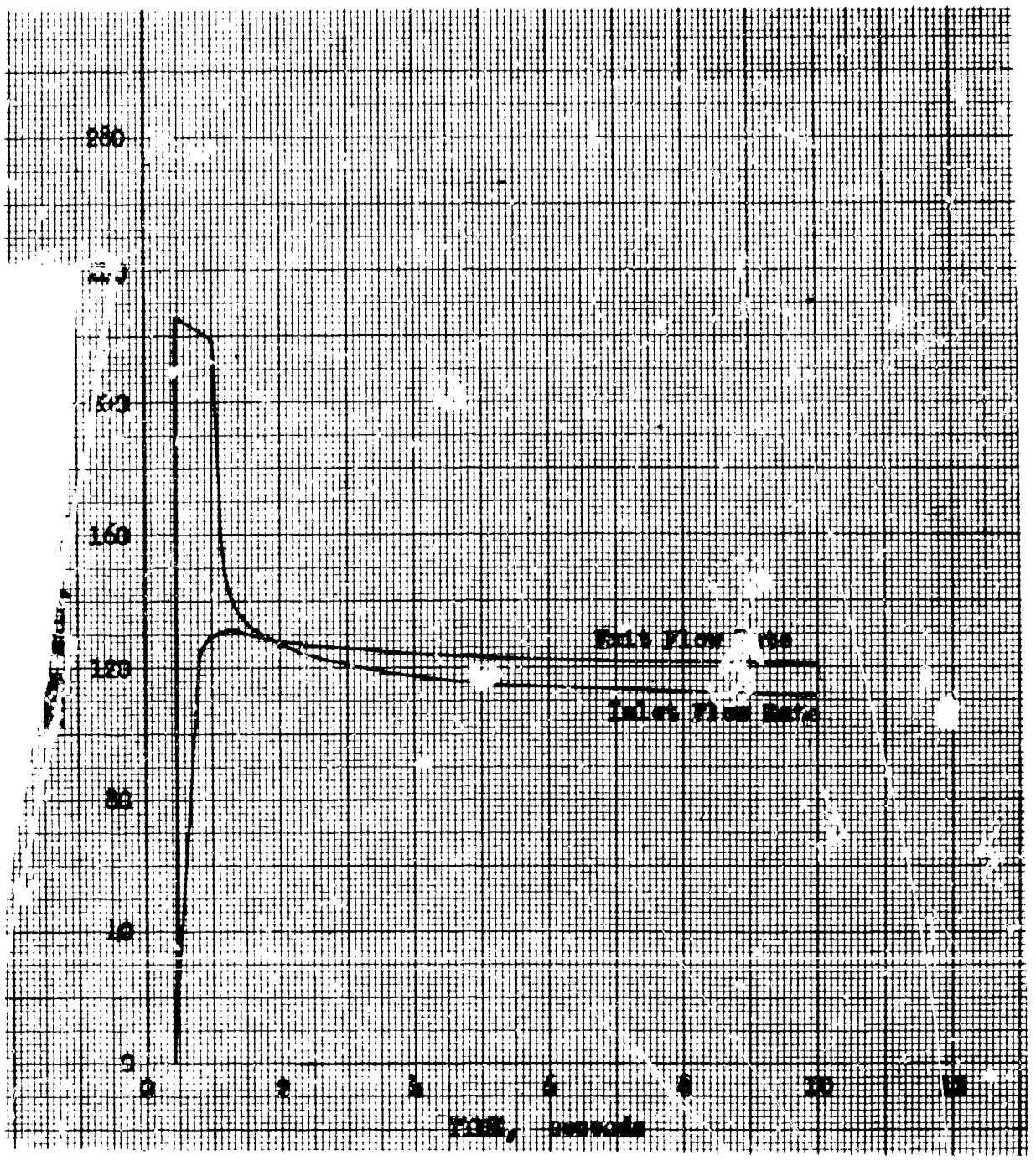

Figure 17. Inlet and Exit Flowrates with Orifices Used for High-Pressure, Low-Flowrate Tests (Run 55B)

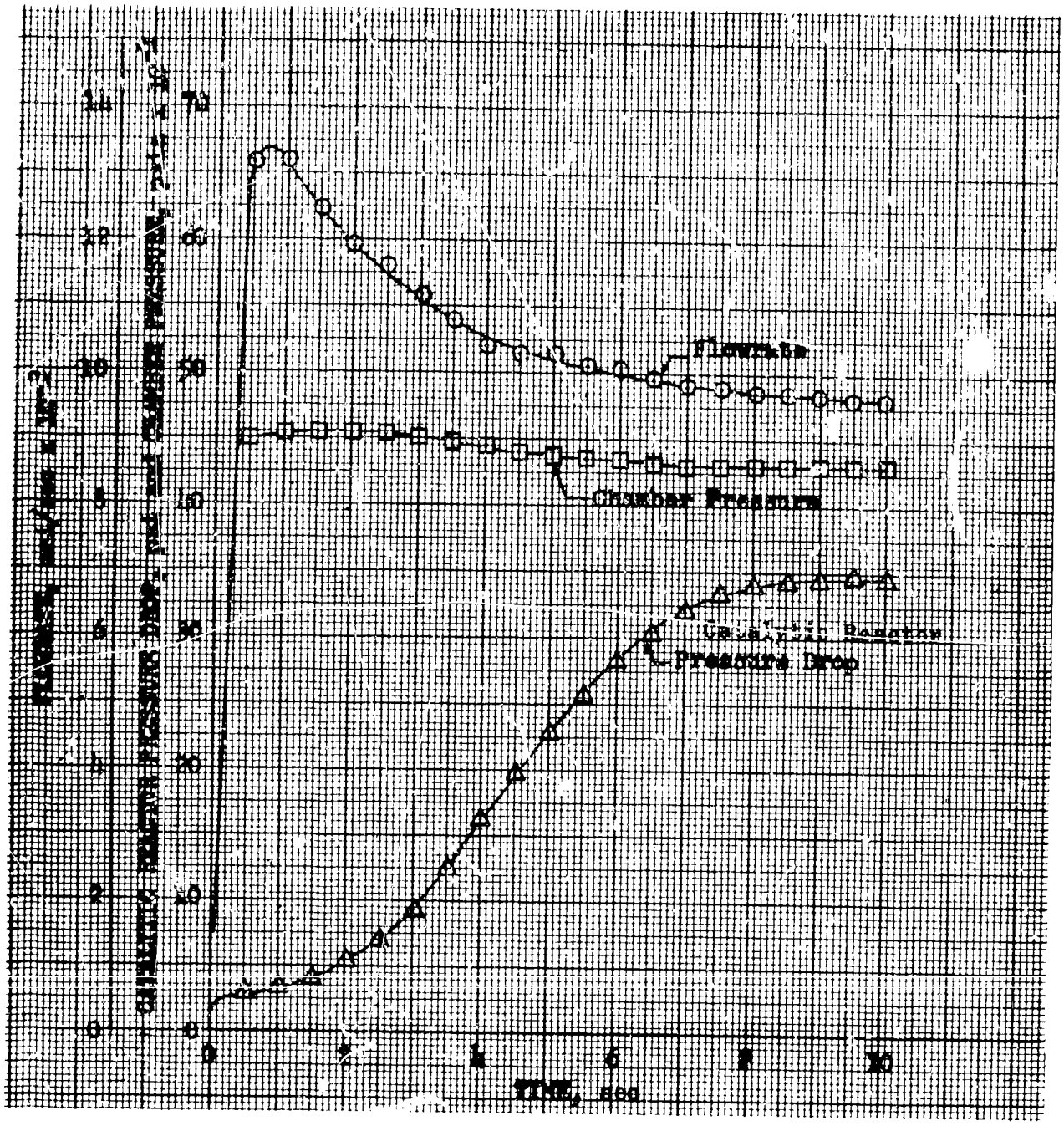

Figure 18. Flowrates, Chamber Pressures, and Catalytic Reactor Pressure-Drop Characteristics for High-Flowrate, High-Pressure, Ambient Mixture Temperature Test (Test 67C

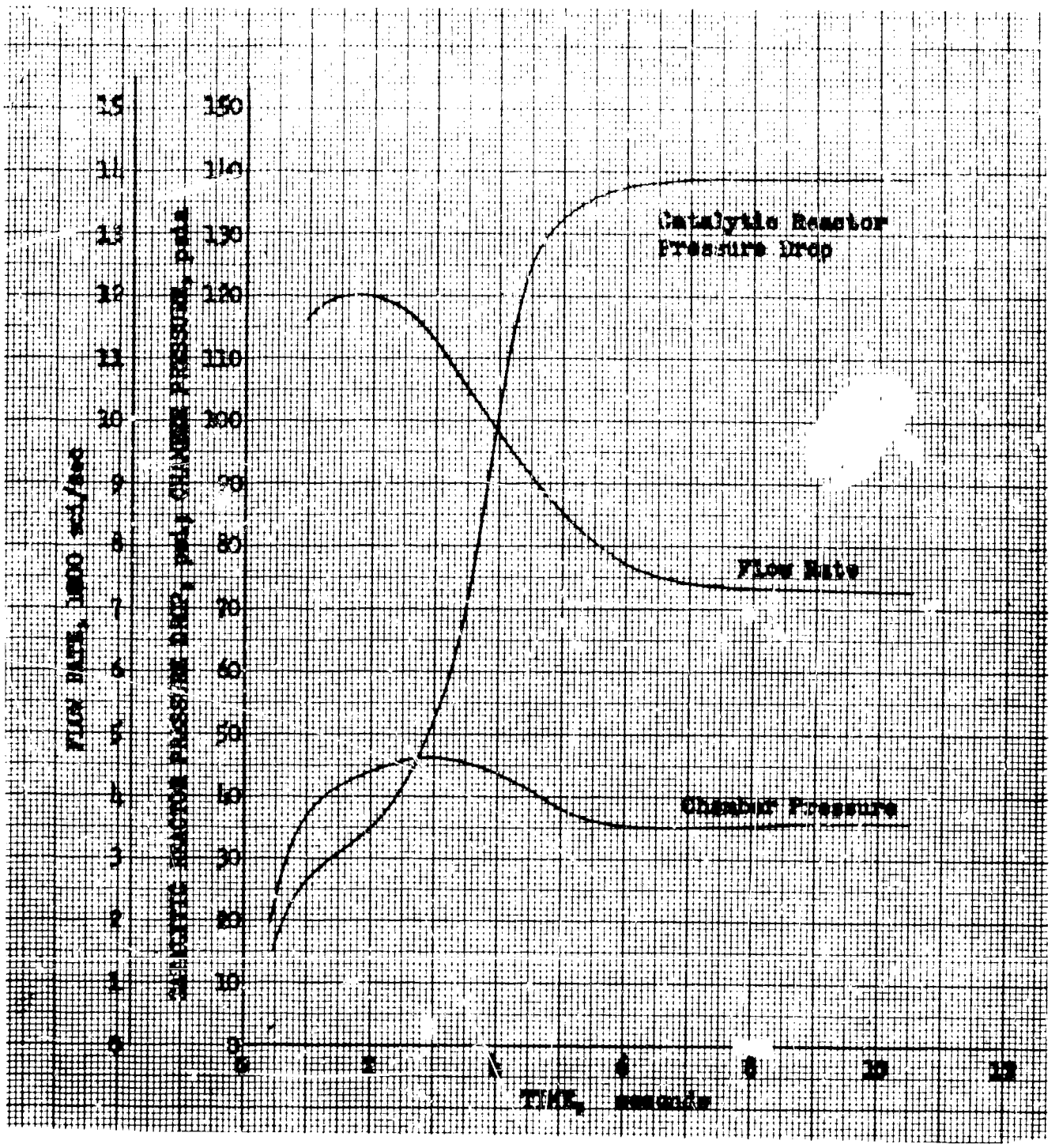

Figure 19. Flowrate, Chamber Pressure, and Catalytic Reactor Pressure-Drop Characteristics for a High-Flowrate, Low-Pressure, Ambient-Blend Temperature Test (Test 70E)

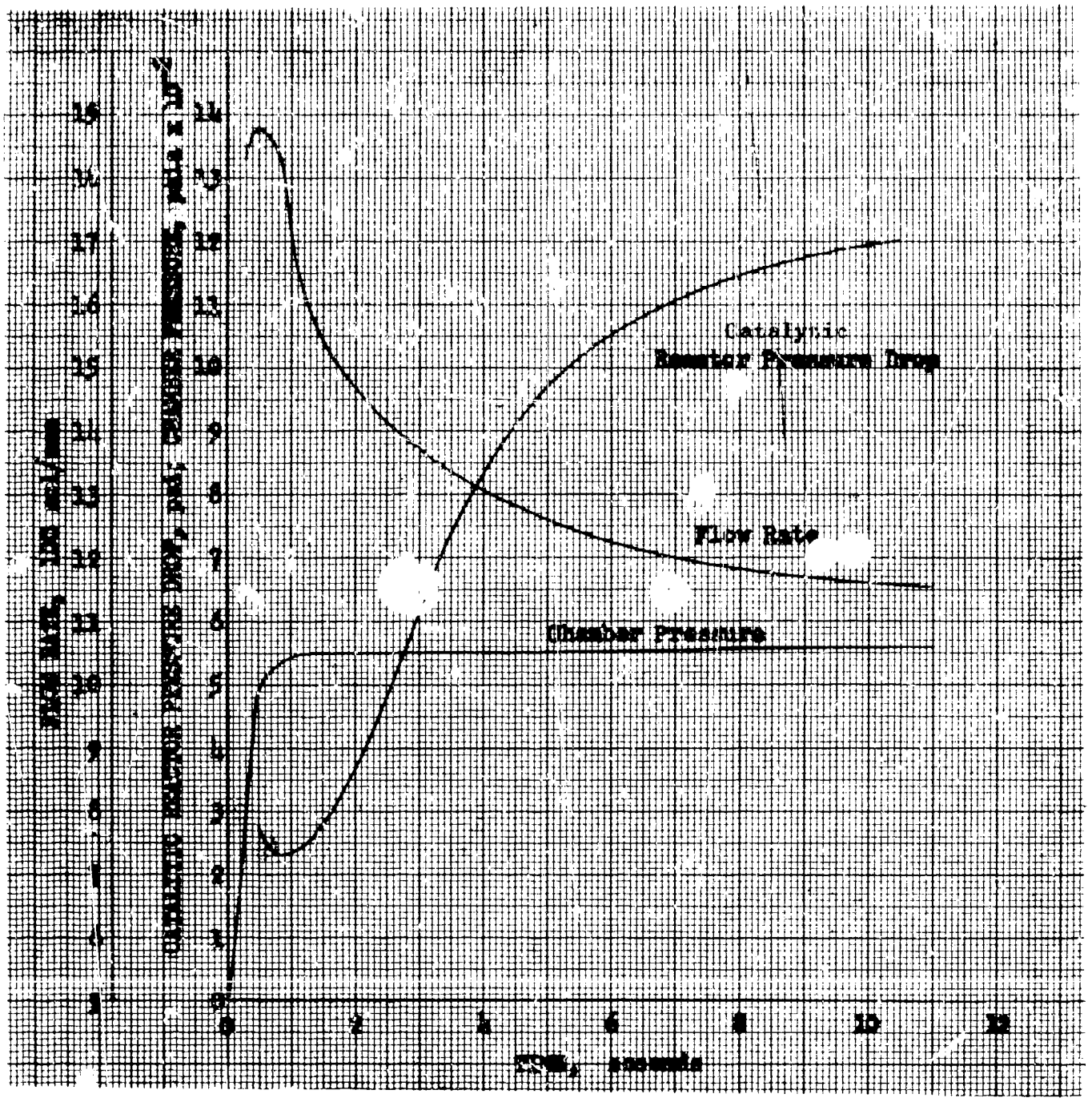

Figure 20. Flowrate, Chamber Pressure, and Catalytic Reactor Pressure-Drop Characteristics for a High-Pressure, High-Flowrate, Cold-Blend Temperature Test (Test 71E)

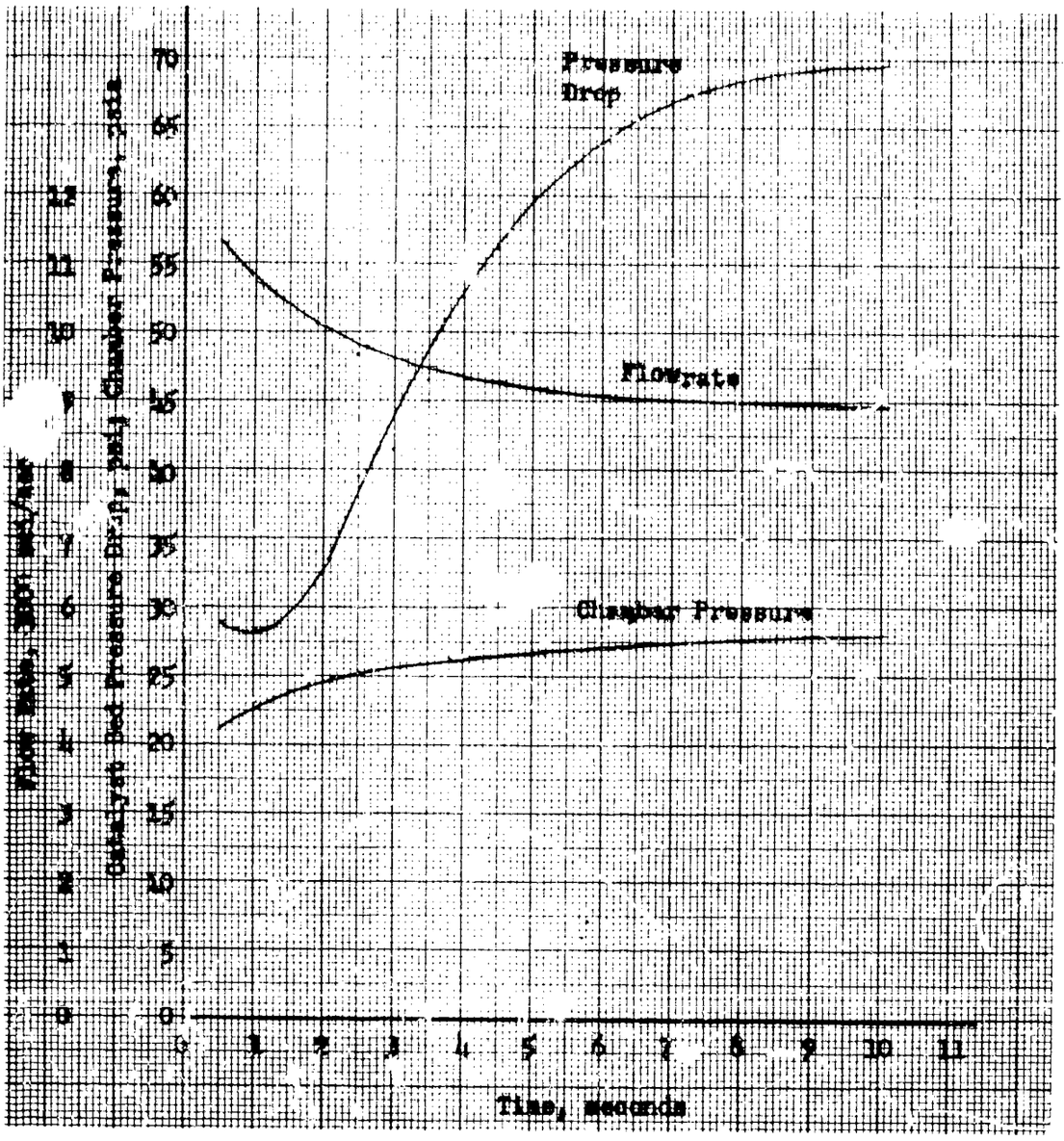

Figure 21. Flowrate, Chamber Pressure, and Catalytic Reactor Pressure-Drop Characteristics for a Low-Pressure, High-Flowrate, Cold-Blend Temperature Test (Test 72A)

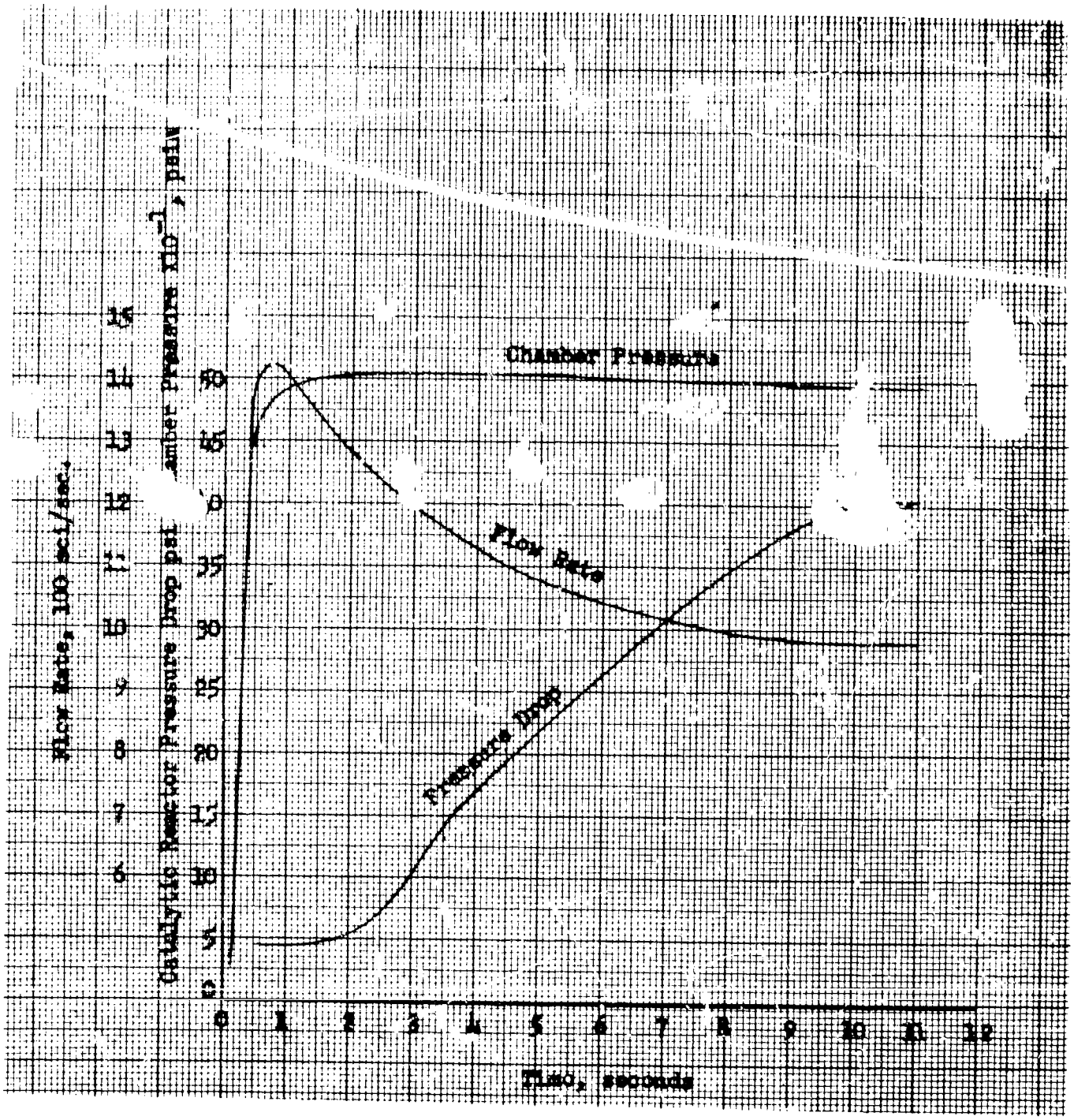

Figure 22. Flowrate, Chamber Pressure, and Catalytic Reactor Pressure-Drop Characteristics for a High-Pressure, High-Flowrate, Hot-Blend Temperature Test (Test 76A)

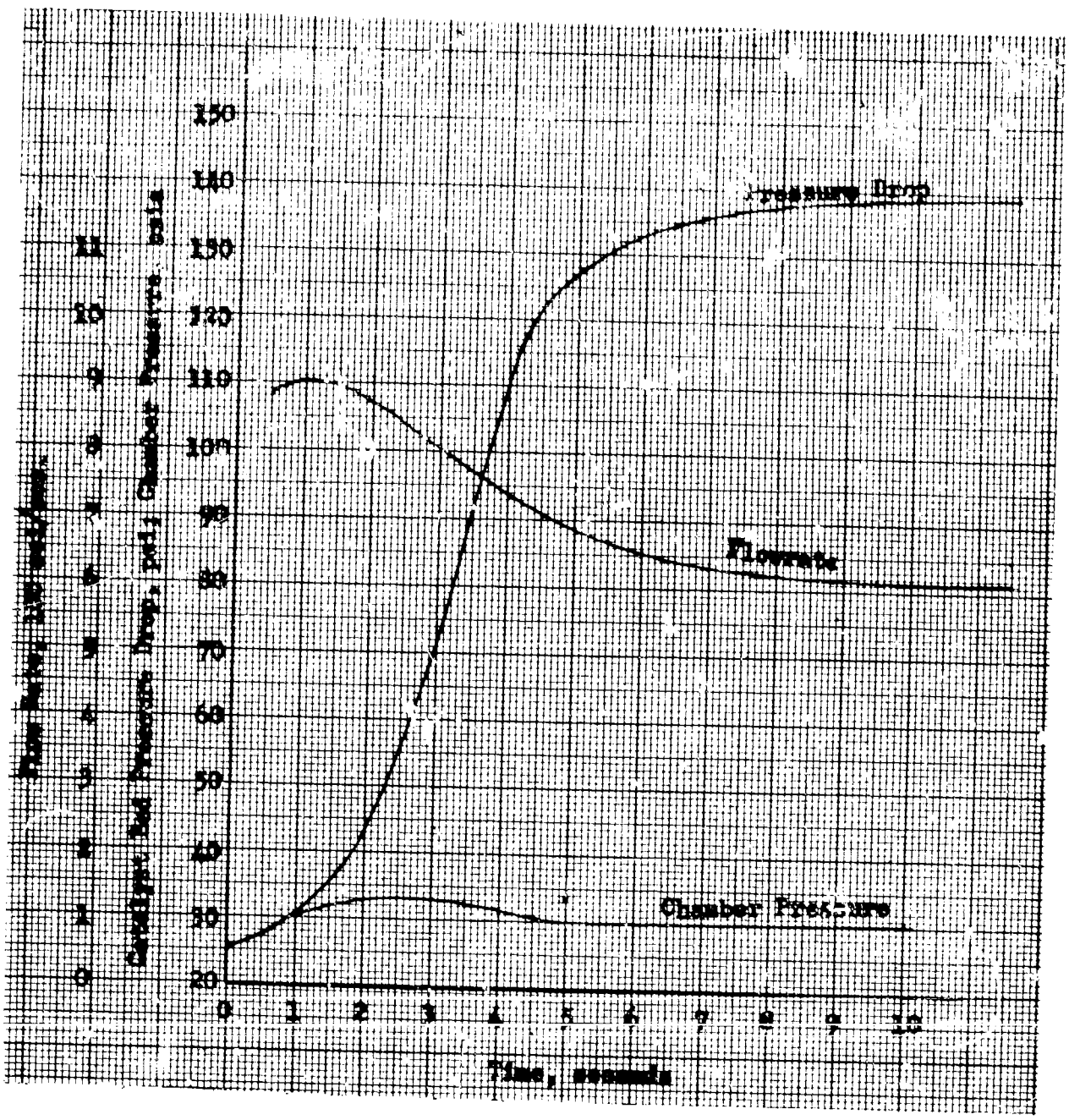

Figure 23. Flowrate, Chamber Pressure, and Catalytic Reactor Pressure Drop Characteristics for Low-Pressure, High-Flowrate, Hot-Blend Temperature Test (Test 77A)

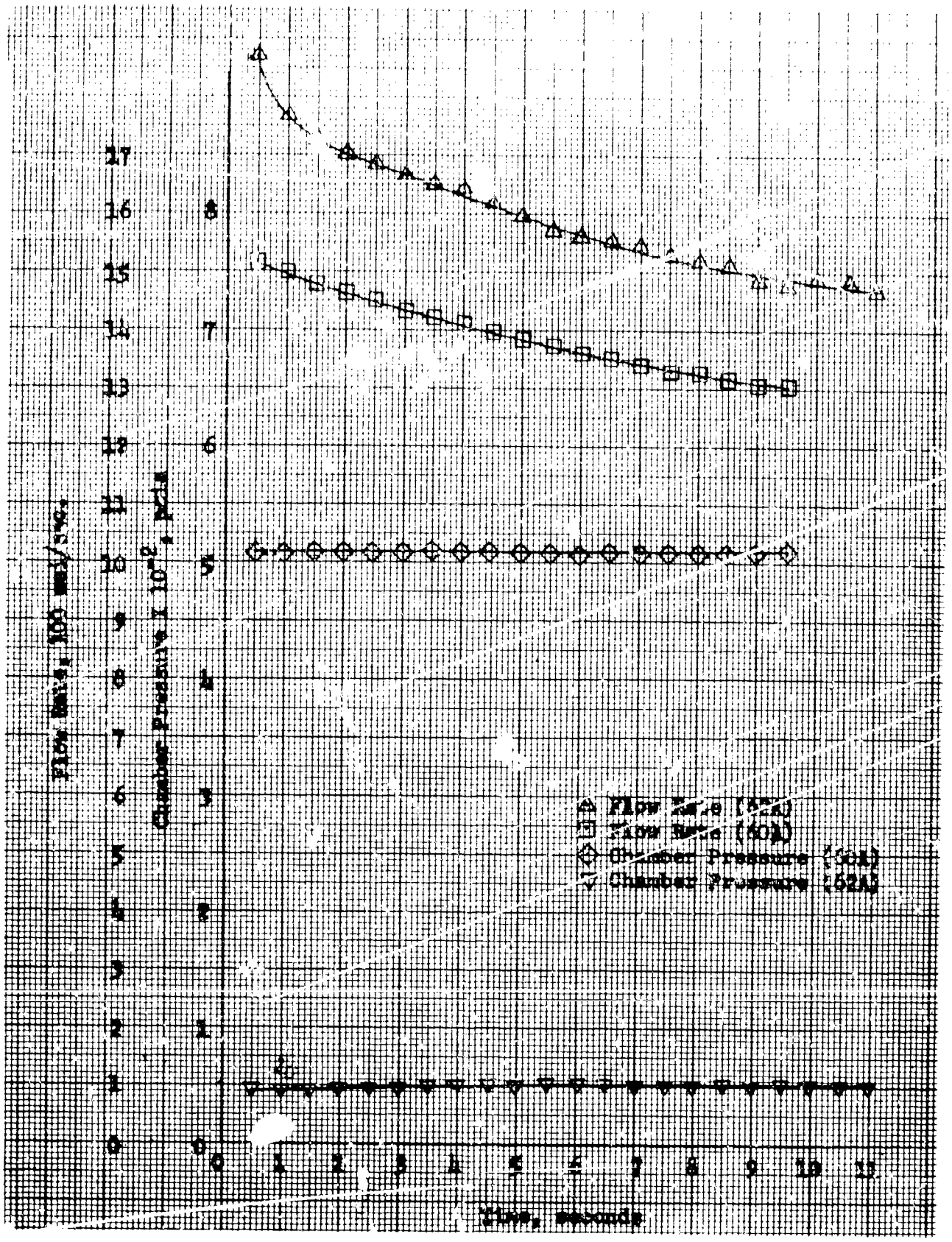

Figure 24. Flowrate and Chamber Pressure for Low-Flowrate Tests 60Z & 62A)

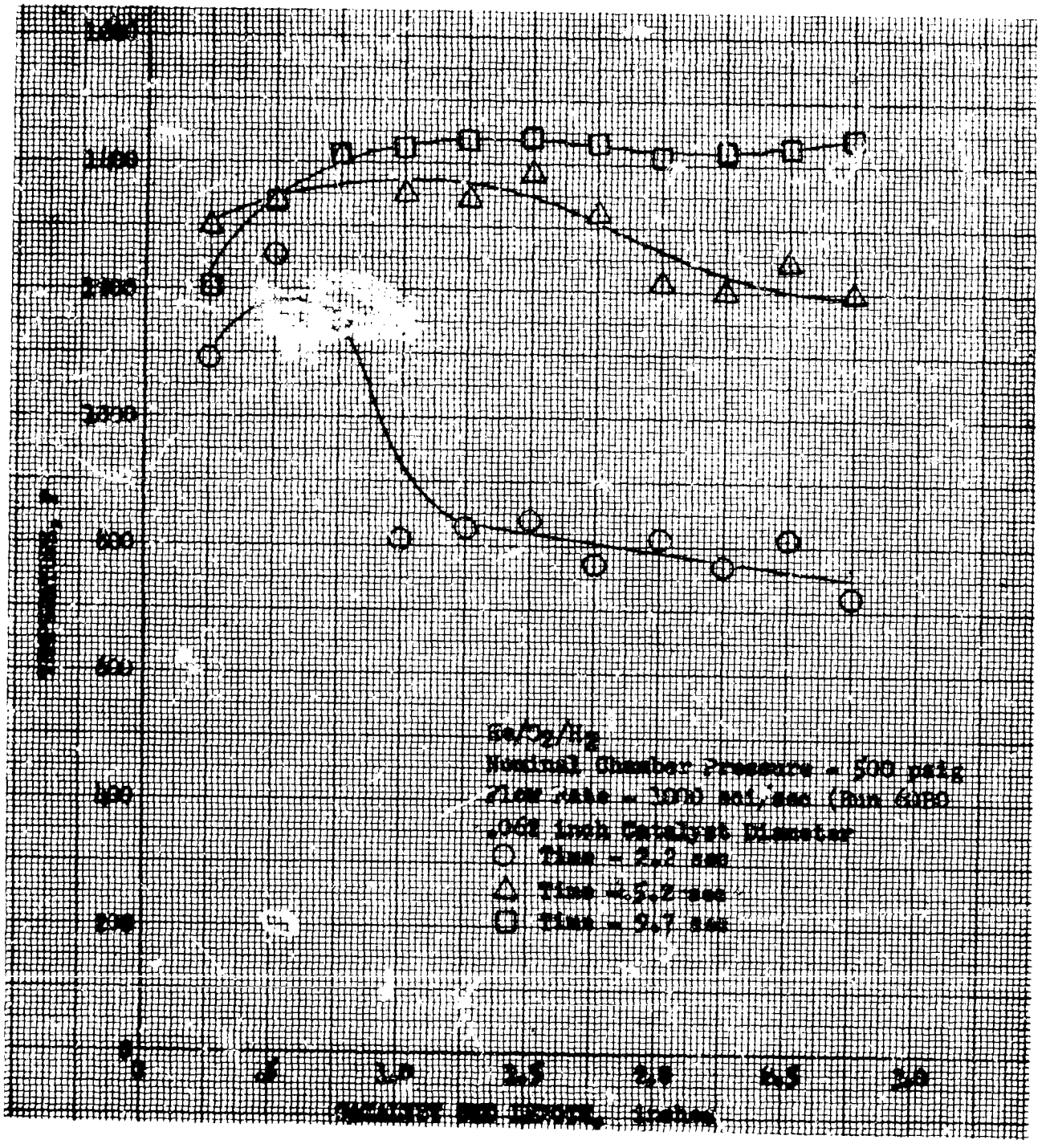

Figure 25. Catalyst Bed Temperature Variation

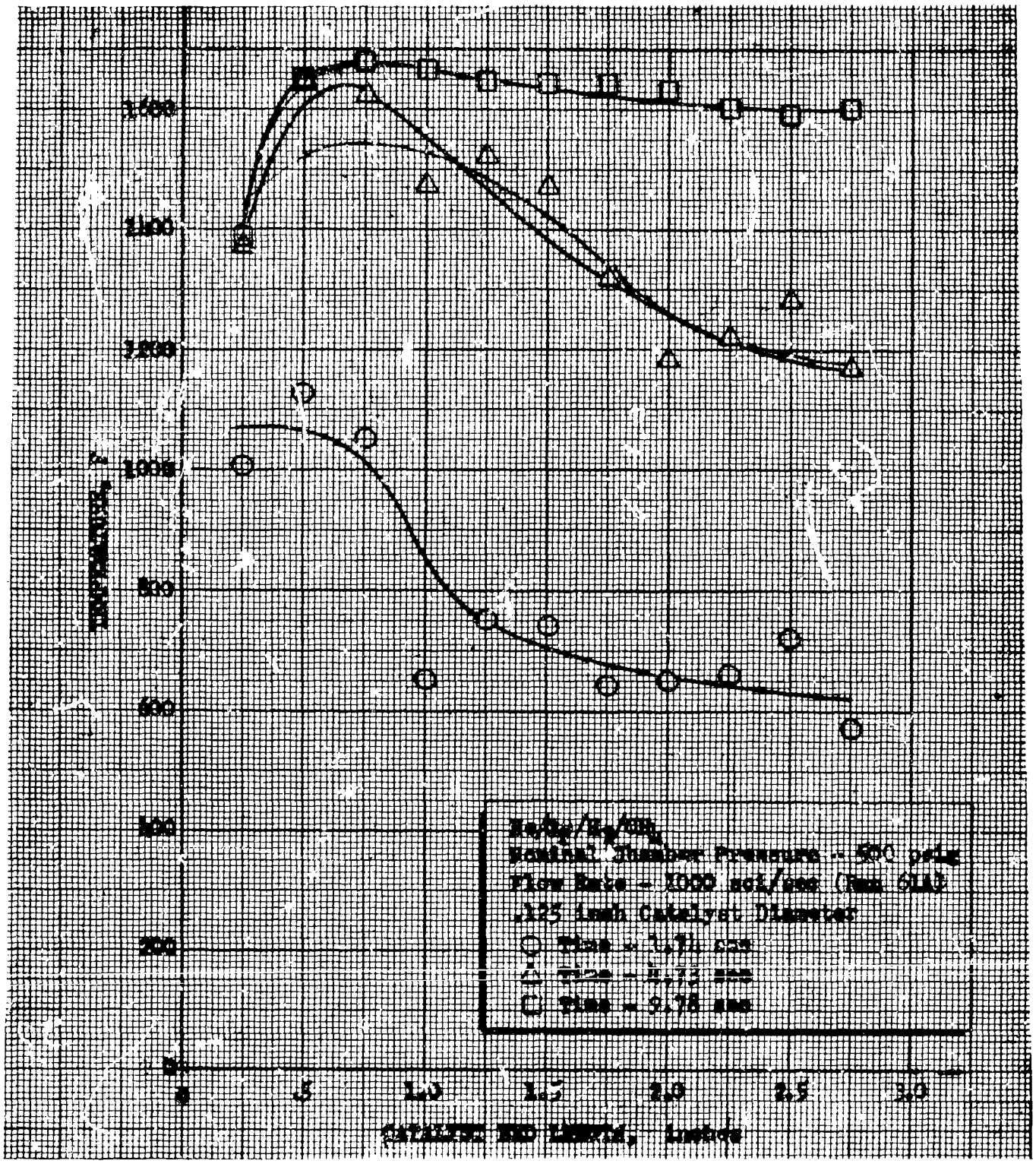

Figure 26. Catalyst Bed Temperature Variation

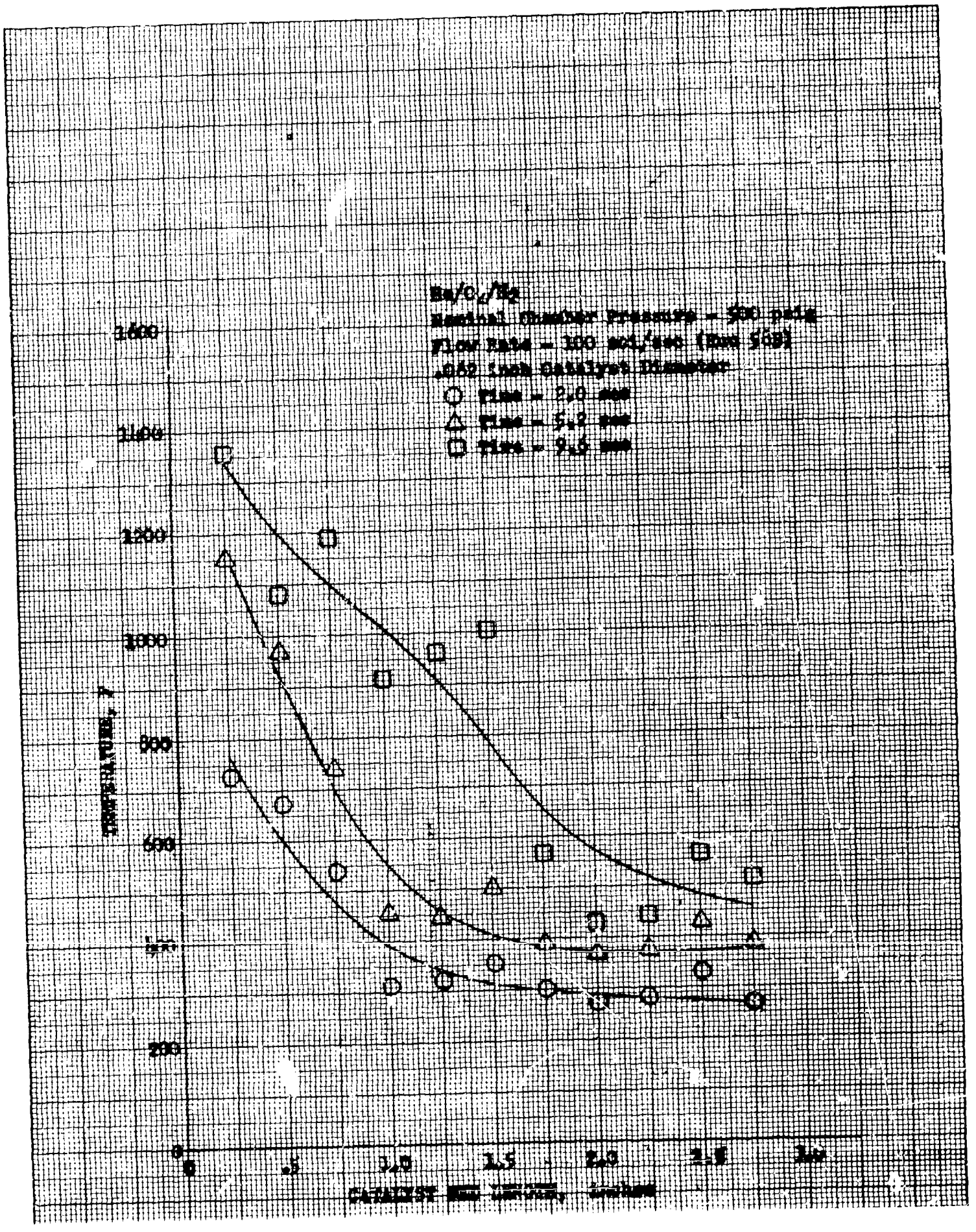

Figure 27. Catalyst Bed Temperature Variation

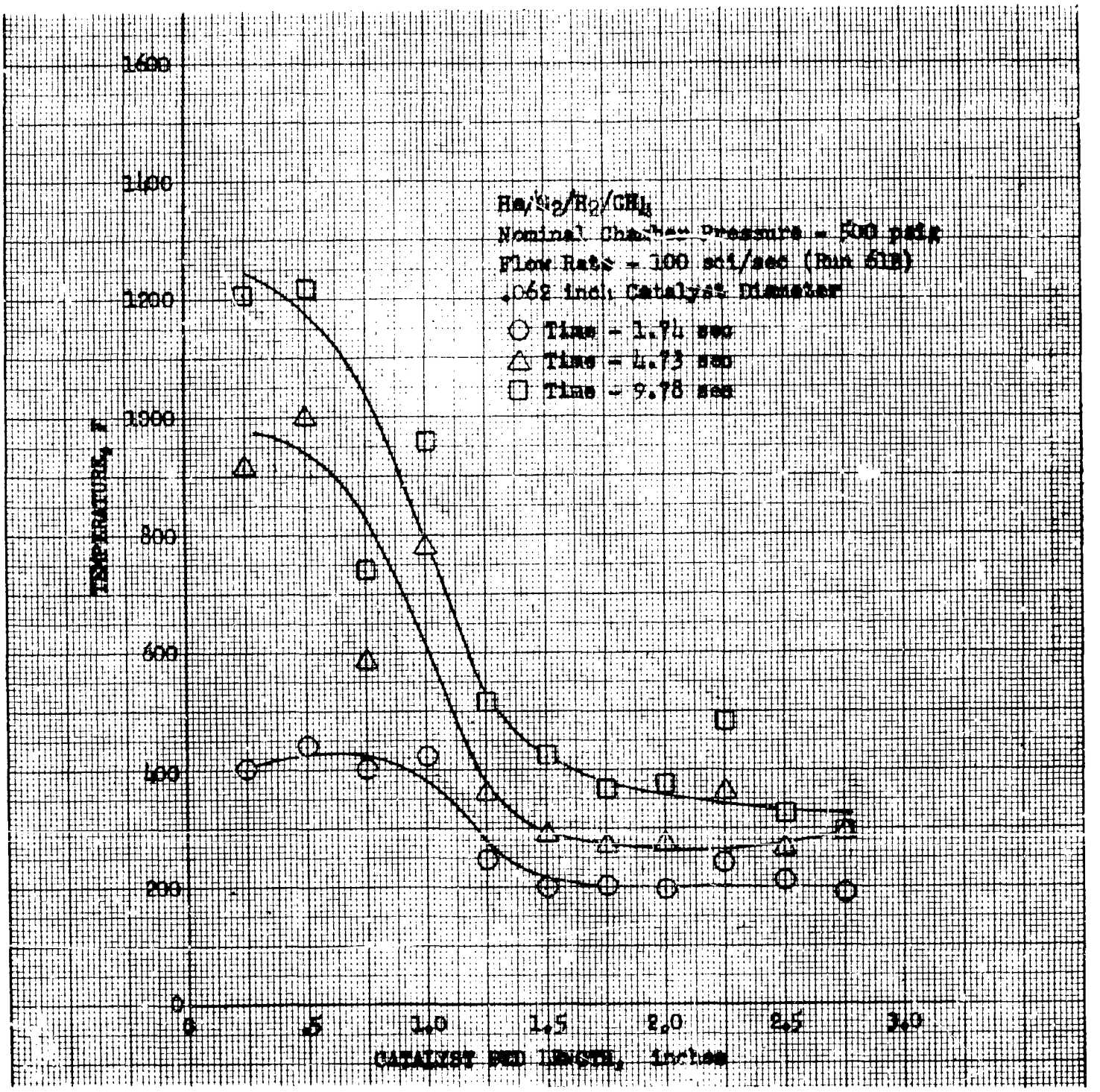

Figure 28. Catalyst Bed Temperature Variation

TABLE 6

MAXIMUM THEORETICAL AND MAXIMUM OBSERVED REACTION TEMPERATURES

Test Series Employing Gas Charge	Mixture	O_2 Partial Pressure, psia	Highest (1) Injection Gas Temperature, F	Theoretical Reaction Temperature, F	Maximum (2) Observed Reaction, F
56, 57	$He/O_2/H_2$	36.0	80	1550	1565
58		34.0	70	1460	1475
60		34.0	70	1460	1463
62		34.4	70	1480	1585
64, 65		34.3	60	1480	1507
67, 68		35.8	80	1540	1586
71, 72		35.8	130	1400	1359
75, 76, 77, 78		33.8	200	1580	1587
80, 81, 82, 83		34.3	110	1530	1500
84			90	1530	1490
85, 86, 87, 88		34.3	90	1530	1457
59	$He/O_2/H_2/CH_4$	43.7	90	1620	1700
61		43.7	90	1620	1700
63		42.8	100	1600	1538
66		42.8	20	1530	1550
69, 70		42.5	47	1530	1548
73, 74		42.8	-115	1400	1389

(1) Highest injection temperature employed with particular gas mixture used

(2) Maximum temperature observed in any test of the series

conversion is occurring across the bed. It is readily apparent that the heat transfer characteristics far override catalytic conversion as a factor in determining capability of delivering maximum reaction temperature gas at the exit of the bed.

(U) Effects of Pellet Diameter. Figure 29 shows data comparing the performance of 0.125- and 0.062-inch catalyst pellets with $He/O_2/H_2$. The high-flowrate data indicate equal temperature response characteristics. The low-flowrate curves have similar shapes with the 0.062-inch pellets yielding slightly higher temperatures during the start transient.

(U) Figure 30 presents similar data for $He/O_2/H_2/CH_4$. Again, little difference in response time is noted for the high-flowrate cases. The flowrate curves indicate a slightly better temperature response for the 0.062-inch pellets than that of the 0.125-inch pellets, although the latter had a higher initial temperature. The reactor pressure-drop data show little difference for the two catalyst sizes. This is surprising, since pellet size was expected to have a significant effect. The pressure-drop data are discussed in more detail in another section of this report.

(U) Effect of Bed Geometry. The effects of bed geometry are shown in Fig. 31 and 32. Because of the unexpected low temperatures obtained during run 85B, an investigation of the hardware was made and revealed a possible leak around the periphery of the bed liner. Subsequent calculations indicate as much as 40 percent of the total flow could have bypassed the bed. Figure 31, for high-flowrate conditions, shows that all of the 1-inch-diameter beds have approximately the same response at this station in the bed, indicating that no performance loss would be anticipated as a result of bed shortening. However, the results of low-flowrate tests (Fig. 32) indicate that the largest-volume bed has the best response. The latter results can be explained as a result of heat losses. Under low-flowrate conditions, delayed response would be expected since an increased portion of heat input (heat of reaction) is lost to the chamber walls and Rigimesh injector. Heat loss is accentuated for smaller beds,

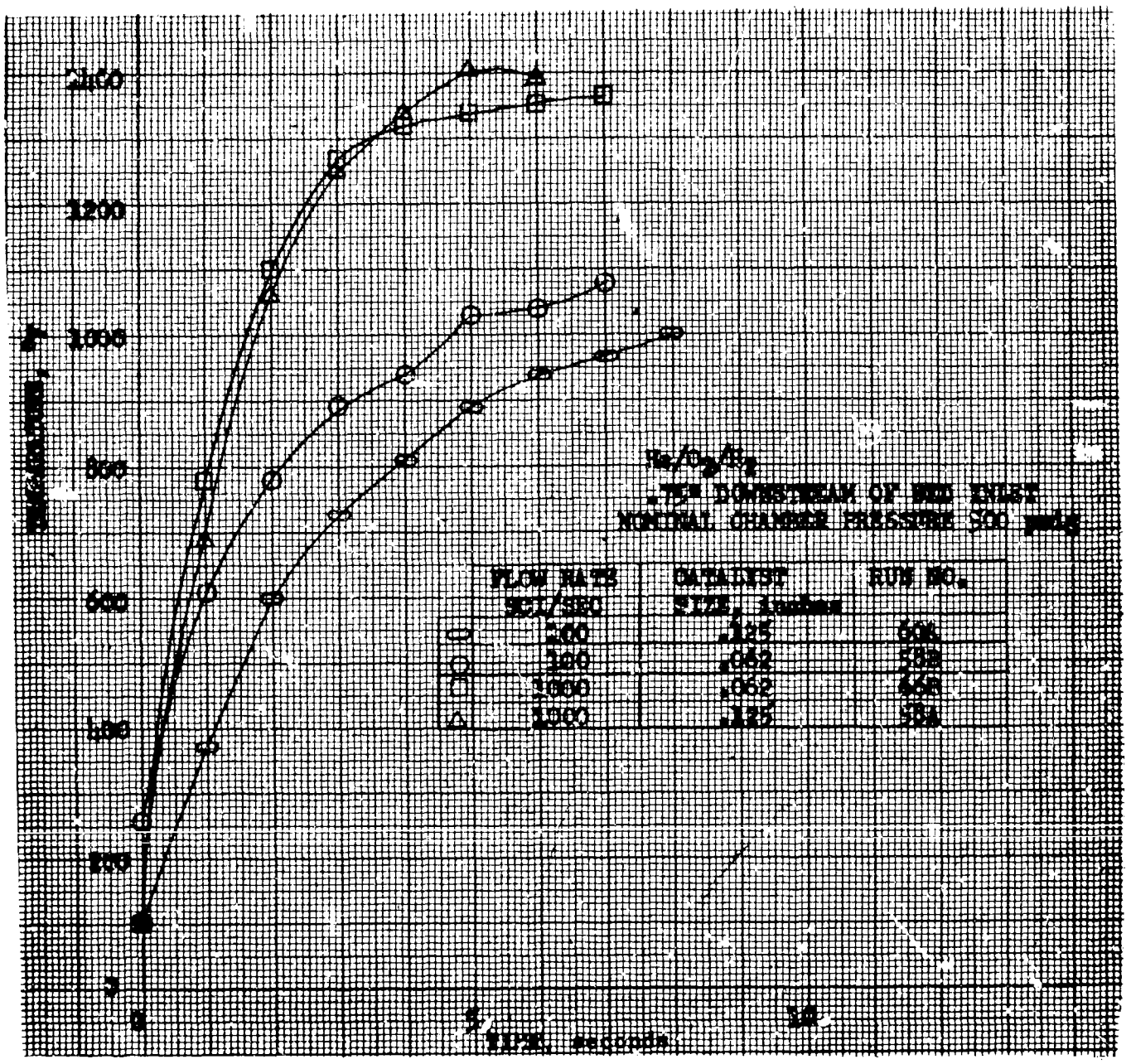

Figure 29. Effects of Catalyst Pellet Diameter on Temperature Response Time

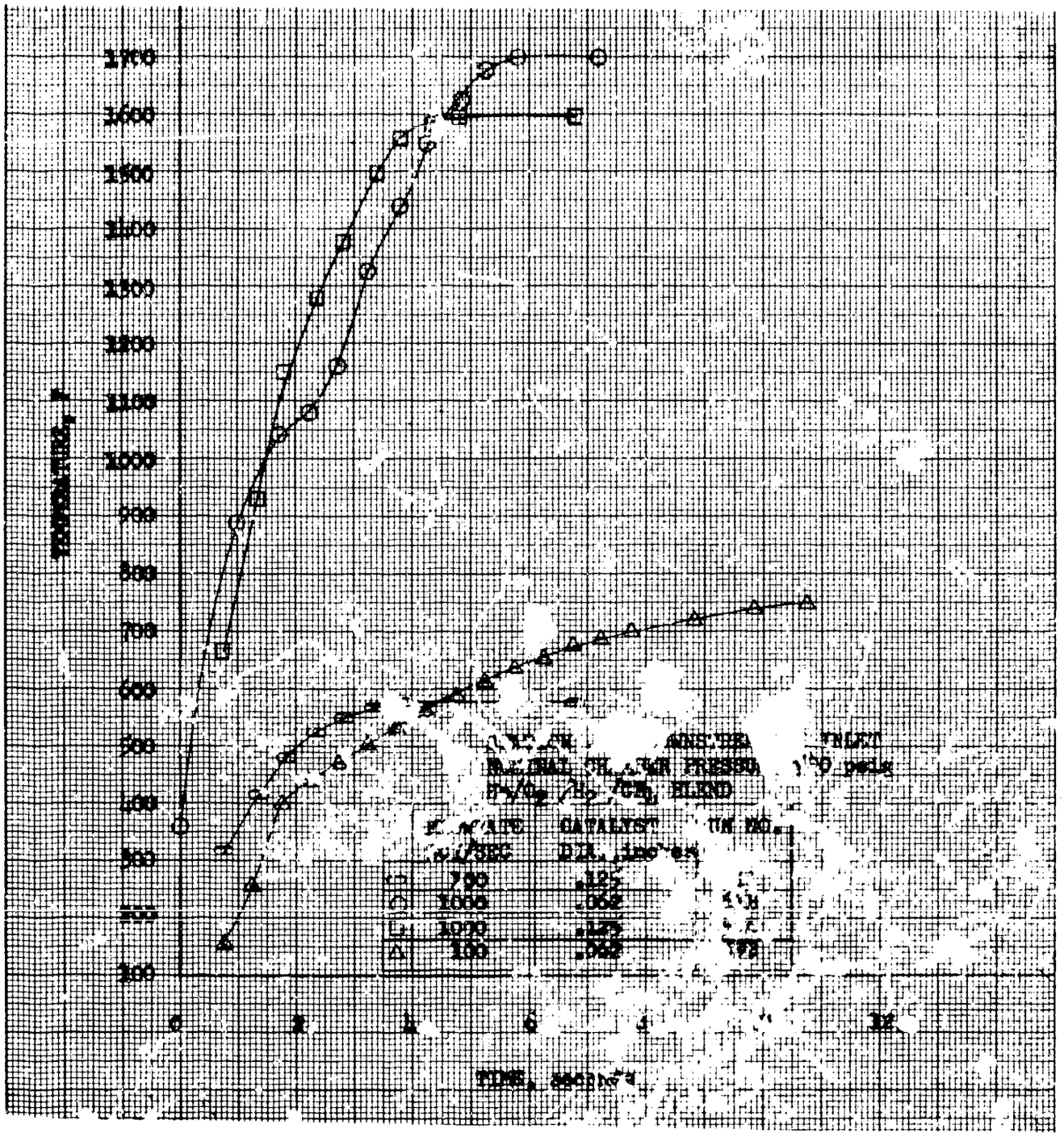

Figure 30. Effects of Catalyst Pellet Diame[illegible] on Te[illegible]perature [illegible]esponse Time

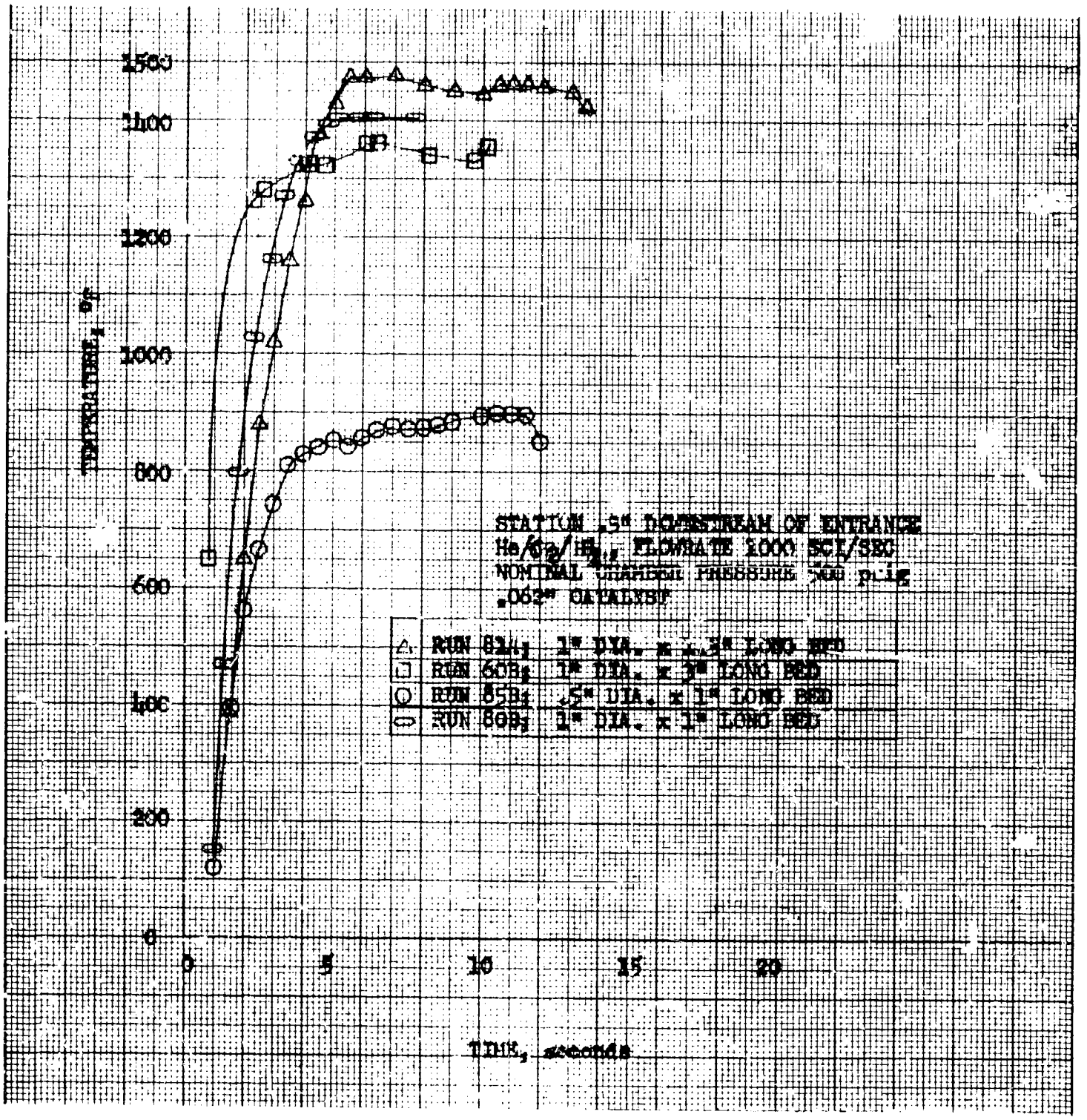

Figure 31. Effects of Bed Geometry on Temperature Response Time

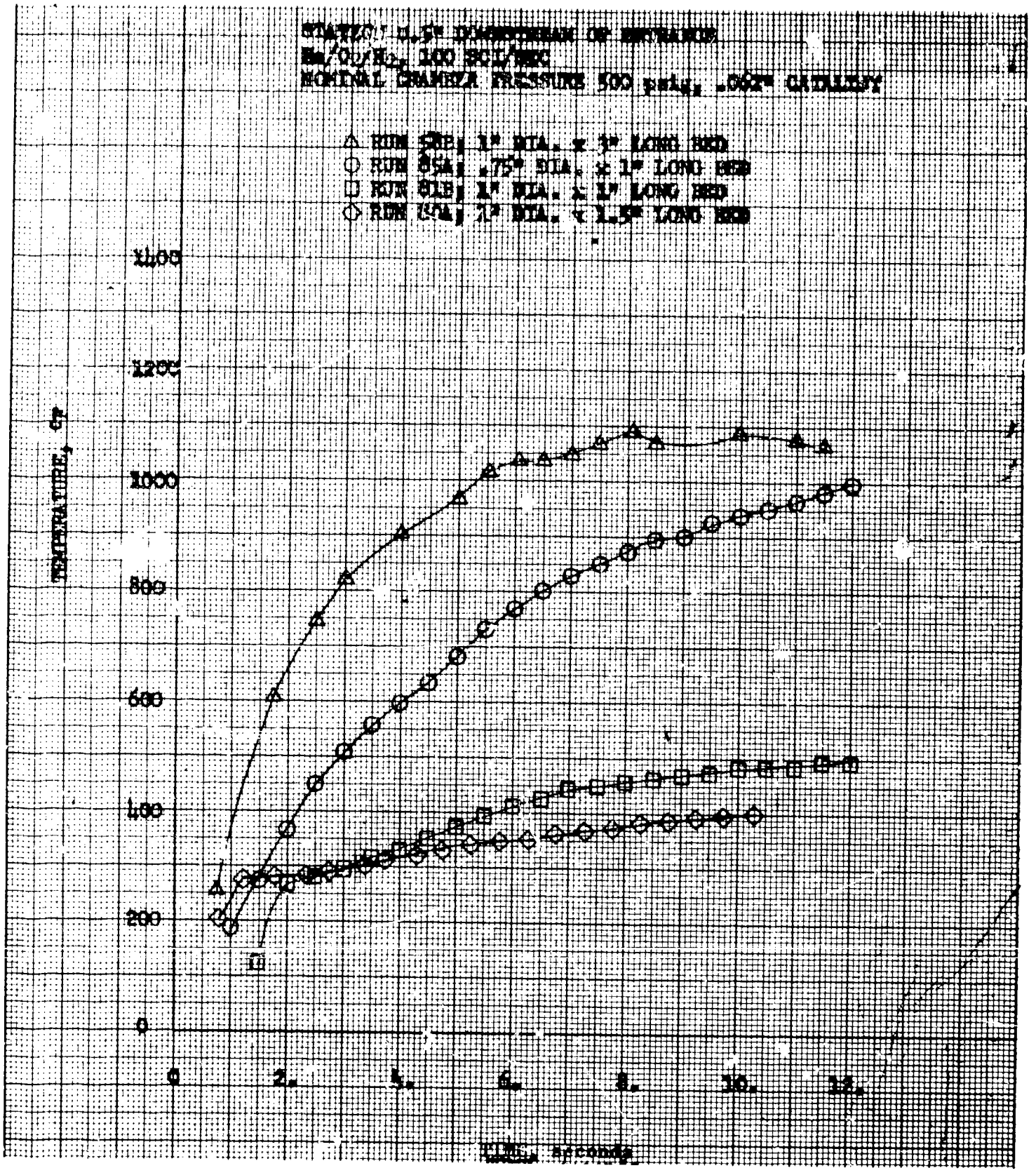

Figure 32. Effect of Bed Geometry on Bed Response Time

since the ratio of external bed area to bed volume is increased. Furthermore suppressed temperatures (particularly when less than 500 F) suppress the reaction rate, which lowers the heat input rate. The geometry variation tests are listed in Table 7.

(U) Effect of Initial Bed Temperature. Many experiments were conducted with initial bed temperatures ranging from -100 to 1500 F. High initial catalyst bed temperatures were obtained by restarting the flow a few seconds after initial-flow shutdown. Typical temperature traces for these experiments are shown in Fig. 33. Start and cessation of gas flow are also shown, and were obtained from the inlet pressure traces. Virtually instantaneous and complete reaction occurs at the elevated bed temperatures.

(U) Figures 34 and 35 show the effect of initial catalyst bed temperature on subsequent bed temperatures for both the $He/O_2/H_2/CH_4$ and $He/O_2/H_2$ blends having an inlet gas temperature of -100 F. Comparisons of the different bed conditions shown in Fig. 34 indicate that a greater bed length is required to achieve a given degree of reaction as the bed temperature is decreased. Figure 35 shows that the required bed length needed for complete combustion also varies with initial bed temperature for the $He/O_2/H_2$ blend.

(U) Figure 36 shows temperature traces for two stations with both ambient and low initial catalyst bed temperatures. The temperature response rate resulting from the high initial temperatures is much greater than the low-bed temperature cases, as would be anticipated.

(U) Cryogenic Temperature Tests. The study of low initial catalyst bed temperatures was extended to -290 F by chilling with purge gas cooled with liquid nitrogen. With the injection temperature of the gas at 60 F, response was quite good as shown in Fig. 37. These data are for the 0.75-inch bed station. The rate of temperature rise is approximately the same as for catalyst initially at ambient temperature. Comparing with other data, the low bed temperature acts to delay the time of

TABLE 7

SUMMARY OF REACTOR BED TEST WITH VARIOUS BED GEOMETRIES

Run No.	Injection Pressure, psia	Flow-rate	Bed Diam ter, inches	Bed Length, inches
80A	520	Low	1	1.5
80B	560	High	1	1
81A	510	High	1	1.5
81B	530	Low	1	1
82A	95	High	1	1.5
82B	90	Low	1	1
83A	85	Low	1	1.5
83B	125	High	1	1
84*	95	Low	1	1.5
85A	550	Low	0.75	1
85B	540	High	0.50	1
85C	550	Low	0.75	1
85D	540	High	0.50	1
86A	530	High	0.75	1
86B	640	Low	0.50	1
87A	70	High	0.75	1
87B	60	Low	0.50	1
88A	60	Low	0.75	1
88B	115	High	0.50	1
89A*	700	Low	0.75	1

All tests were conducted with an $He/O_2/H_2$ blend, 0.062-inch-diameter catalyst pellets, and ambient-gas inlet temperature.

* Long-duration tests: Test 84, in excess of 800 seconds; Test 89, in excess of 500 seconds

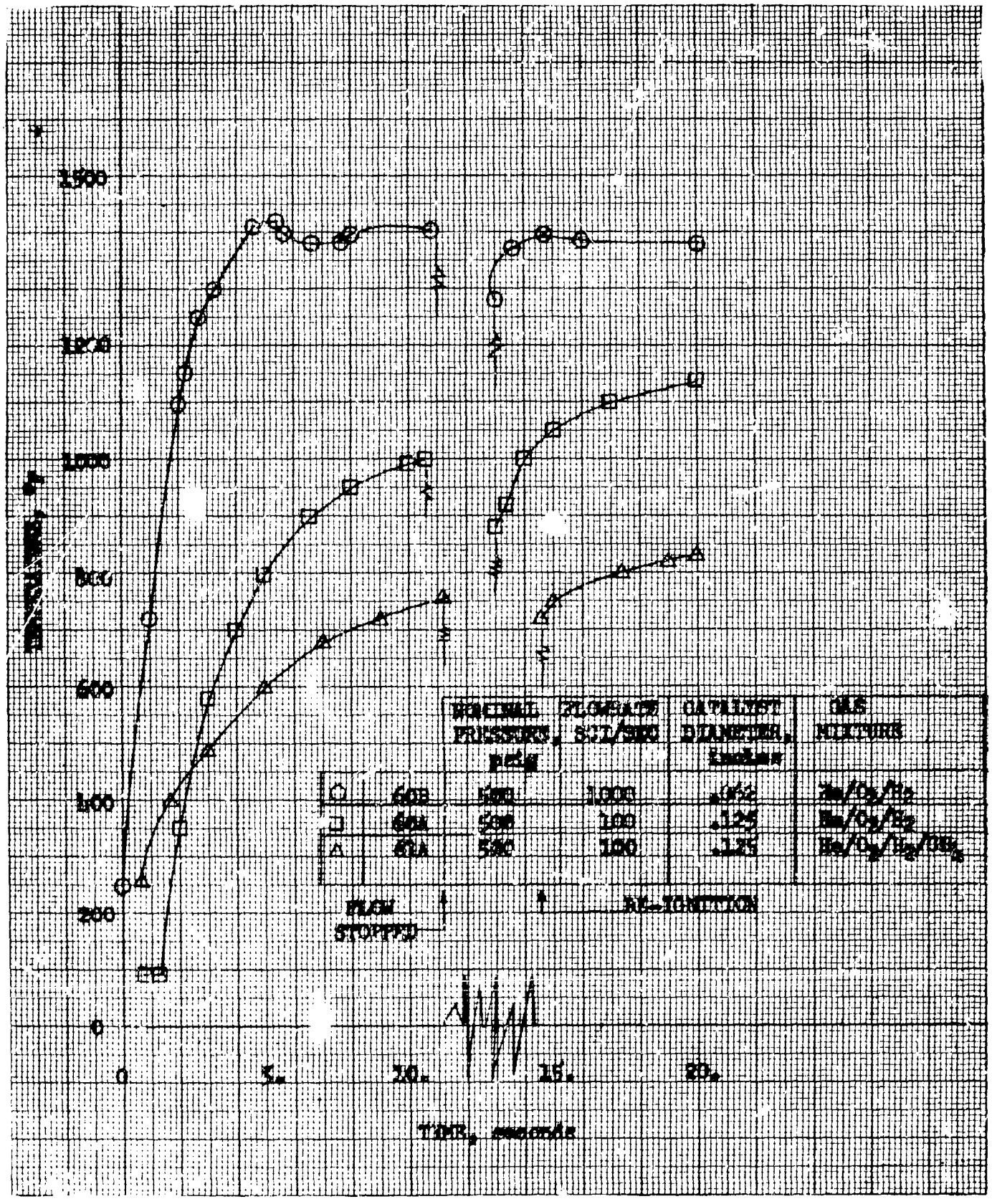

Figure 33. Re-Ignition Characteristics

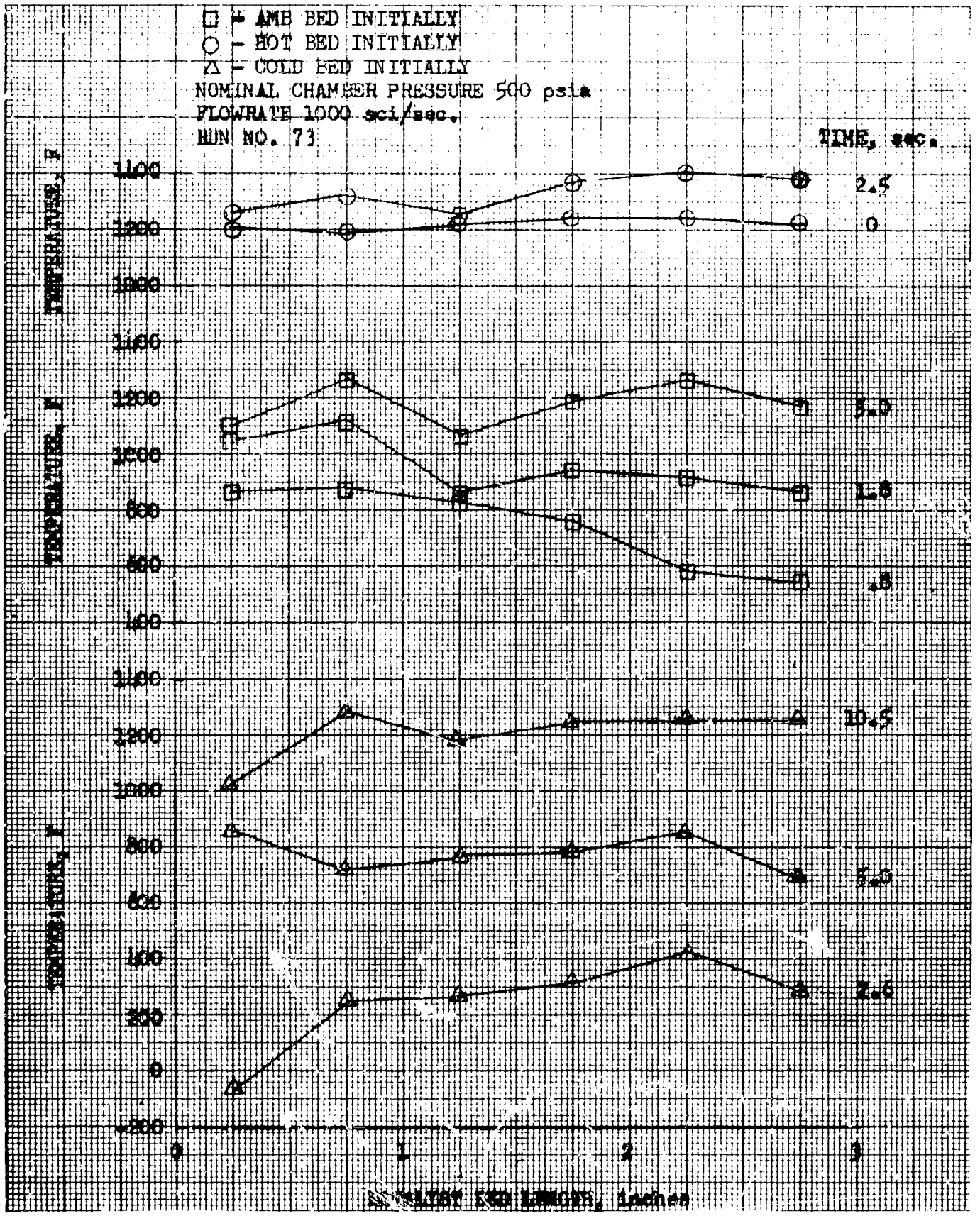

Figure 34. Effects of Initial Bed Temperature on $He/O_2/H_2/CH_4$ Combustion

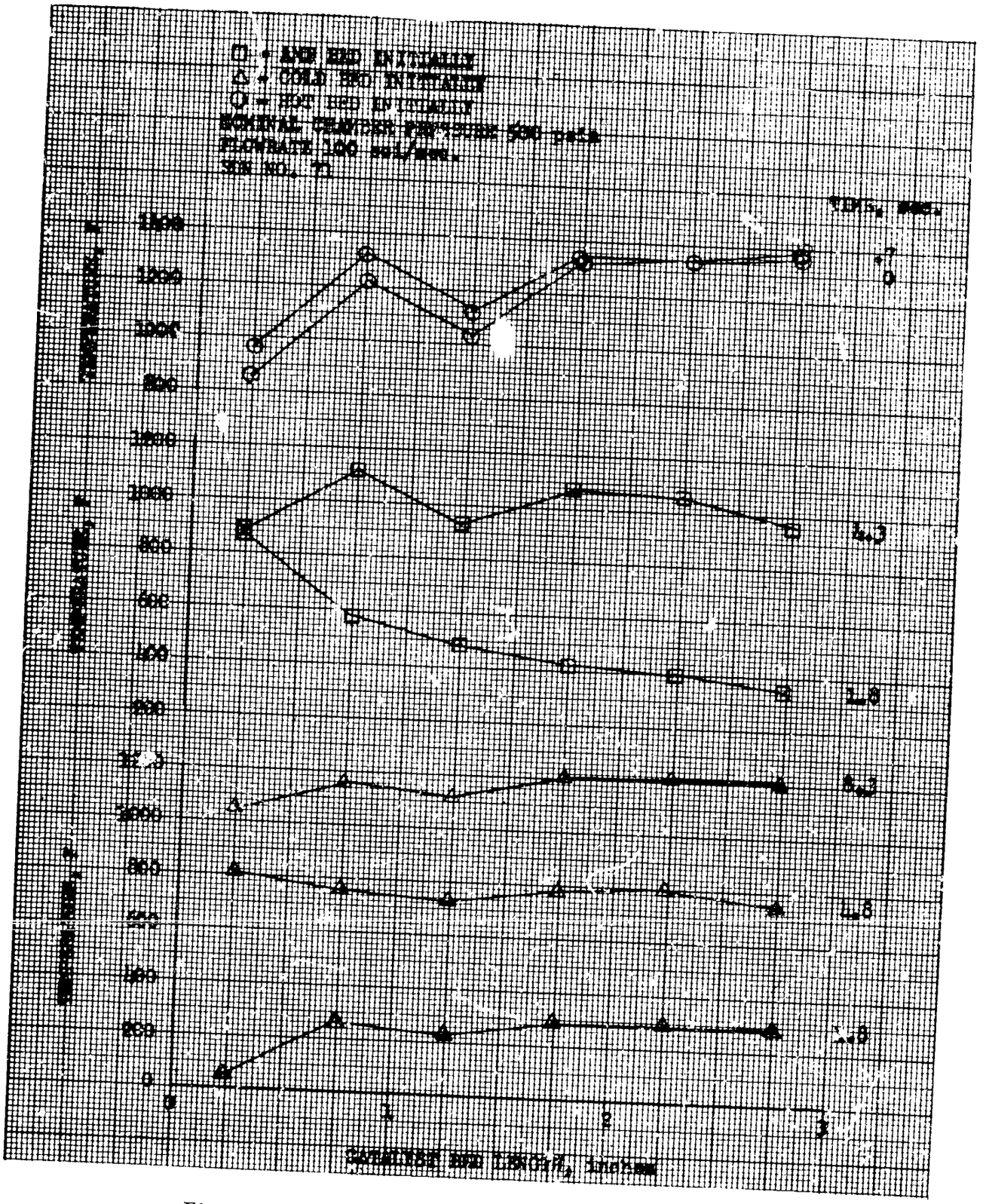

Figure 35. Effects of Initial Bed Temperature on $He/O_2/H_2$ Combustion

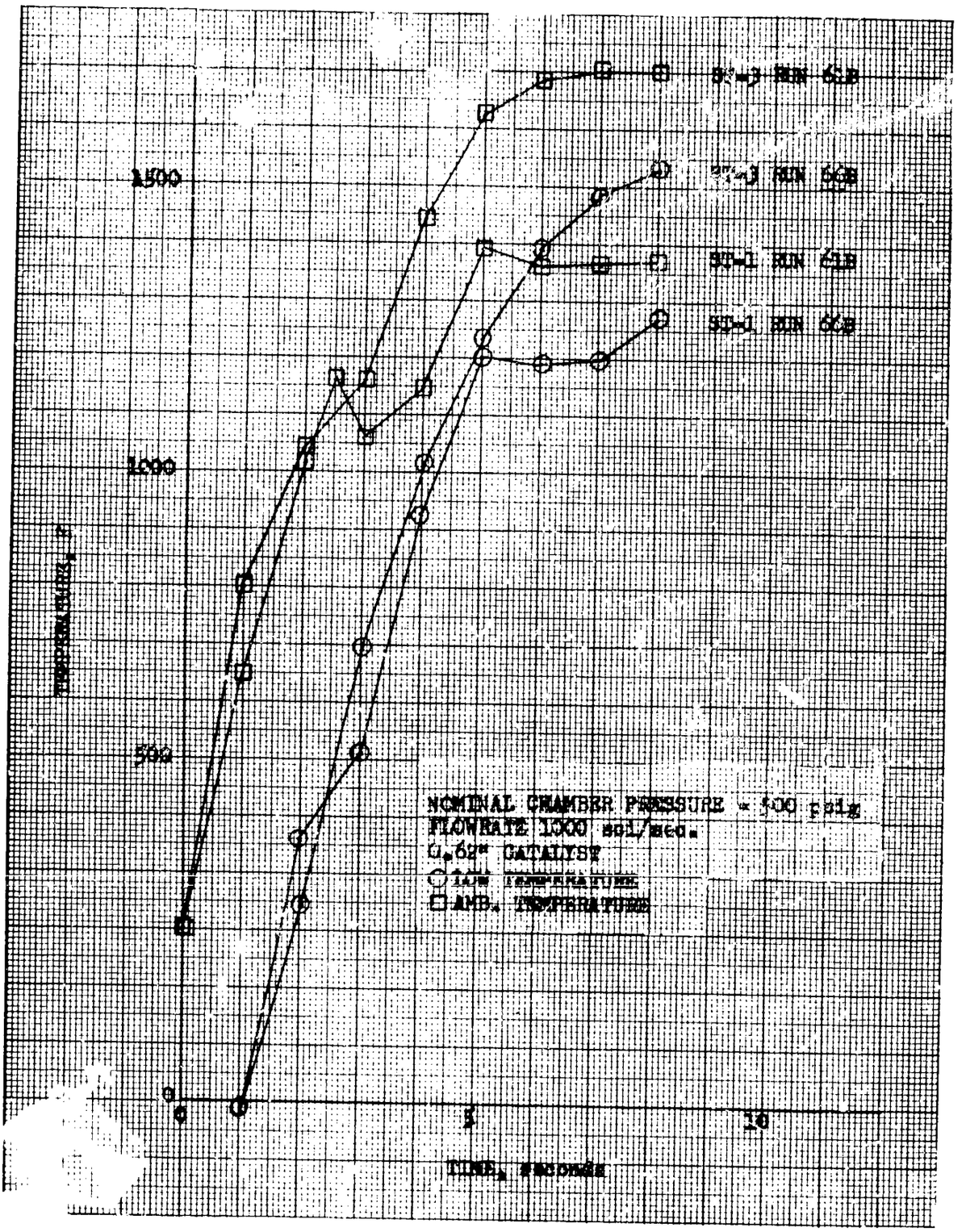

Figure 36. Effect of Initial Bed Temperature on Response Time

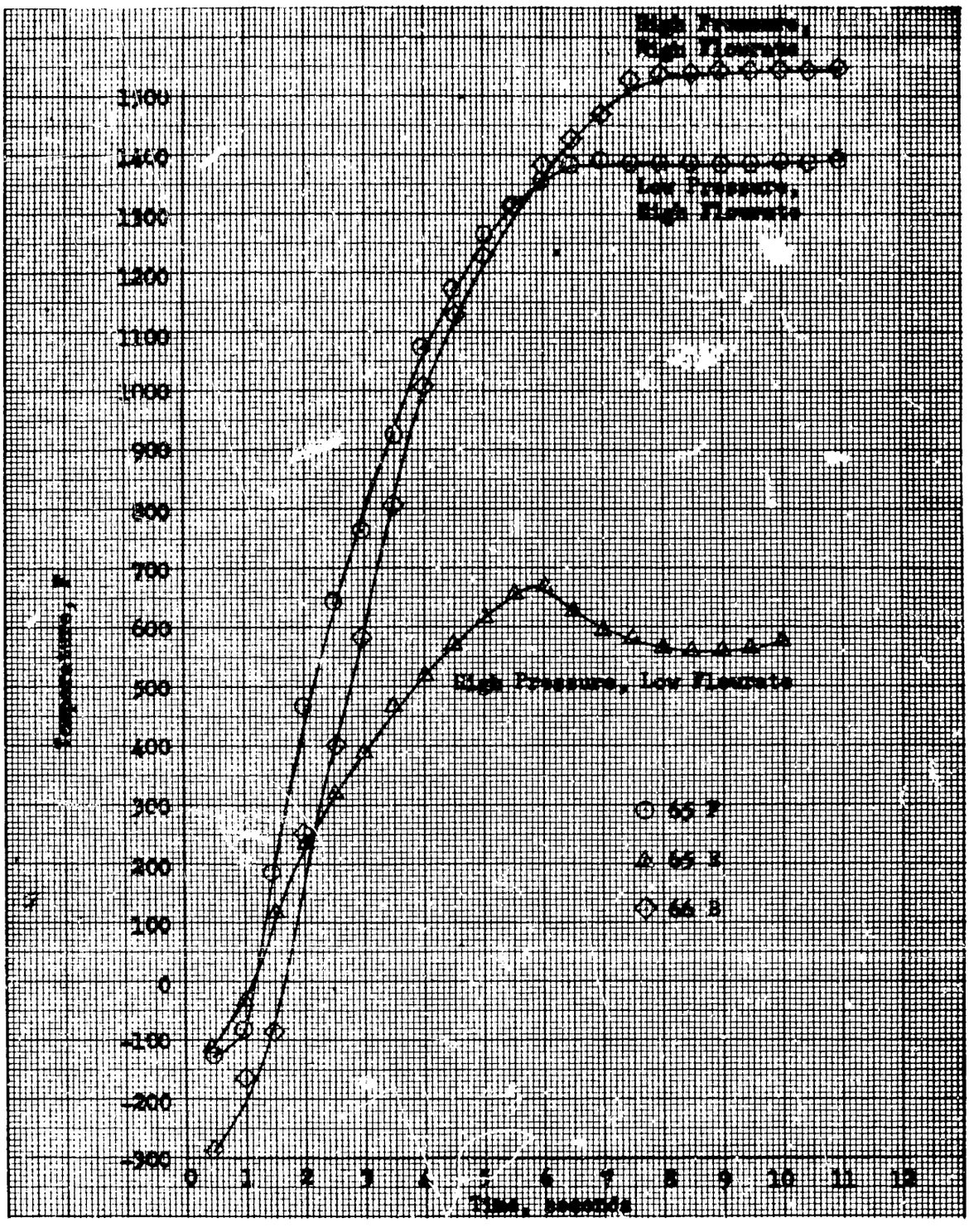

Figure 37. Catalyst Bed Temperature at 0.75 inch with Initial Bed at Cryogenic Temperatures

reaching maximum temperature by 2 to 3 seconds. This results from the extra enthalpy required to heat the bed to the steady-state temperature.

(U) When the gas temperature was also lowered to LN_2 temperature, the catalyst failed to initiate a reaction over a 5- to 10-second interval. This is the result of either a reduced catalytic activity at these low gas-solid temperatures or to fractionally condensing the oxygen from the gas mixture.

(U) Effect of Injection Gas Temperature. Figures 38, 39, and 40 present temperature-time data for the $He/O_2/H_2$ blend at three different bed stations and initially at three different inlet temperatures. Figure 39 shows the hot-catalyst bed yields the fastest initial response followed by the ambient-temperature bed and the low-temperature bed. The low steady-state combustion temperatures and long response times experienced at this station in the bed are caused by the short bed length (0.25 inch) which is insufficient to complete the reaction.

(U) Catalyst Durability. The durability of the catalyst was evaluated in two ways during the reactor tests. Single charges of catalysts were employed during the bulk of the reactor studies, and two specific long-duration runs were made with the same catalyst. The catalyst used for the major portion of the reactor studies was subjected to greater than 75 runs of at least 10 seconds duration without any noticeable deterioration. This multiple restart capability and extended service life effectively demonstrates an excellent life potential.

(U) In addition, a charge of the 0.062-inch catalyst was used in two long-duration tests, one in excess of 800 seconds and the other in excess of 500 seconds. Again no deterioration was noted over the accumulated service of greater than 1300 seconds.

(U) These results are in agreement with other durability results for catalysts in related service (Ref. 5). These results indicated an essentially infinite life, if the reaction temperature is kept in the vicinity of 1500 F. Higher temperatures on the order of 1800 to 2000 F could lead to reduced catalytic activity.

STATION 0.25" DOWNSTREAM OF BED ENTRANCE

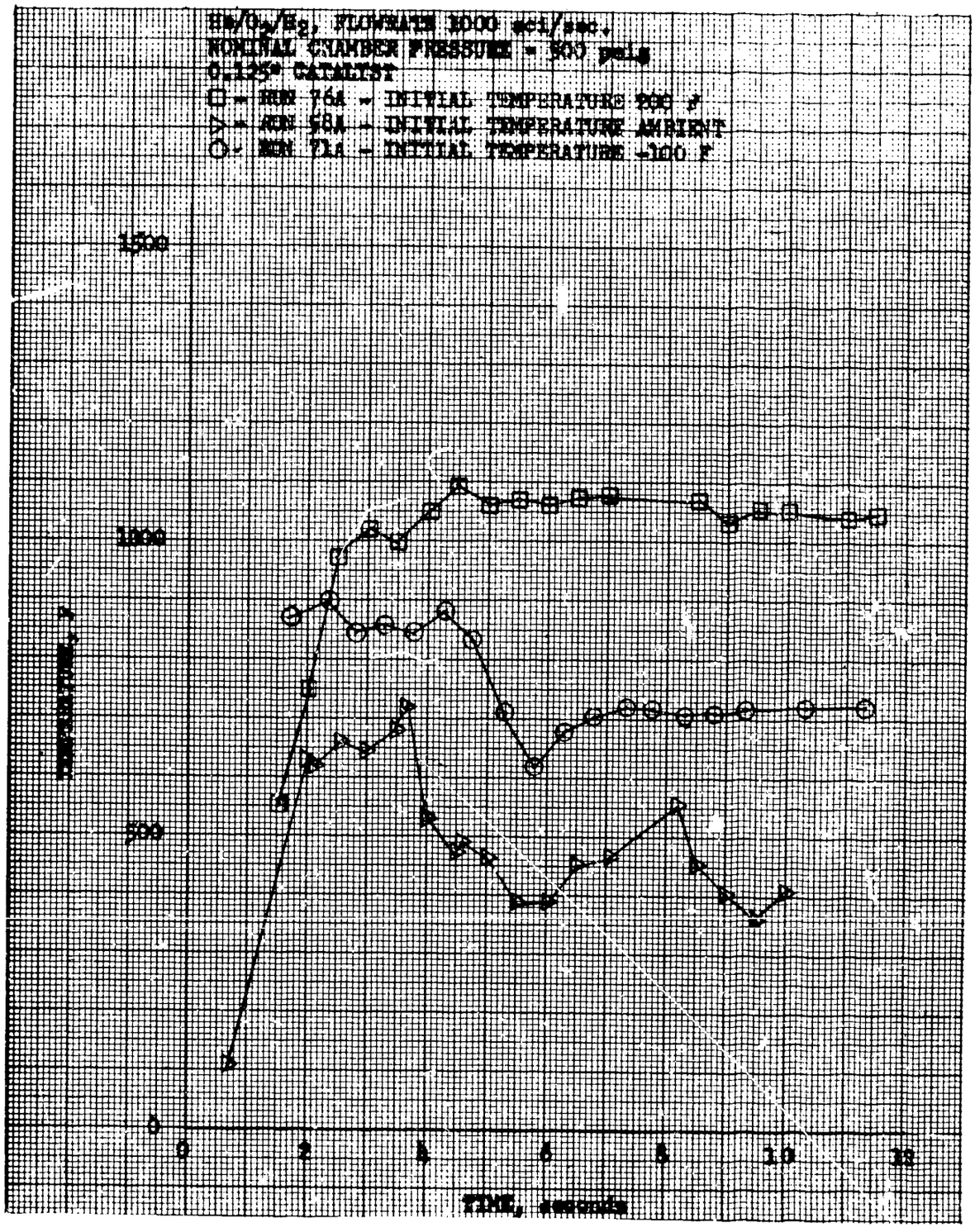

Figure 38. Effect of Initial Gas Temperature on Response Time

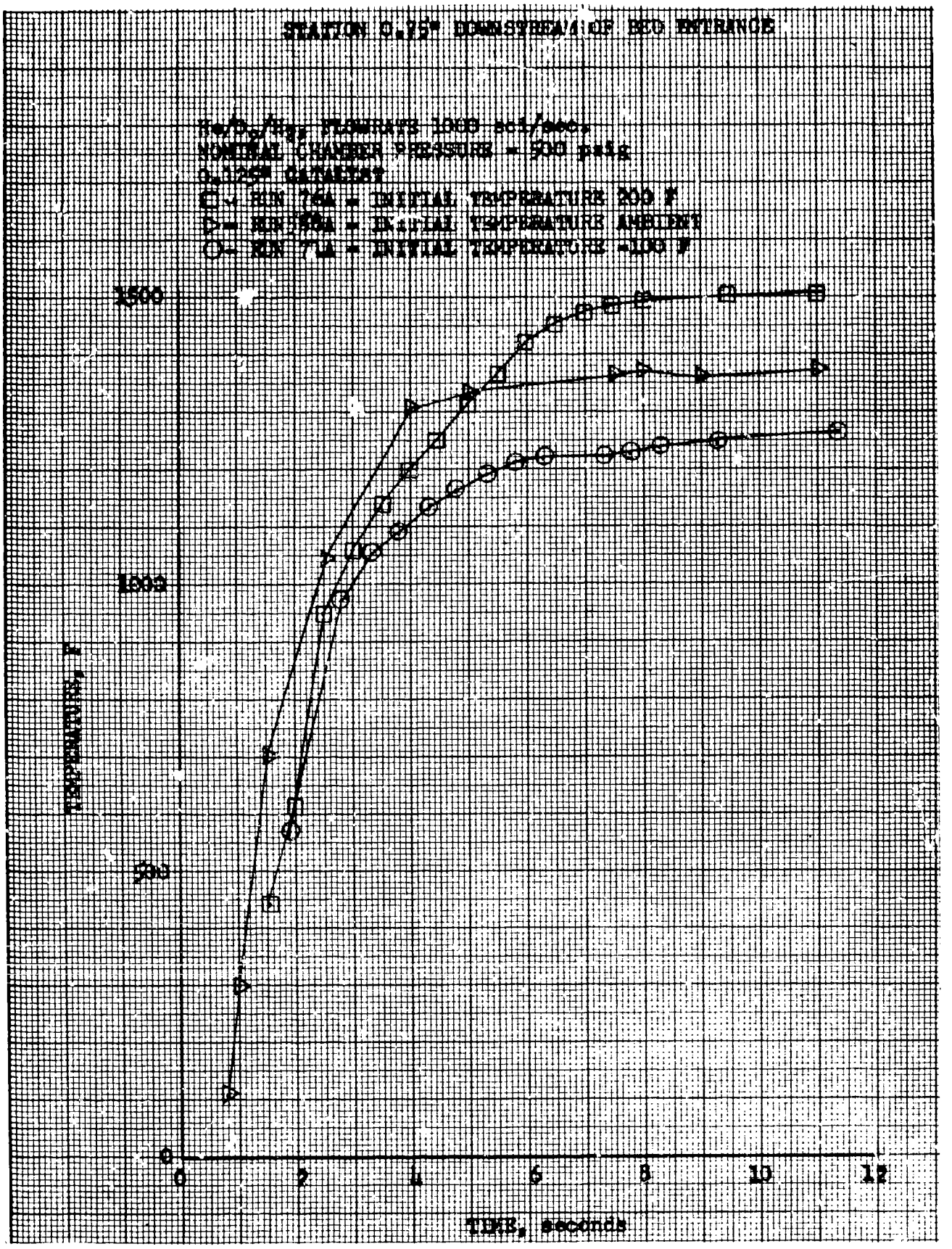

Figure 39. Effect of Initial Gas Temperature on Response Time

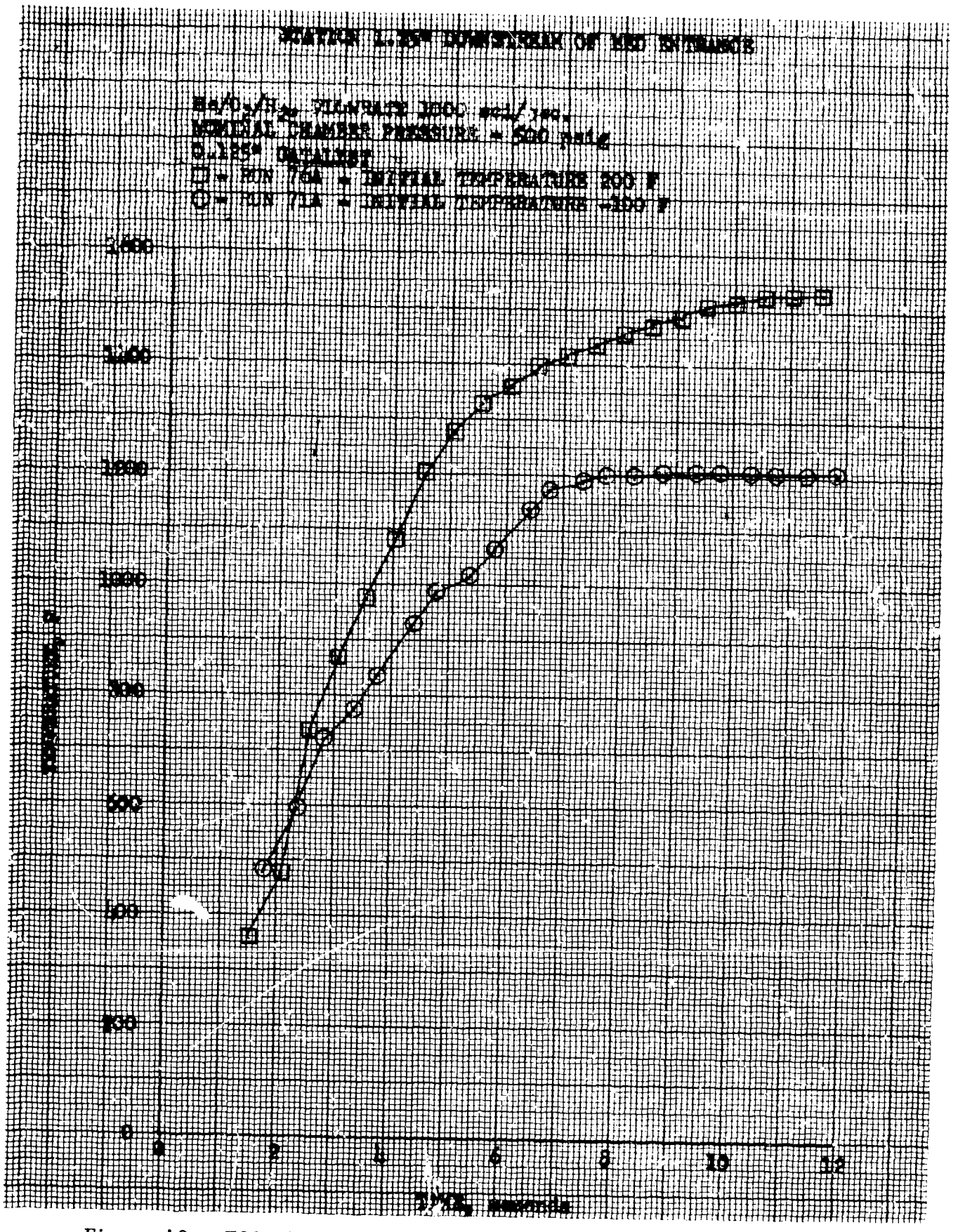

Figure 40. Effect of Initial Gas Temperature on Response Time

(U) Delivered Thermal Efficiency. As a means for measuring the performance of the reactor, a delivered thermal efficiency factor was defined as the temperature rise of the gas (as measured by the chamber temperature) divided by the theoretical temperature rise. Figures 41, 42, 43, and 44 show the delivered thermal efficiency for the cold-gas-temperature series of tests. These particular tests were chosen, since more pronounced variation in performance should occur as a consequence of the low initial gas temperature. For comparative purposes, Fig. 45 shows delivered thermal efficiency curves for the hot-gas temperature test and for the cold-gas temperature test. The zero time point on the ordinate of the subject figures was defined as the time when the main valves were energized. The unexpected aspect of Fig. 45 is that the hot-gas curve lies below the cold-gas curve, indicating better performance and better response for the cold-gas conditions. A possible explanation is that a greater relative quantity of heat is lost to the chamber and injector walls under the higher temperature conditions; thus, relative performance would be impaired for the higher temperature condition.

(U) A study of the aforementioned curves reveals some interesting aspects. These are: (1) no significant difference in delivered thermal efficiency can be attributed to the difference in gas mixtures; (2) a cold initial catalyst temperature does not appear to have any appreciable effect at low-pressure conditions while it does at higher pressure; (3) at the low-flow conditions, performance is poor and response is indecisive; and (4) the curvature is approximately the same for the high-flowrate curves at ambient and low initial-catalyst temperature conditions. The poor response characteristics of the low-flow tests show the need for the delivered heat of reaction to be significantly greater than heat losses if response time is to be reasonably short and performance acceptable.

(U) The similarity of the curvature for the high-flowrate curves indicates a similar time constant may apply to all high-flowrate conditions. The delivered thermal efficiency is, in fact, a response term. Furthermore, the response time of the exit gas should be approximately equivalent to the overall response time of the bed. Inspection of data of many tests showed that the exit gas temperature (chamber temperature) was nearly the same as the average temperature of the bed.

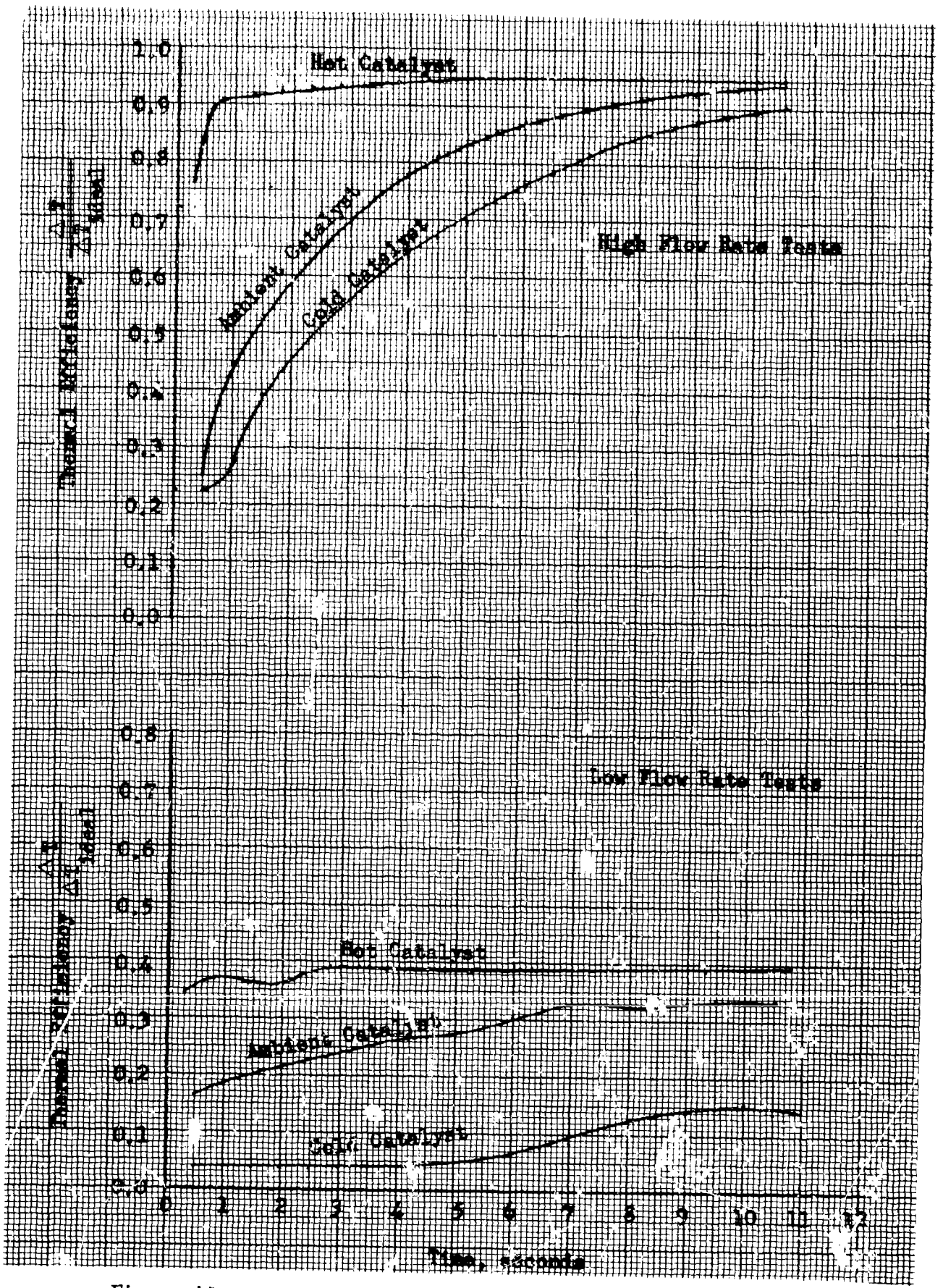

Figure 41. Delivered Thermal Efficiency for $He/O_2/H_2$ at -135 F and High Injection Pressure (Tests 71-A-F)

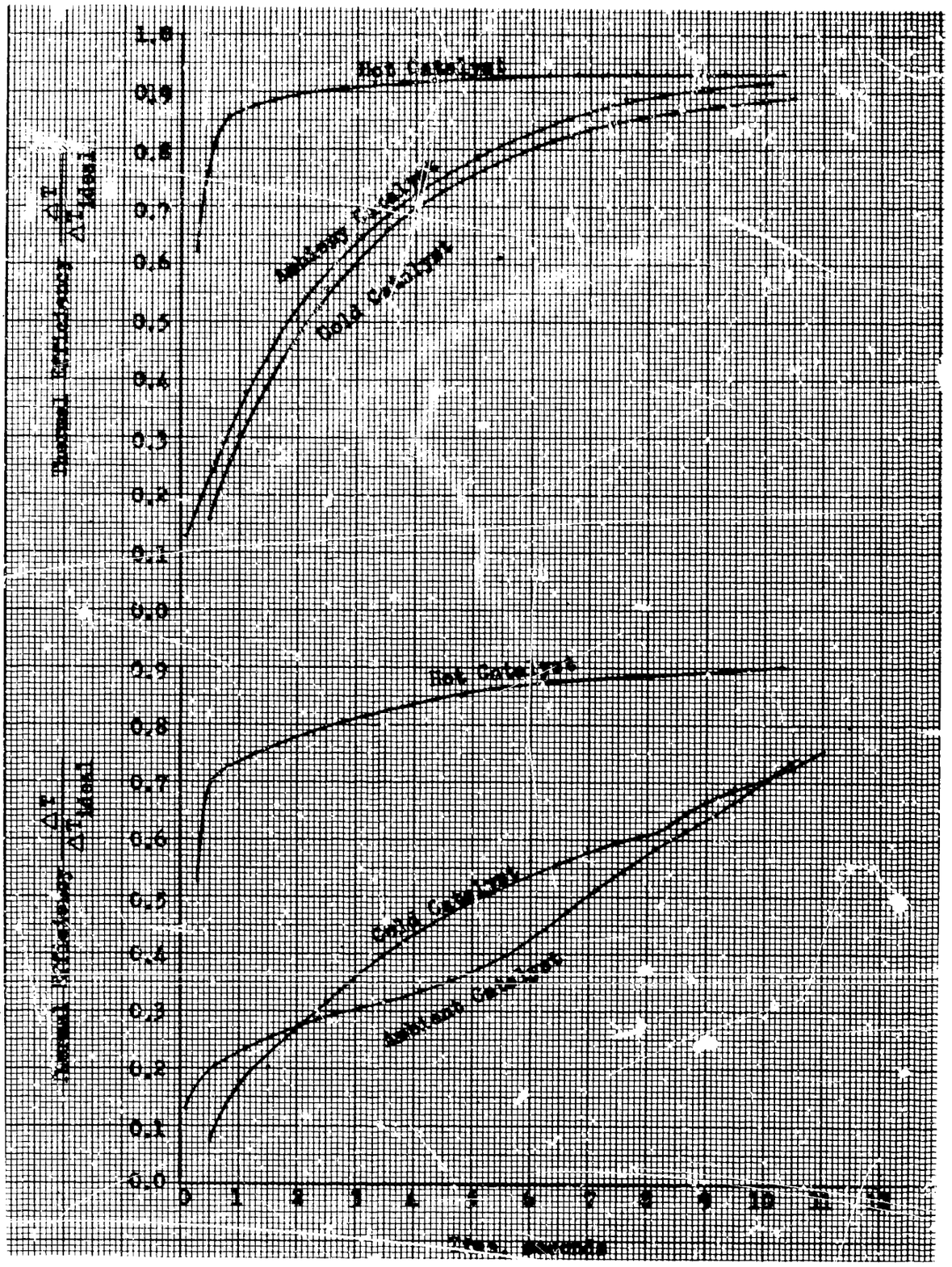

Figure 42. Delivered Thermal Efficiency for $He/O_2/H_2/CH_4$ at -133 F and Low Injection Pressure (Test 72 A-F)

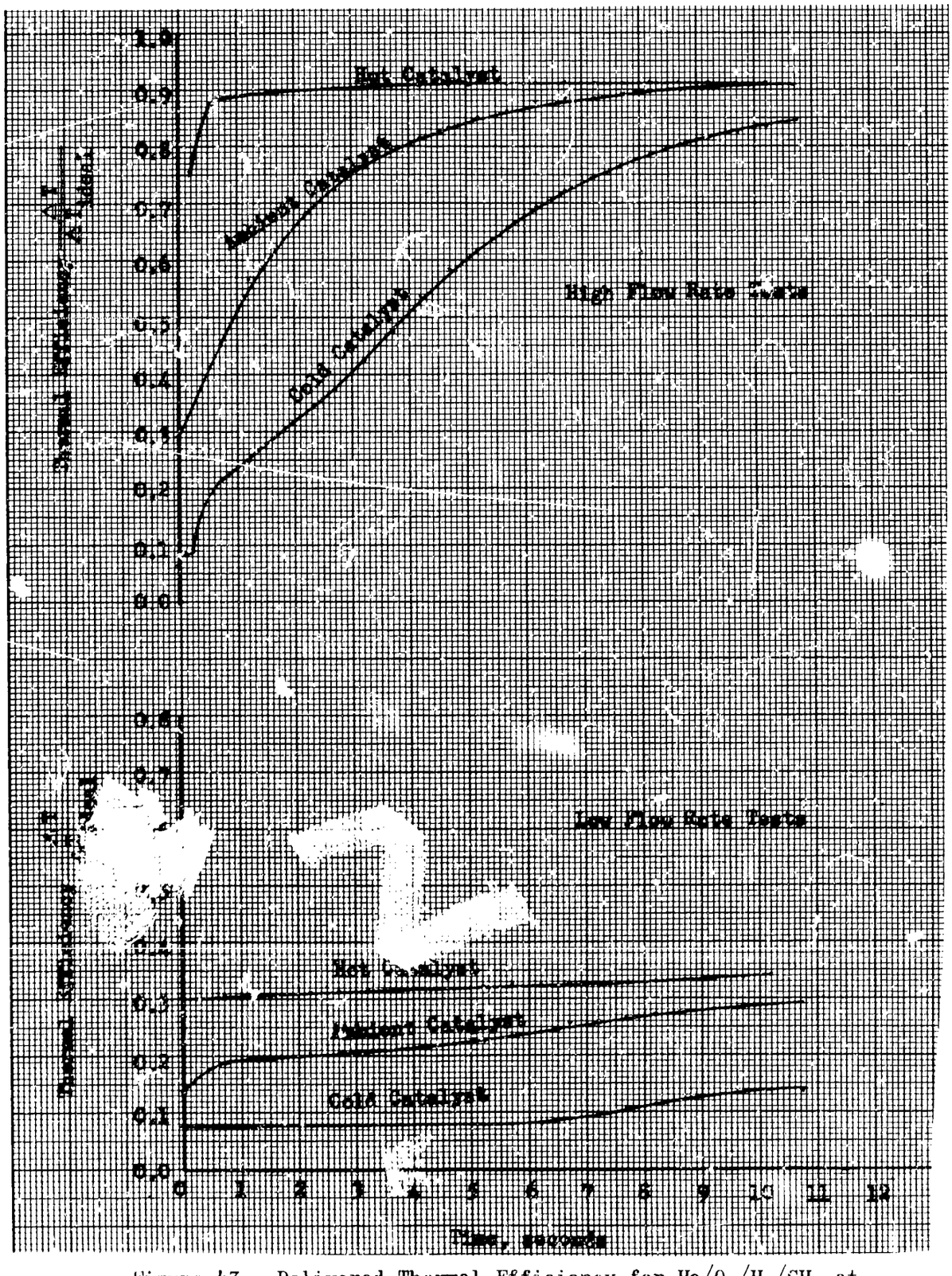

Figure 43. Delivered Thermal Efficiency for $He/O_2/H_2/CH_4$ at -120 F and High Injection Pressure (Test 73 A-F)

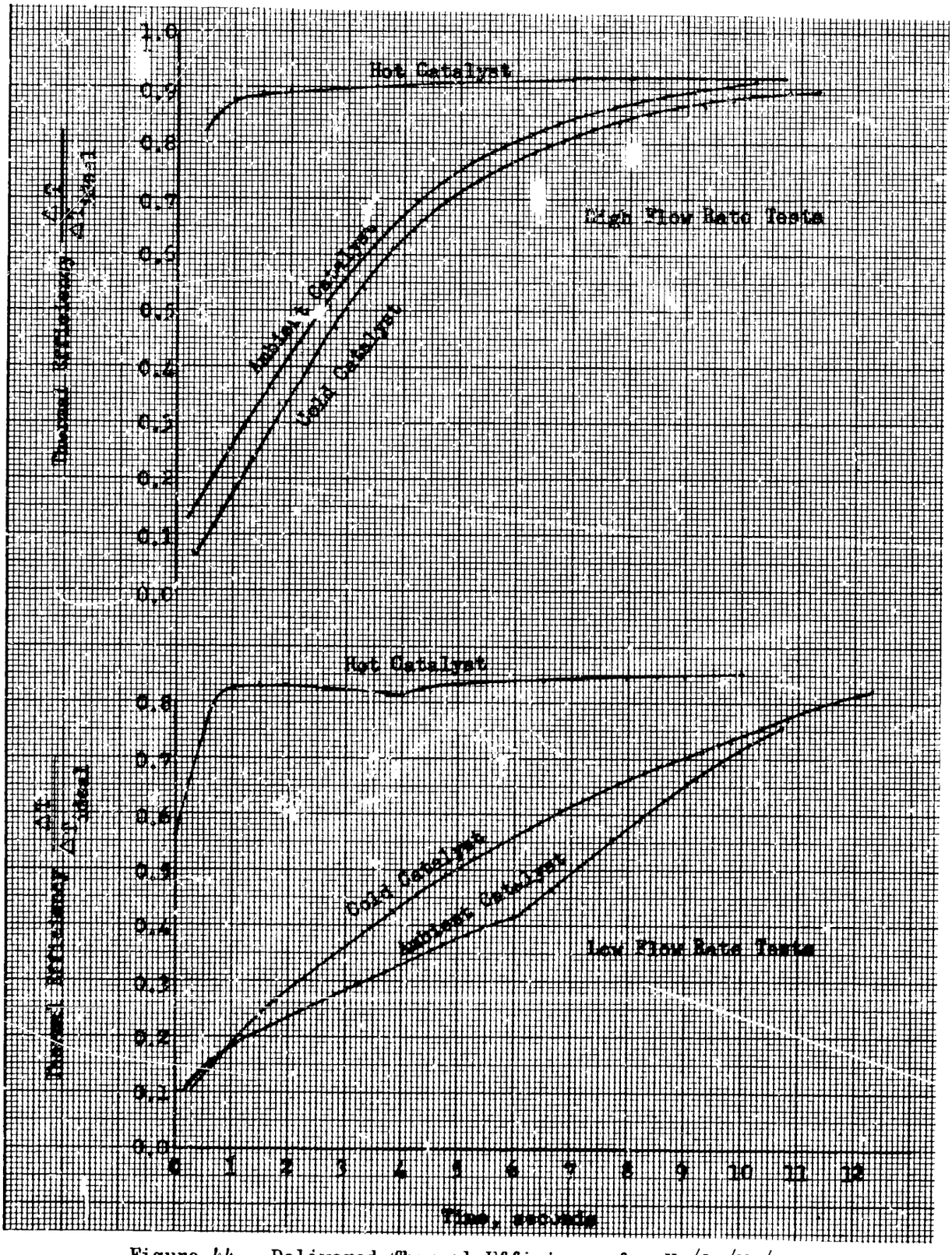

Figure 44. Delivered Thermal Efficiency for $He/O_2/H_2/CH_4$ at -115 F and Low Injection Pressure (Tests 74 A-F)

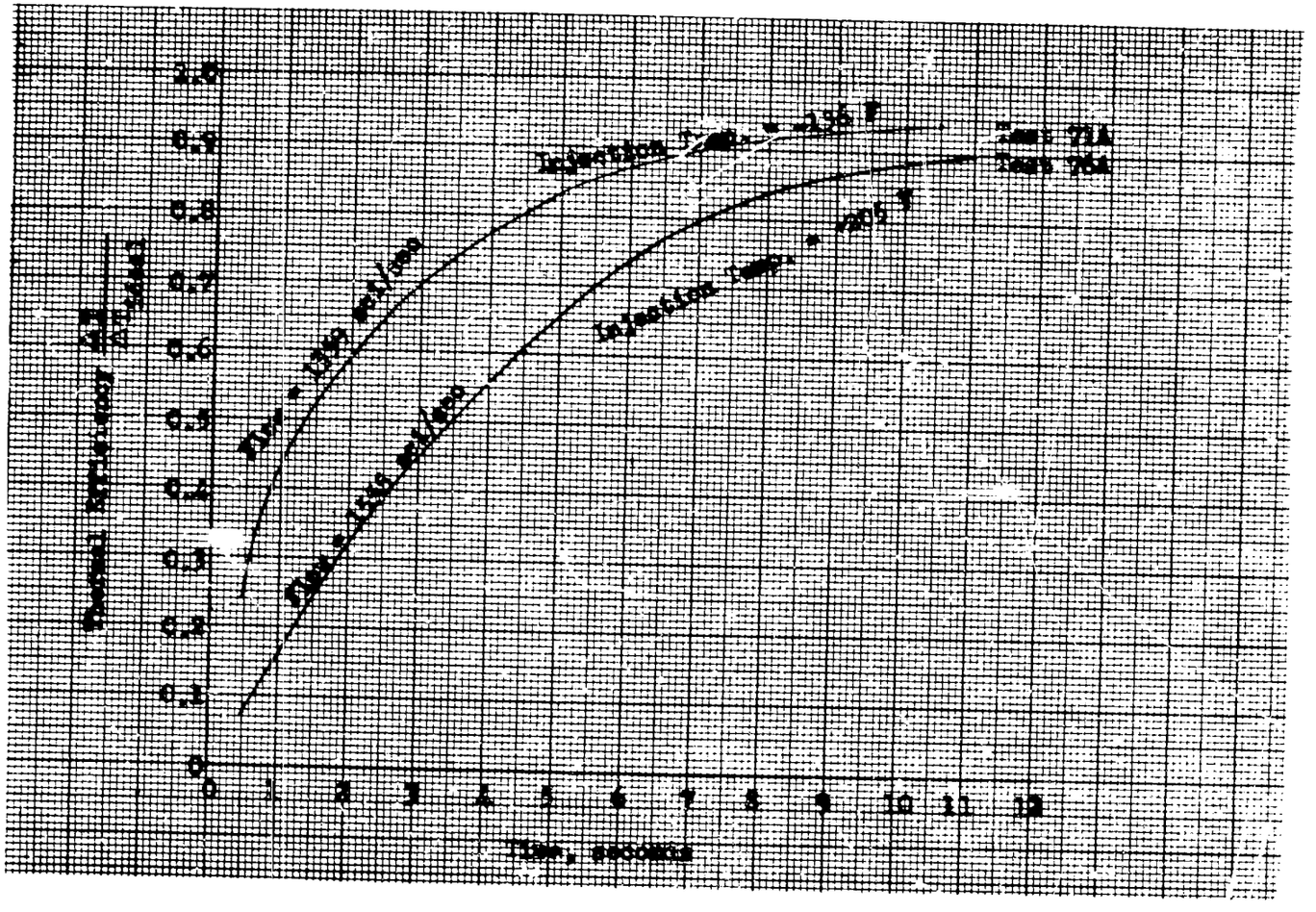

Figure 45. Injection Temperature Comparison

The response time to a catalyst bed may be estimated as:

$$\frac{T_f - T}{T_f - T_o} = \exp -\left(\frac{\dot{w}\, c_p}{M_B c_b}\right) t = \exp\,(-kt) \qquad (1)$$

$$k = \frac{\dot{w}\, c_p}{M_B c_b} \qquad (2)$$

(U) Using the data of the high-flowrate, ambient-catalyst temperature curve of Fig. 41 (by plotting the log of $(T_f - T)/T_f - T_o)$ vs time and taking the slope of the resulting straight line) an experimentally determined k of 0.372 sec^{-1} was obtained. This compares with a calculated k (from the $\dot{w}\, c_p/M_B c_b$ term) of 0.54 sec^{-1}. The difference between these two values is attributed to heat losses to the chamber and retaining screens, so that the effective heat sink capability is increased to a value greater than the $M_B c_b$ term.

(U) Reactor Pressure Drop. Reactor pressure drop was found to be extremely sensitive to temperature, both the temperature of the entering gas and the hardware temperatures. Intercomparison of the data of Fig. 17 through 23 illustrates this point. Table 8 lists the pressure drop experienced across the reactors for a variety of operating conditions. The wide differences in the data again illustrate the pressure-drop sensitivity to temperature and also allude to the problem of correlating the data.

(U) By selecting the terminal conditions of those tests where the axial temperature distribution was essentially constant, suitable data for a pressure-drop correlation were obtained. These data are presented in

TABLE 8

CATALYTIC REACTOR PRESSURE DROP VALUES
FOR A VARIETY OF CONDITIONS
(Catalyst Bed, 3.0 inches in Length)

Run No.	Injection Temperature, F	Chamber Temperature, F	1/2 (Injection Pressure + Chamber Pressure), psia	Flowrate, sci/sec	Catalyst Diameter, inches	Reactor Pressure Drop, psi
67A	64	3337	495	965	0.125	34.0
67B	86	1286	496	973		34.6
67C	86	1340	499	950		33.8
71A	-139	1267	569	1136		10.0
71C	-139	1282	572	1138		8.8
71E	-137	1195	577	1155		12.0
77A	204	1369	515	970		40.9
77A	204	1428	106	619		140
68A	64	1337	83.5	621		112
68C	84	1342	78.9	620		113
68E	79	1450	80.9	645		114
72A	-114	1210	74.9	893		69.5
72C	-134	1215	72.4	898		74.0
72E	-133	1193	66.5	760		66.5
62B	105	1472	149	1540	0.0625	142
62D	102	1301	134	1805		131
62F	97	1465	111	1160		102

TABLE 8

(Concluded)

Run No.	Injection Temperature, F	Chamber Temperature, F	1/2 (Injection Pressure + Chamber Pressure), psia	Flowrate, sci/sec	Catalyst Diameter, inches	Reactor Pressure Drop, psi
68B	25	402	47.3	155	0.0625	1.2
68D	66	431	47.6	154	↓	1.2
68F	70	1070	49.0	120		1.6
61B	107	1522	532	969		34.5
61D	107	1540	534	970		33.1
61F	63	1477	528	977		26.9

Fig. 46. A linear normalization of the data to 1500 F and 500 psia for the high-pressure tests and 50 psia for the low-pressure tests was employed. These data are somewhat scattered, but the data can be reasonably represented by two straight lines on a log-log plot.

The Ergun equation,

$$g \frac{\Delta P \rho D_p}{G_o^2 L} \frac{\epsilon^3}{1-\epsilon} = \frac{150 (1-\epsilon)}{\frac{D_p G_o}{\mu}} + 1.75 \qquad (3)$$

which is one of the better equations for describing pressure drop through packed beds, is also shown in Fig. 46 for the two pressure conditions of 500 and 50 psia. The experimental data are six-fold higher than the Ergun equation for the high-pressure data, and two-fold higher for the low-pressure data.

(U) In addition to these deviations from the predicted pressure drops, the experimental pressure drop does not appear to be a function of pellet size; data for the two pellet sizes fall in the same area. This is again a deviation from an analytical prediction of packed-bed, pressure-drop characteristics. The one aspect that tends to shift the curves is gas temperature. A few data points for cold and hot gaseous mixtures depart considerably from the curves, and illustrate the effects of injection temperature.

(U) The experimentally observed pressure drops being considerably in excess of theoretical indicates that much of the pressure drop occurred outside the bed. This is further substantiated by the absence of a pellet-size effect. As mentioned previously, a 0.15-inch Rigimesh disk served as a distribution plate. It appears that the major portion of the pressure drop occurred across the Rigimesh.

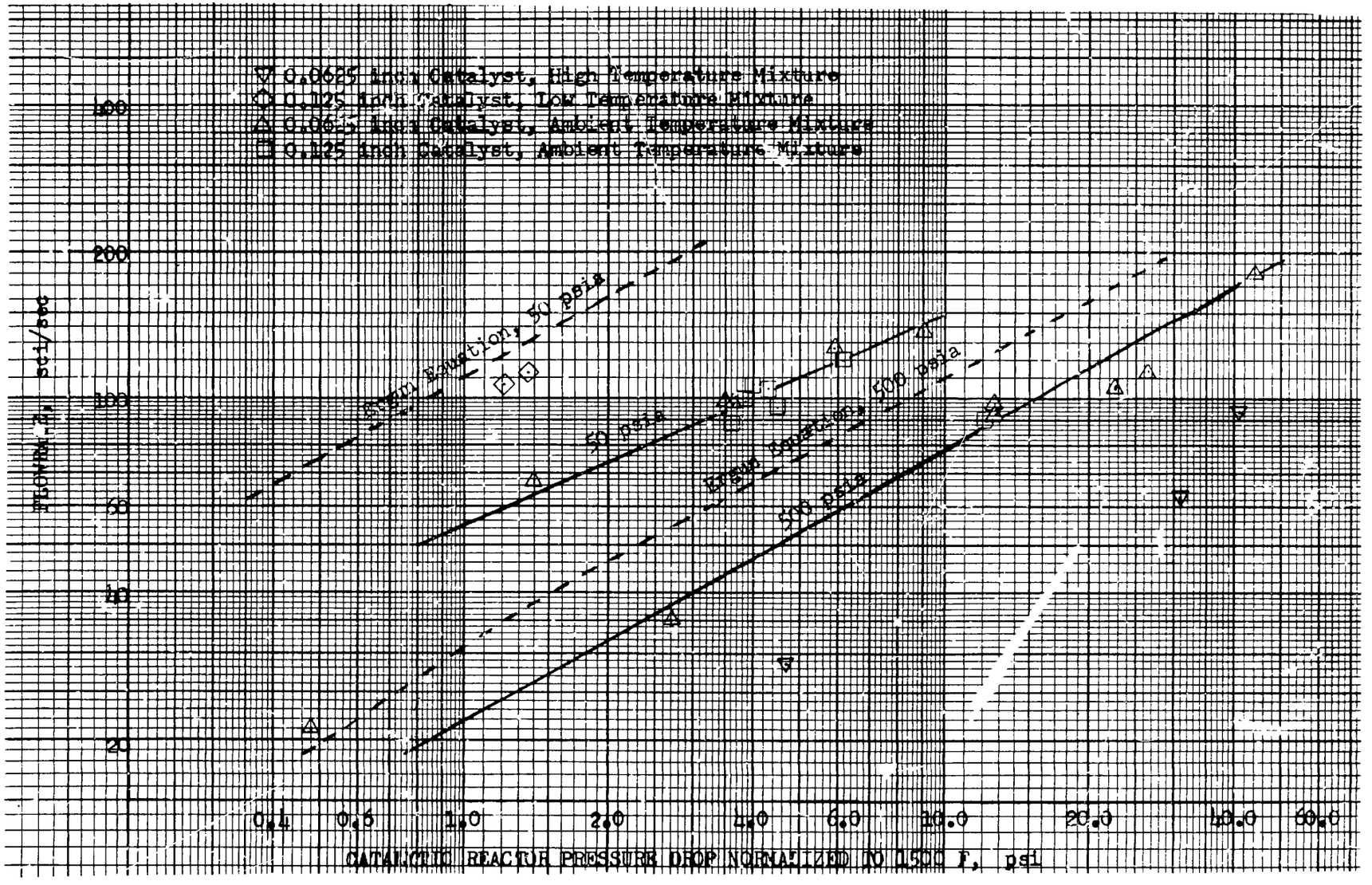

Figure 46. Catalytic Reactor Pressure Drop Normalized to 1500 F and Indicated Pressures of 500 and 50 psia, respectively

Thermal Analysis

(U) The catalyst in a reactor and the reactor body components act as heat sinks to delay the full thermal response of the pressurant during initial firings when the reactor is at a relatively low temperature. The energy transfer from the gas to the reactor lowers the enthalpy and the reacted temperature of the gas. This loss in temperature is reflected in a decrease in the pressurization capability of the mixture. A simplified model has been developed to evaluate the thermal response of the reacting mixtures. The catalyst bed is considered to be infinitely conductive and in thermal equilibrium with the gas. A more realistic model would assume each radial cross section of the system to be at a uniform temperature with a temperature variation longitudinally. However, such a model cannot be described by a simplified mathematical approach, and the model described below was developed to give an approximate value of the thermal response.

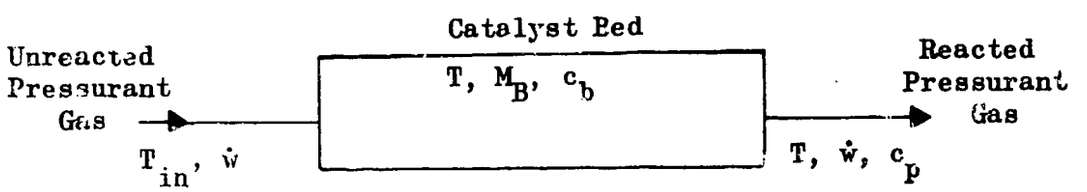

(U) The system corresponds to the catalyst bed plus the engine hardware. The energy equation is given by:

$$\dot{w}\, c_p\, (T_{in} - T)\, dt = M_B\, c_b\, dT \tag{4}$$

with the boundary condition given by:

$$T_{in} = T = T_o \text{ for } t \leq 0;\ T_{in} = T^* \text{ for } t > 0 \tag{5}$$

The solution to Eq. is:

$$\frac{(T^* - T)}{(T^* - T_o)} = \exp - \frac{\dot{w}\, c_p\, t}{M_B\, c_b} \tag{6}$$

(U) The response calculated from Eq. 6 will represent minimum response times as the decrease in flame temperature is not considered. Table 9 presents the solutions to Eq. 6 for all of the conditions of interest. Additionally the total enthalpy loss from the pressurant gases is also shown along with the ratio of reactor wall to catalyst pellet heat transfer coefficients. This latter parameter has been computed from equations presented by McAdams (Ref. 6)

$$\frac{h_p}{h_w} = \left[1.06\ Re^{0.59}\ Pr^{1/3}\ \frac{K}{D_p}\right]\left[\frac{e^{6\ D_p/D_t}\ D_t}{0.812\ Re^{0.9}\ K}\right] \qquad (7)$$

$$\approx \frac{1.212}{Re^{0.31}}\left(\frac{D_t}{D_p}\right)$$

(U) Table 9 shows the total heat loss to the reactor bed liner is a small portion of the total heat loss, and the liner response time is less than 0.1 of the response time of the catalyst pellets. Therefore, it is necessary to minimize the catalyst volume for each application to minimize the heat loss and maximize the bed response time.

(U) For example, if the bed were optimized for a pressurant flowrate of 100C sci/sec using 0.125-inch-diameter catalyst pellets, the total heat loss (including the liner) would be approximately 5.08 Btu and the bed response time would be on the order of 0.88 second (assuming no change in flame temperature). These values are based on an initial temperature of 0 F.

(U) Table 9 also shows the catalyst bed response time for the low flowrates is on the order of 35 to 40 seconds, illustrating that the bed volume for the 100 sci/sec experimental flowrates is approximately one order of magnitude too large. The analytical heat transfer rates presented in Table 9 show the heat transfer coefficient of the catalyst granules is much larger than the heat transfer coefficient of the wall. It is therefore evident that the major initial thermal loss occurs in heating the pellets.

TABLE 9

SUMMARY OF REACTOR BED THERMAL PARAMETERS

Flowrate, sci/sec	Catalyst Pellet Diameter, inches	Catalyst Response Time,* seconds	Reactor Bed Liner Response Time,** seconds	Loss to Catalyst,* Btu	Loss to Bed Liner,** Btu	Reynolds Number Based on Pellet Diameter	$\frac{h_{pellet}}{h_{wall}}$
1,000	0.125	3.54	.293	18.75	1.55	675.	2.74
1,000	0.062	3.76	.293	20.0	1.55	337.5	4.64
100	0.125	35.4	2.93	18.75	1.55	67.5	5.59
100	0.062	37.6	2.93	20.0	1.55	33.8	9.48

*Bed geometry: Cylindrical 1-inch diameter and 3 inches long

**Liner geometry: Hollow cylinder 1-inch inside diameter 3 inches long, 0.035 inch-thick

Conclusions.

(U) The results of the reactor evaluation tests substantiate the feasibility of employing a catalytic reactor to heat propellant pressurizing gases. The development of this concept of improved propellant pressurization will not be jeopardized by catalytic reactor limitations or performance. In more specific terms, the following statements may be made regarding this study.

1. The 1-inch-diameter reactor hardware responded suitably for nominal flowrates of 1000 sci/sec at pressures ranging from 40 to 700 psia. Bed lengths as short as 1 inch appear suitable.

2. Temperature response at a nominal 100 sci/sec were characteristically slow, but this can be explained as largely resulting from excessive heat loss in proportion to heat input. Additional effort with smaller-diameter reactors is needed to define optimum geometries for these low flowrates.

3. Maximum bed temperatures equivalent to the theoretical reaction temperatures indicate catalytic conversion is essentially complete under conditions of insignificant heat loss. Additionally, under steady-state firing conditions, delivered thermal efficiencies of up to 95 percent were achieved.

4. Low initial catalyst bed temperatures (-100 F), of themselves, do not severely impair temperature response.

5. The catalyst is responsive and durable for an extensive number of firings (> 75 starts) and a long accumulated firing time (> 1300 seconds) when the maximum temperatures do not greatly exceed 1500 F.

EXPULSION DEMONSTRATIONS

(U) The experimental expulsion demonstrations were performed to illustrate the use of a catalytically reacted pressurant system, and to provide a comparison between the expulsion capabilities of ambient temperature helium and a reacted mixture. The nominal blend composition selected was 3.6 volume percent oxygen, 7.2 percent hydrogen, and 89.2 percent helium. The liquid propellants expelled were isopropyl alcohol, simulating a storable propellant, and liquid nitrogen, simulating a cryogenic propellant.

Experimental Apparatus

(U) The apparatus used in these demonstrations, (Fig. 47) consisted of a blend storage tank, pressurant fluid flow regulation system, catalytic reactor, propellant tank and liquid propellant metering system. The catalytic reactor was selected on the basis of the results of the catalytic reactor evaluations, and consisted of the previously described 1-inch-diameter reactor filled with a 1-inch-long catalyst bed composed of 0.052-inch-diameter catalyst pellets. The catalyst used was the Engelhard Industries, Inc., MFSA material, also previously described. The pressurant metering system consisted of a turbine flowmeter, thermocouple, and pressure transducer mounted in the line immediately upstream of the pressurant main valve.

(U) The propellant tank was a nominally 25-gallon, stainless-steel vessel rated at approximately 1700 psia, and heavily insulated to minimize propellant boiling during the simulated cryogenic propellant (liquid nitrogen) demonstrations. The propellant metering system consisted of a turbine flowmeter installed in the discharge line. An overflow pipe level indicator system was used to establish the liquid level prior to initiation of the run.

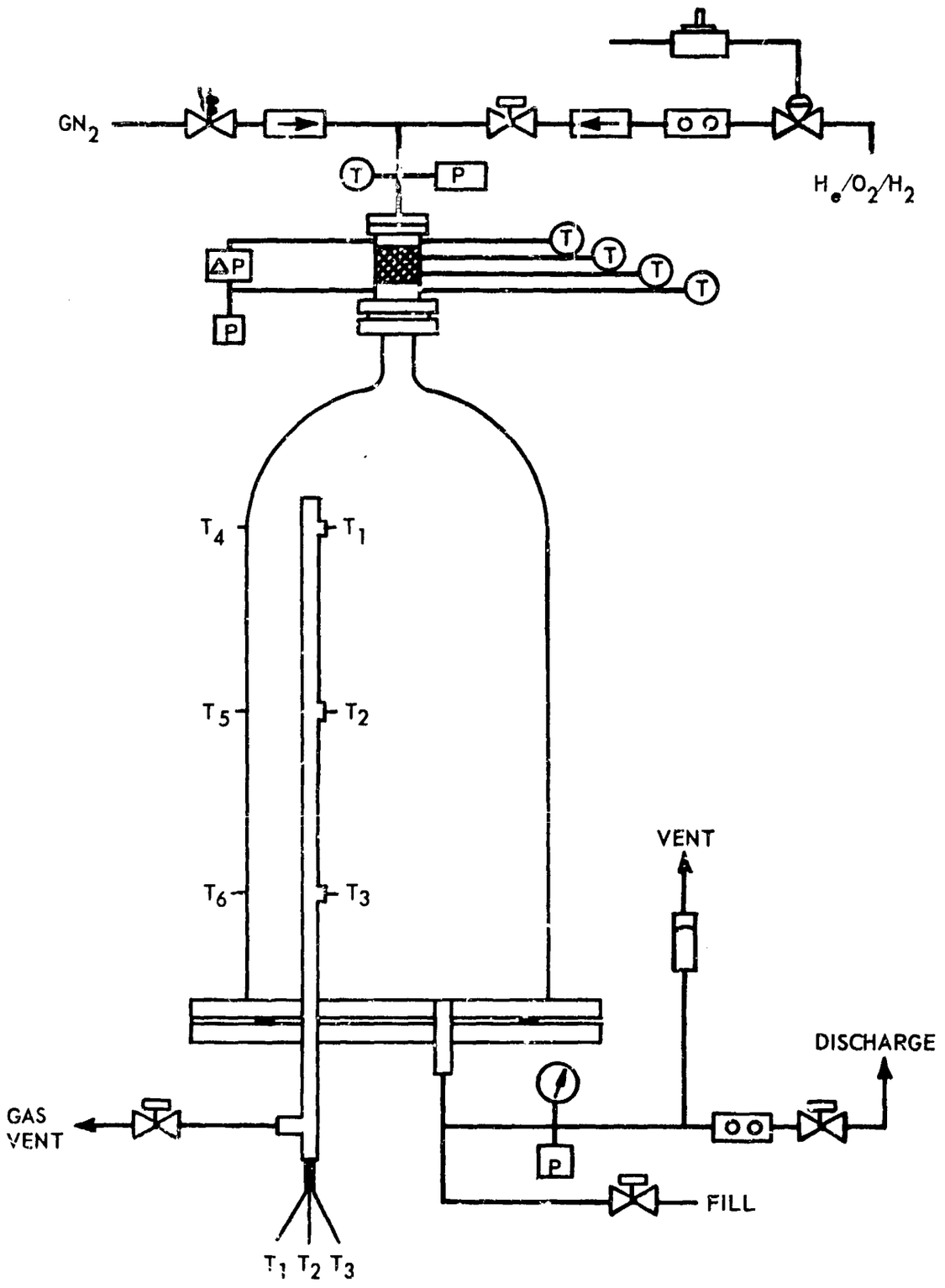

Figure 47. Expulsion System Schematic

Experimental Procedures

(U) The demonstration expulsions with each expellant were conducted first with ambient helium and then with the reacted pressurant. This affords a direct comparison between the helium and heated-gas expulsion capabilities. The blend expulsions were accomplished in three steps: (1) filling the propellant tanks, (2) preparing the pressurant fluid, and (3) accomplishing the expulsion. The helium expulsions included only the first and last steps. In filling the propellant tank, the simulant fluid was introduced through the bottom tank port. The overflow line was inserted into the tank leaving an ullage space which represented only a small fraction of the tank capacity when liquid overflowed through the stand pipe. Temperature measurements were made both inside the tank and on the external tank wall. The pressurant fluid was prepared following the propellant filling operation. This was accomplished using the procedure described in previous sections.

(U) The final step was the actual expulsion run. With the isopropyl alcohol, the expulsion was performed in a three-stage cycle. In each stage, approximately one-third of the propellant was expelled. Conversely, in the demonstrations involving the use of liquid nitrogen, the expulsion was performed as a single steady run.

Results and Discussion

(U) Storable Propellant Expulsions. The expulsions of the storable propellant simulant, isopropyl alcohol, were conducted at a nominal propellant tank pressure of 250 psia in the manner previously discussed. The results are summarized in Table 10 and Fig. 48 and 49. In each instance the three-stage experiment resulted in uniform expulsion of liquid propellant, providing an excellent comparison of the relative performance of helium and blend pressurants. The single difficulty encountered during the runs was the inability to measure the gas temperature accurately inside the tank during the blend expulsion run.

TABLE 10

SUMMARY OF RESULTS OF ISOPROPYL ALCOHOL EXPULSION EXPERIMENTS

	Pressurant			
	Helium		Blend	
	Initial	Final	Initial	Final
Propellant weight, pounds	182	0	182	0
Pressurant injection temperature, F	73.3	51.3	1685	1648
Propellant tank pressure, psig	251.7	175.0	219.6	164.3
Internal tank temperature, F				
Top position	72.6	72.6	74.0	305.9
Middle position	72.5	77.9	74.0	314.4
Bottom position	73.1	75.2	74.0	308.1
External tank wall temperature, F				
Top position	72.3	72.3	74.9	111.1
Middle position	68.5	69.2	71.5	84.2
Bottom position	75.1	75.7	80.4	75.9
Pressurant consumption, pounds	- - -	0.585	- - -	0.324

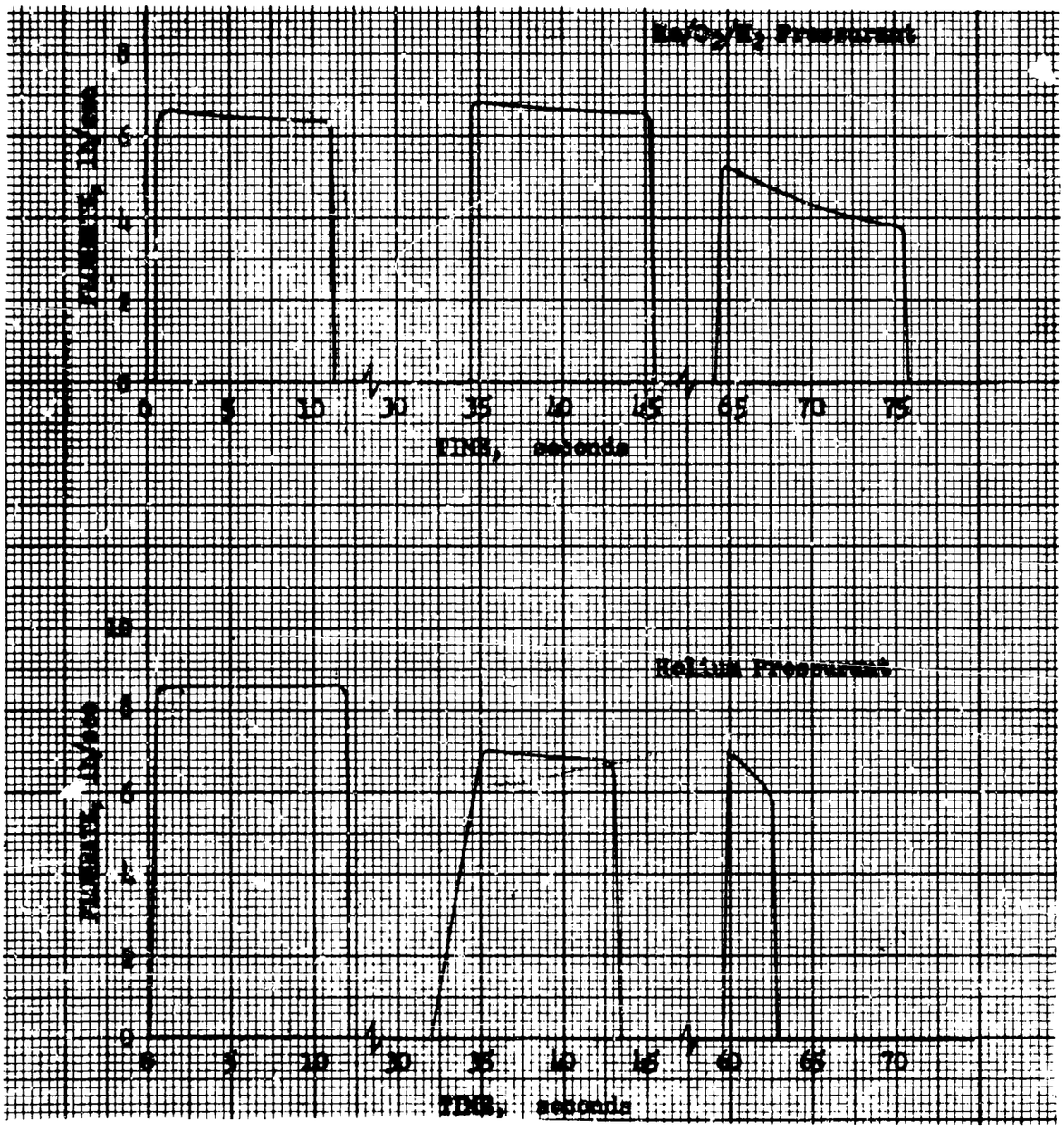

Figure 48. Alcohol Flowrate as a Function of Time for Expulsion Demonstration Tests

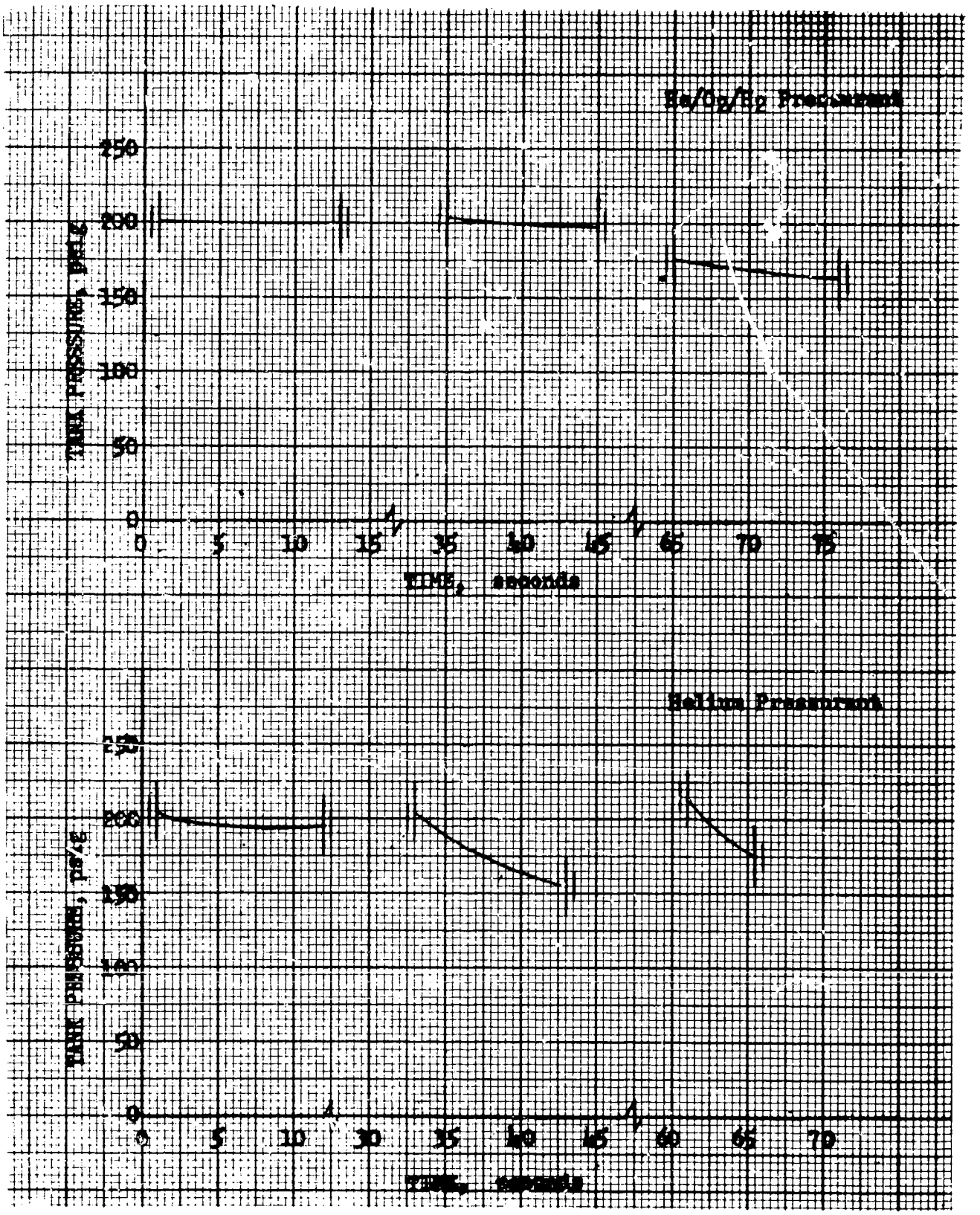

Figure 49. Tank Pressure as a Function of Time for the Alcohol Expulsion Tests

(U) Each of the three thermocouples located in the propellant reservoir indicated a maximum temperature of approximately 315 F. Since this temperature coincides with the isopropyl alcohol boiling temperature at the tank pressure, it is presumed that the thermocouples were "wet" with alcohol throughout the run and that this alcohol was slowly boiling away during the run. This inaccuracy in the gas temperature measurement does not affect the determination of the blend requirements for expulsion, however, because the requirements could be calculated from supplimentary measurements.

(U) The results presented in Fig. 48 and 49 illustrate the liquid expulsion rate and propellant tank pressure as functions of time for the helium and blend expulsions. Comparison of the figures indicate the experimental runs were very similar. Comparison of the pressurant requirements show the blend requirements to be approximately 55 percent of the ambient helium requirements (Table 10). This is particularly significant in view of the fact that heavy heat-sink hardware was used in the expulsions. A more precise analysis of comparable applications in flight-weight hardware is presented in a subsequent section of this report.

(U) An attempt was made to evaluate the condensation characteristics of the blend reaction products in the alcohol. Samples of alcohol were taken during both the helium and blend pressurant runs. Each sample was analyzed for water content, since water is the only appreciably soluble reaction product. The samples from the helium and blend expulsions were analyzed and showed water contents of 0.05 and 0.24 weight percent, respectively. However, a material balance on the blend shows the maximum water contamination from this source to be 0.11 weight percent. This indicates that either the sample was contaminated or the alcohol used for the blend expulsions absorbed a significant quantity of water.

(U) Cryogenic Propellant Expulsions. Following completion of the expulsion experiments with the simulated storable propellants, similar runs were made with liquid nitrogen simulating a cryogenic propellant. These runs differed slightly from the previous runs with alcohol, the primary difference being that the cryogenic runs were conducted as a single steady expulsion rather than in three stages as with the storable propellant. The primary purpose in this run procedure modification was to eliminate propellant boil-off during the downtime between stages.

(U) The results of the expulsion runs are summarized in Table II and Fig. 50 and 51. An aborted run was made prior to the successful expulsion with the blend pressurant. A tantulum plate used to retain the catalyst bed became embrittled and broke immediately upon initiation of the low-temperature, nitrogen expulsion. The plate was replaced with a stainless-steel plate which would not embrittle at liquid nitrogen temperatures, and a successful run was accomplished. Figure 50 shows that the liquid expulsion rate with both the helium and the reacted pressurant decreased with time as the run progressed. This was caused by a drop in propellant tank pressure with time, resulting from the inability of the gaseous supply system to maintain constant pressure in the tank. The decreasing tank pressure was determined to have little effect on the test results. The tank pressure-time relationship is shown in Fig. 51 for both runs.

(U) The results of these runs indicate that the heated gas requirements are approximately 31 percent of those observed with the helium pressurant. The previous remarks concerning pressurant enthalpy loss to the heavy tank walls and flanges apply in this case as well. The problem of measuring gas temperatures inside the propellant tank encountered in the storable propellant expulsion were also observed in the runs with liquid nitrogen. The effect was less pronounced, as the boiling rate of liquid nitrogen on the thermocouple surface was sufficiently fast to provide essentially "dry" thermocouple junctions. Thus, the hot-gas temperature was observed almost immediately after the liquid interface fell below the thermocouple level.

TABLE 11

SUMMARY OF RESULTS OF LIQUID NITROGEN EXPULSION EXPERIMENTS

	Pressurant			
	Helium		Blend	
	Initial	Final	Initial	Final
Propellant weight, pounds	185	0	185	0
Pressurant injection temperature, F	70.5	63.2	1478	1569
Propellant tank pressure, psig	300.4	172.3	321.6	155.2
Internal tank temperature, F.				
Top position	-298	-110	-332	54
Middle position	-277	-260	-308	-192
Bottom position	-276	-309	-286	-314
External tank wall temperature, F				
Top position	-311	-311	-319	-294
Middle position	-323	-323	-319	-318
Bottom position	-302	-395	-296	-318
Pressurant consumption, pounds	- - -	0.781	- - -	0.246

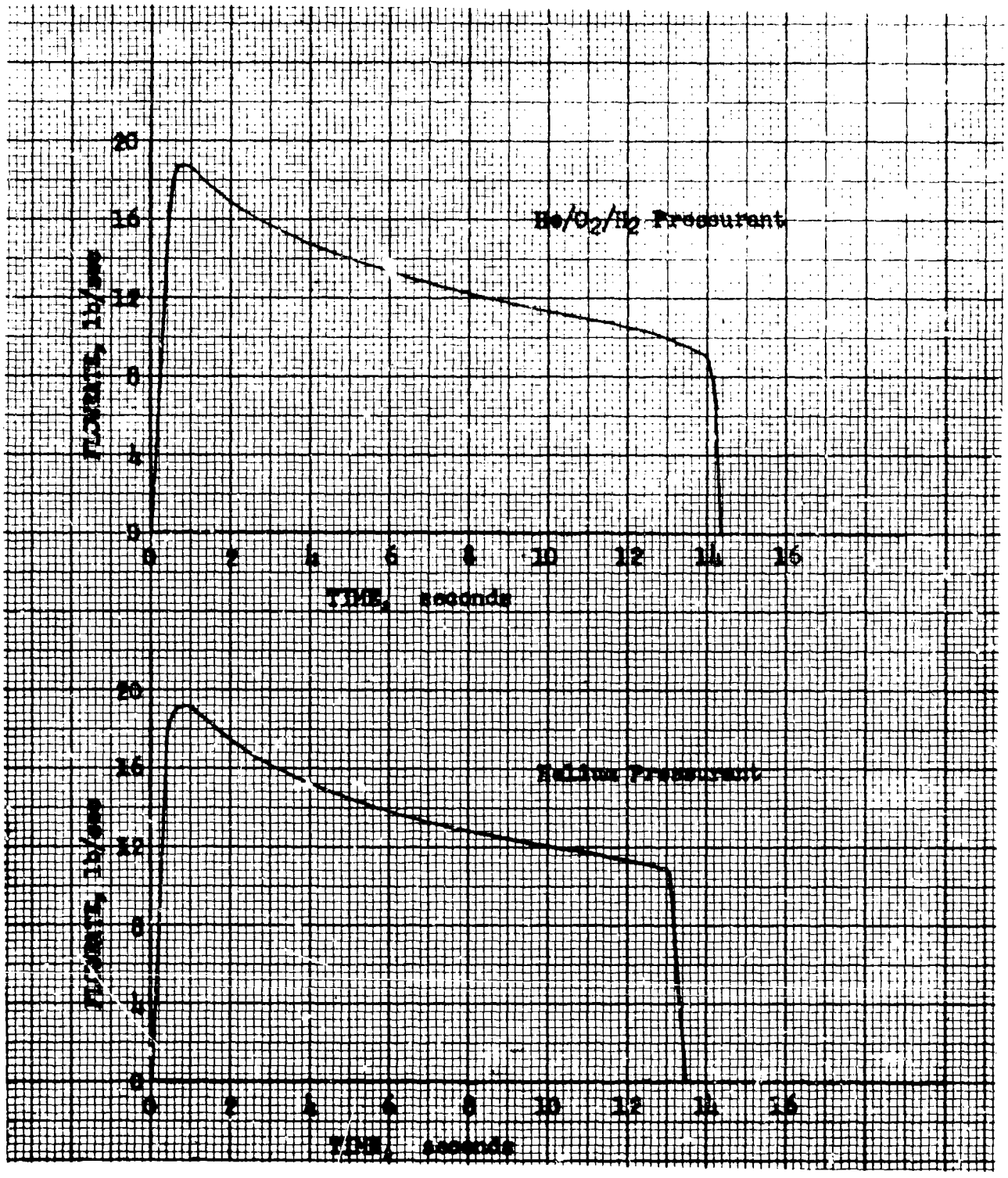

Figure 50. Liquid Nitrogen Flowrate as a Function of Time for Expulsion Demonstration Tests

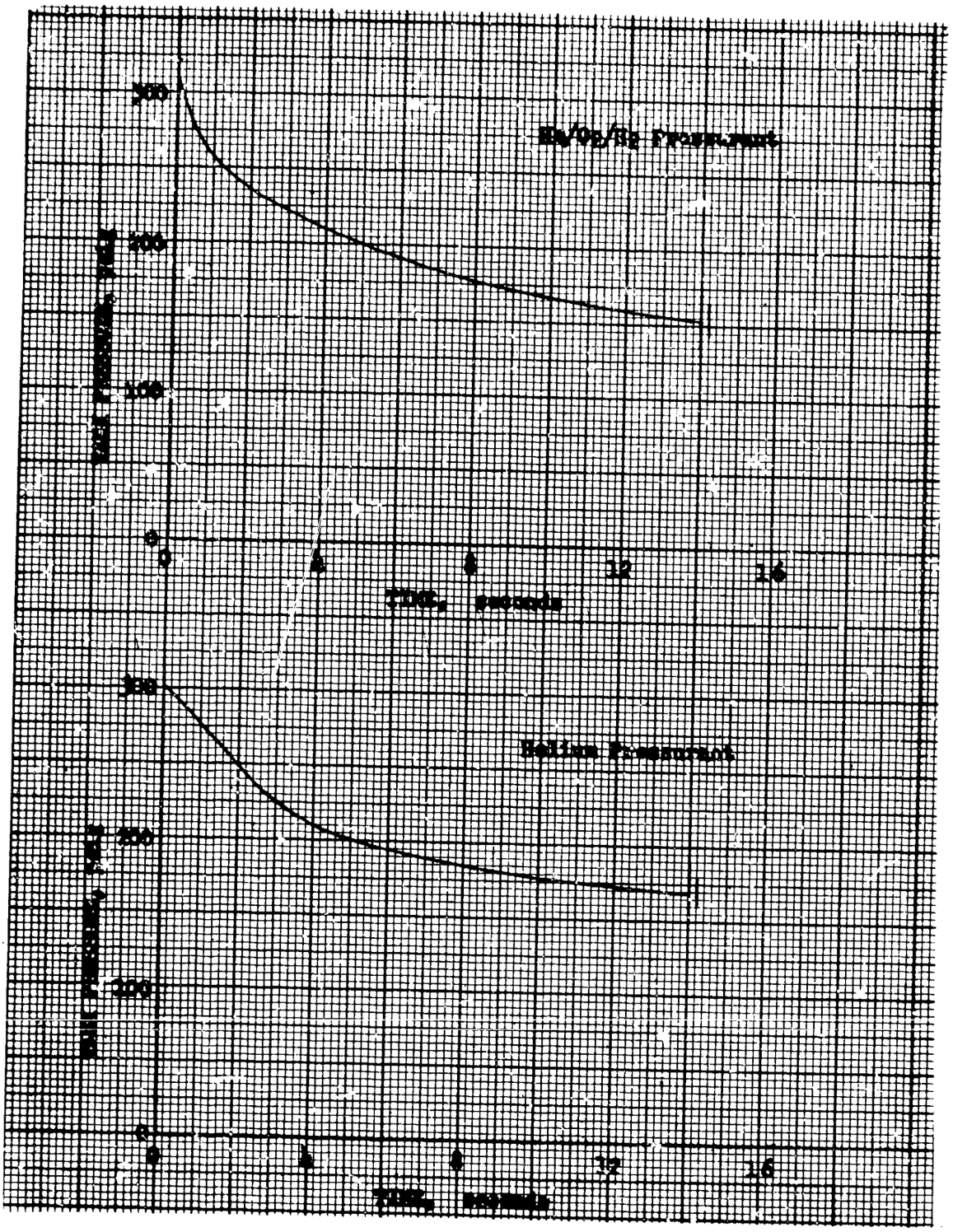

Figure 51. Tank Pressure as a Function of Time for the LN_2 Expulsion Tests

Although the 69 percent reduction in pressurant requirements with the blow as compared to ambient helium is not directly applicable to a flight weight system, this rather conservative comparison indicates a strong application potential for given duty cycles.

PERFORMANCE ANALYSIS

(U) The major analytical tasks of the program consisted of establishing accurate theoretical performance values and in providing performance efficiency determinations. Much of the analytical effort has been integrated into the previous sections in which performance has been discussed. The combustion parameters of the gas mixtures and a comparison of theoretical and experimental pressurization models are presented in this section. Additional details on gas mixture composition are shown in Appendix B.

(U) The Rocketdyne free-energy digital computer program was used to obtain theoretical combustion parameters for four different pressurant mixtures. The mixtures consist of small amounts of reactive gases in stoichiometric proportions homogeneously mixed with an inert diluent. The mixtures for study are:

1. Helium with oxygen and hydrogen
2. Helium with oxygen, hydrogen, and methane
3. Nitrogen with oxygen and hydrogen
4. Nitrogen with oxygen, hydrogen, and methane

(U) Figures 52 and 53 present the combustion parameters for $N_2/O_2/H_2$ and $He/O_2/H_2$, respectively. No effect of combustion pressure was noted in the range considered, 25 to 1000 psia. The helium mixture offers a significant weight advantage over the nitrogen mixture as the combustion products are about one-sixth of the weight of the nitrogen products at equal temperatures, pressures, and displacement volumes. This is shown in Fig. 52 and 53 by the combustion parameter (T/M) which is the combustion temperature (R) divided by the effective molecular weight of the combustion products. The water content of the products is shown as a percentage of total weight. The effect of pressurant water vapor content is strongly dependent on the heat transfer from the pressurant to the propellant tank walls. If the pressurant temperature is lowered sufficiently, condensation occurs. Comparison of Fig. 52 and 53 shows that the $N_2/O_2/H_2$ blend flame temperatures are less sensitive to composition changes than the $He/O_2/H_2$ blend

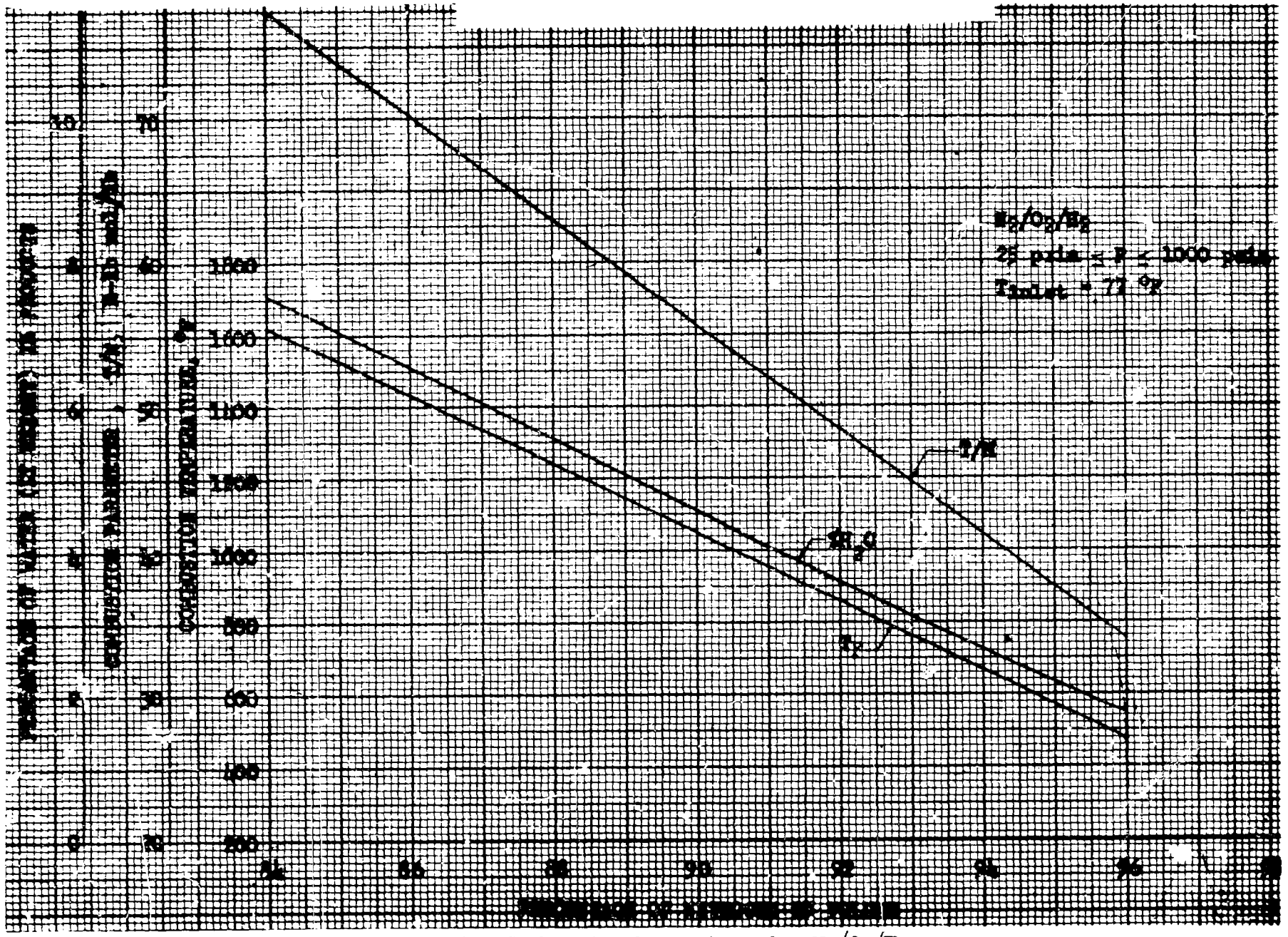

Figure 52. Combustion Parameters for $N_2/O_2/H_2$

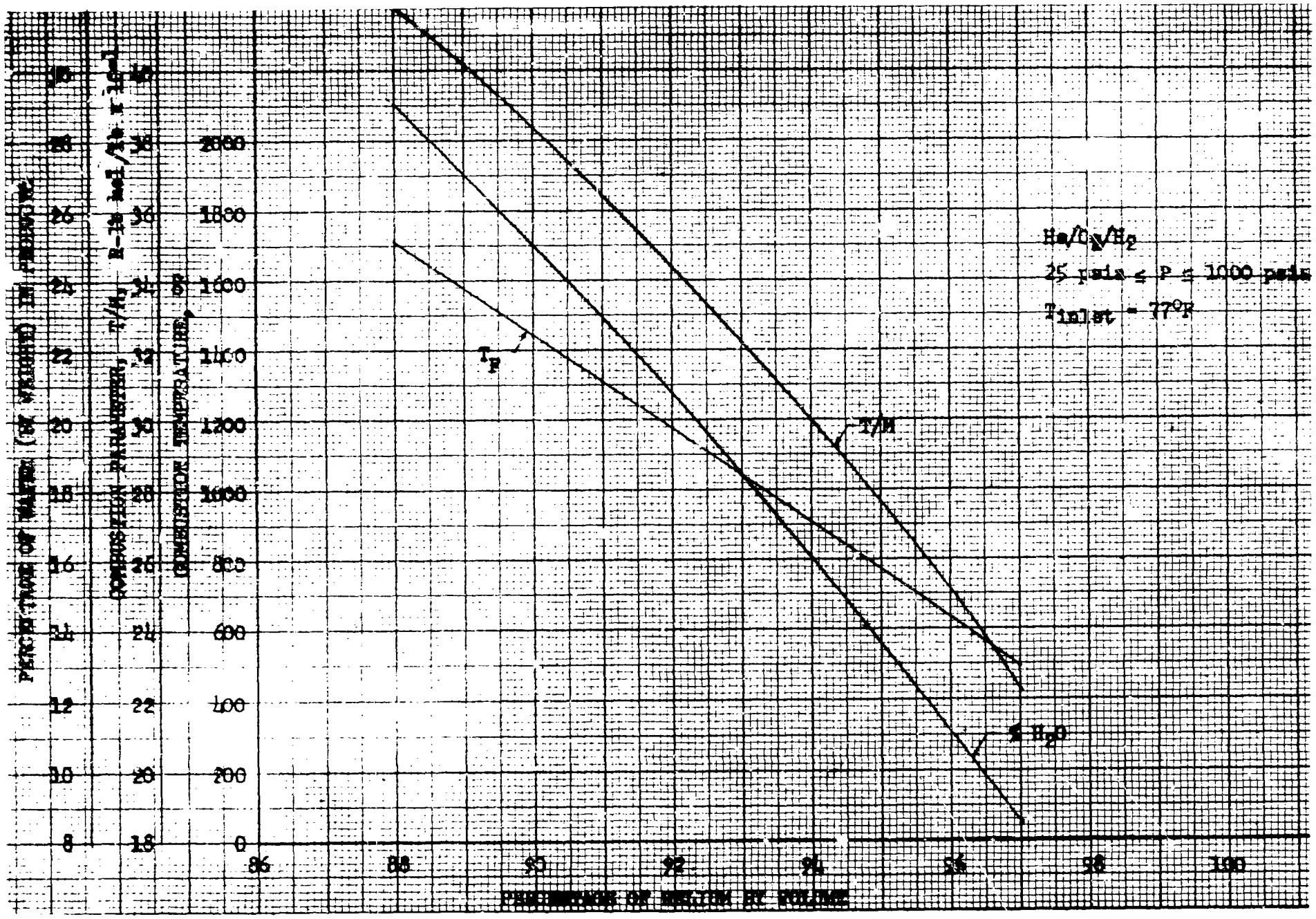

Figure 53. Combustion Parameters for $He/O_2/H_2$

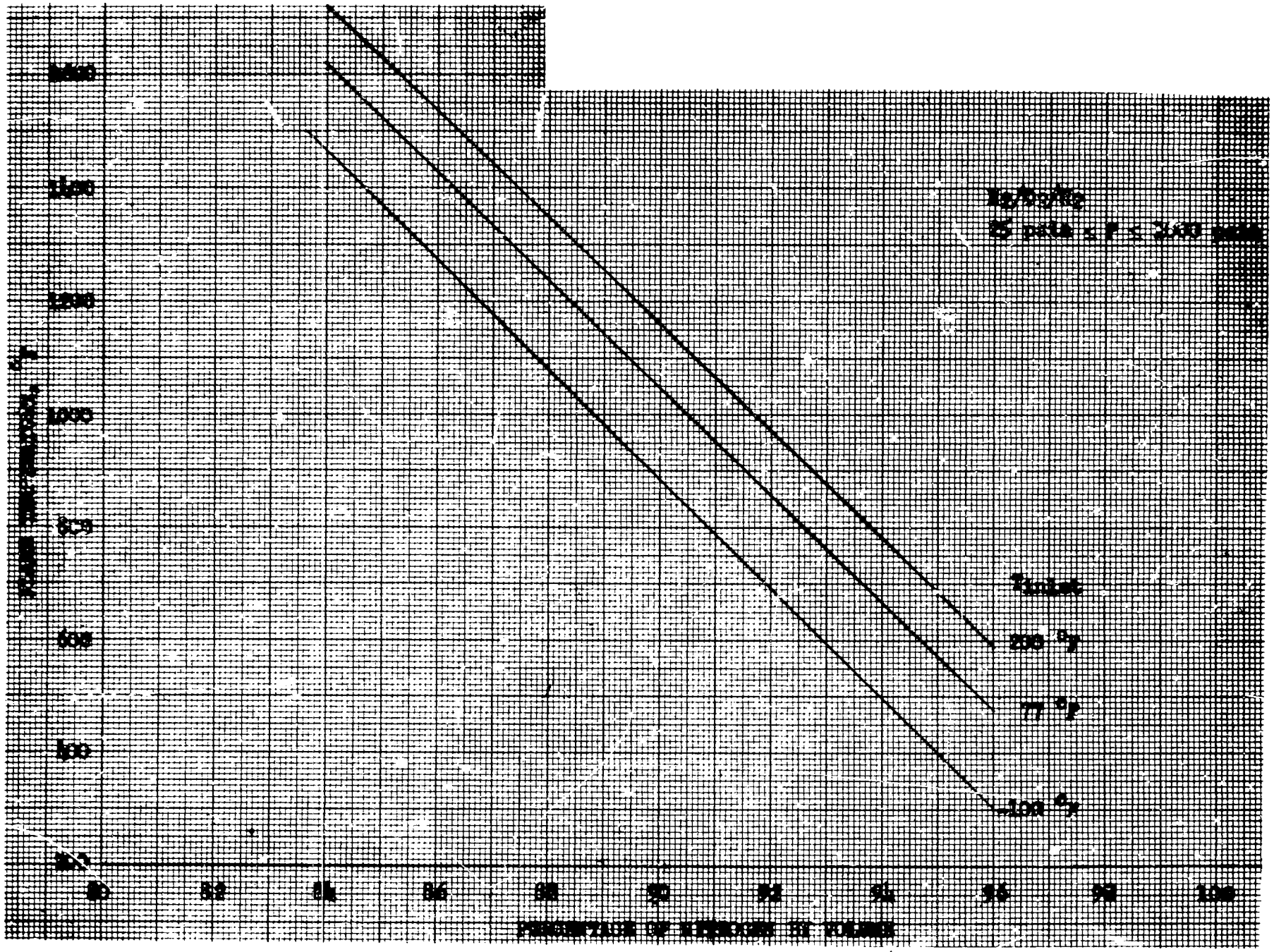

Figure 54. Effect of Inlet Temperature on Flame Temperature for $N_2/O_2/H_2$

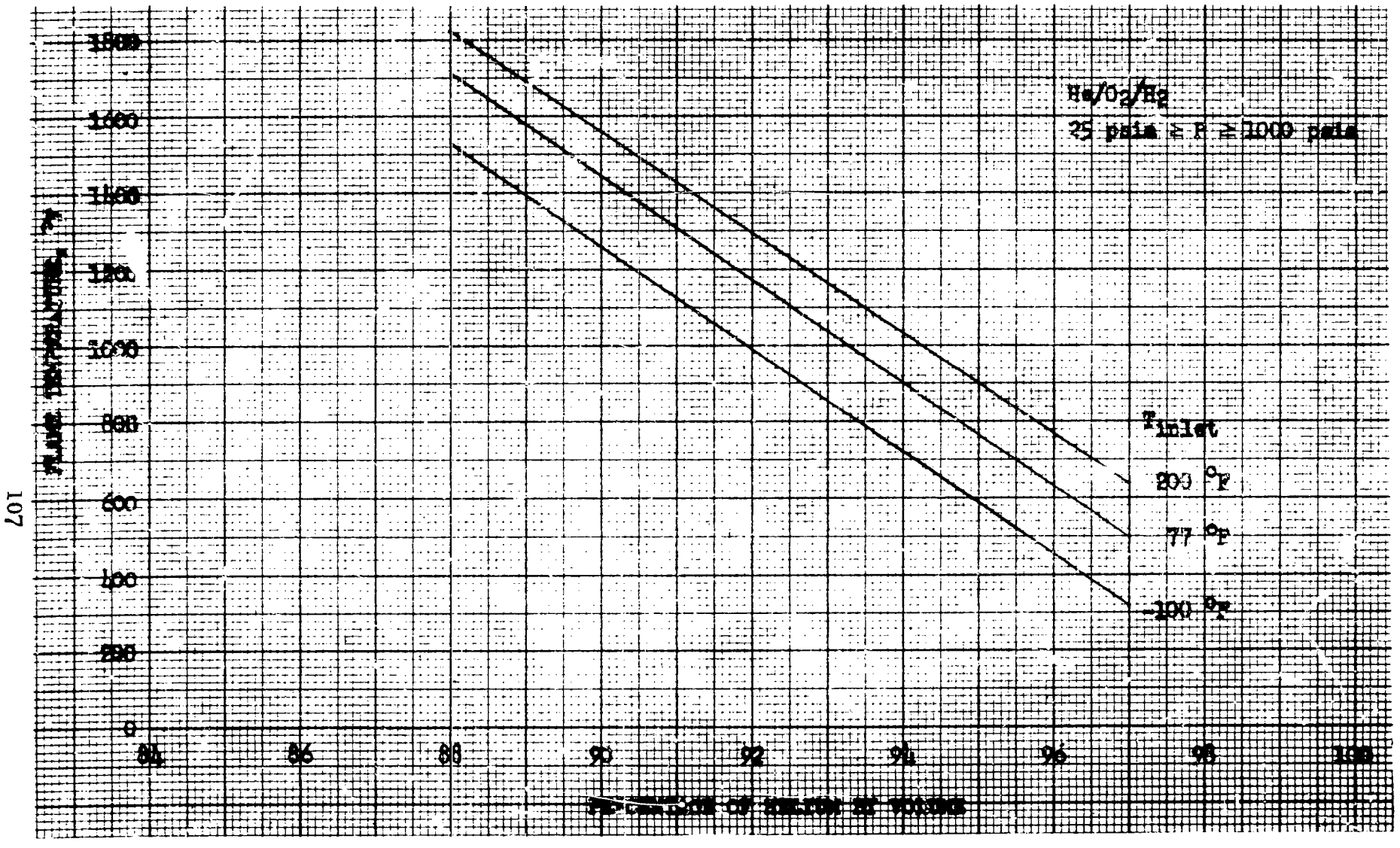

Figure 35. Effect of Inlet Temperature on Flame Temperature for $He/O_2/H_2$

(U) The effect of inlet temperature on the above mixtures is shown in Fig. 54 and 55. At inlet temperatures of 200 F, reactive gas contents of 9.5 percent for the helium mixture and 13.6 percent for the nitrogen mixture should not be exceeded because of the present steady-state operational limit on the catalyst bed temperature of 1500 F.

(U) The effects of substituting methane as an additional reactive agent is shown in Fig. 56 and 57, which present combustion parameters for $N_2/O_2/H_2/CH_4$ and $He/O_2/H_2/CH_4$, respectively.

(U) The methane mixtures were established with sufficient stoichiometric amounts of oxygen and hydrogen to raise the gaseous mixture temperature to at least 500 F. At 500 F, a substantial margin is provided to ensure complete catalytic reaction of the methane and the remaining oxygen. The oxygen-methane reaction has been found to be responsive to catalytic ignition at temperatures of about 300 F.

(U) Figure 58 shows the effects of inlet temperature on combustion temperature for $N_2/O_2/H_2/CH_4$ and $He/O_2/H_2/CH_4$ mixtures. Comparison curves of water content of combustion products as functions of inlet temperatures for the nitrogen and helium mixtures are presented in Fig. 59 and 60.

(U) Using the theoretical data presented in Fig. 52 through 60, a preliminary pressurization system weight estimate was made to screen the candidate propellants for the Phase II and Phase III portions of this program.

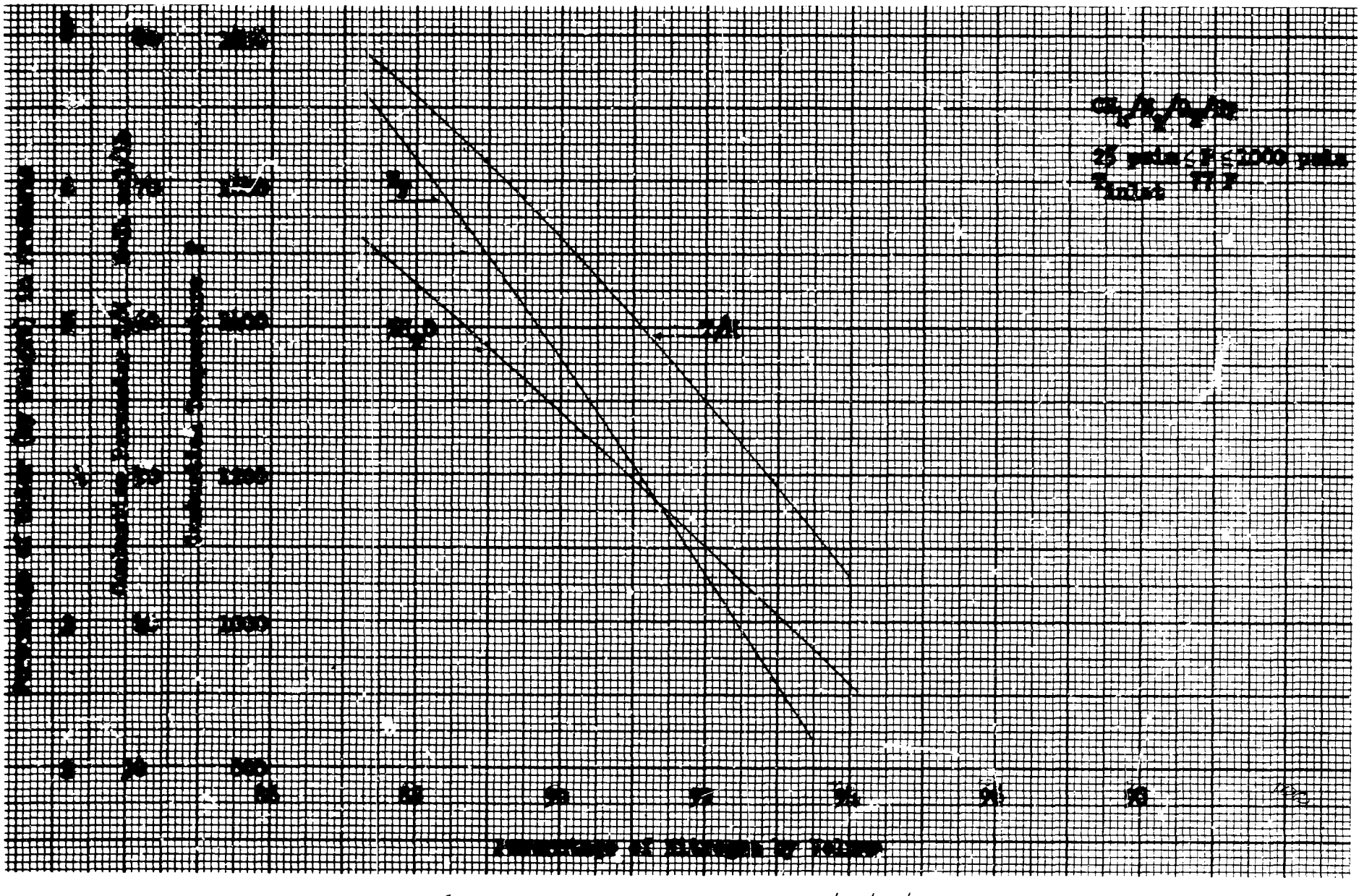

Figure 56. Combustion Parameters for $N_2/O_2/H_2/CH_4$

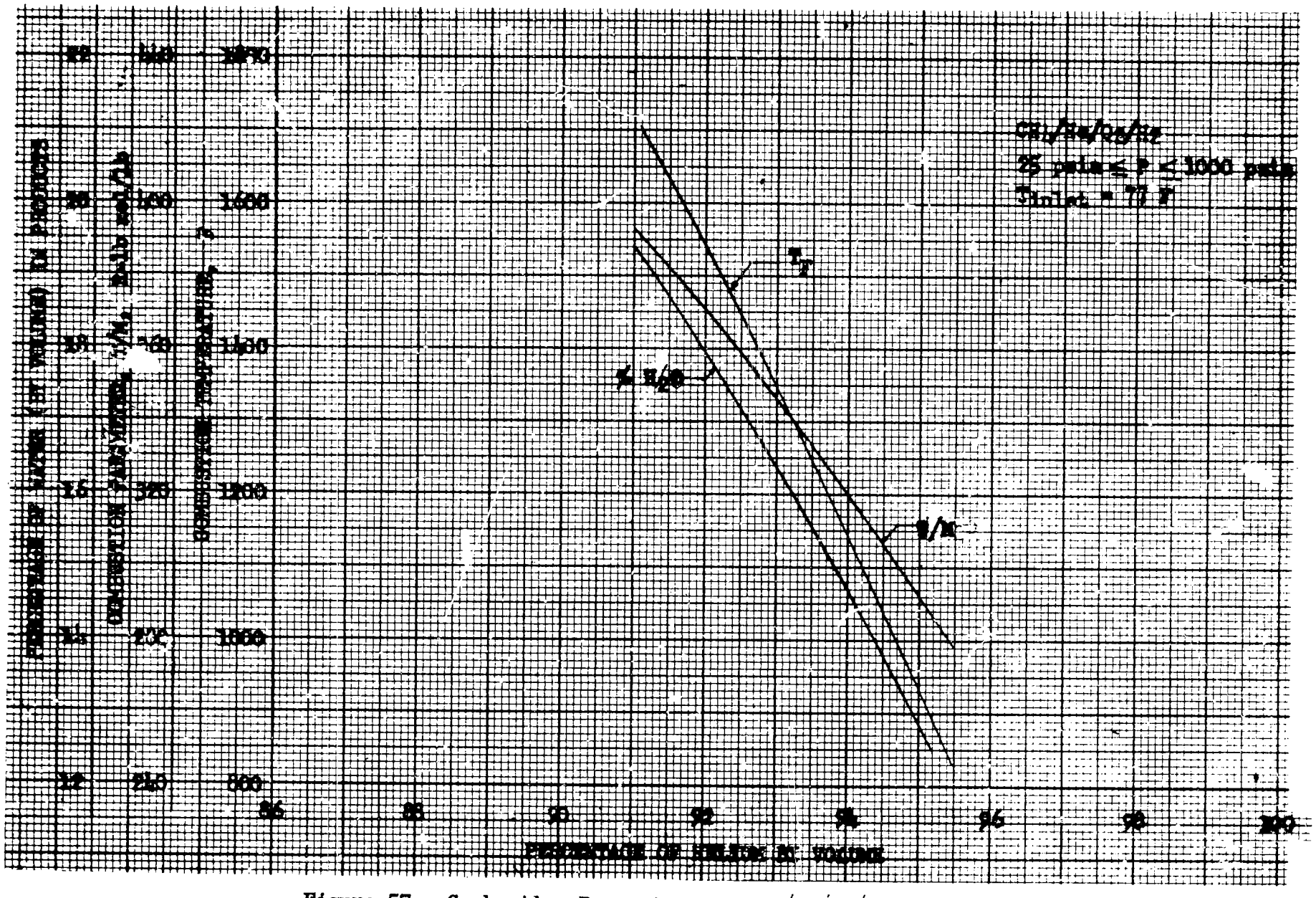

Figure 57. Combustion Parameters for $He/O_2/H_2/CH_4$

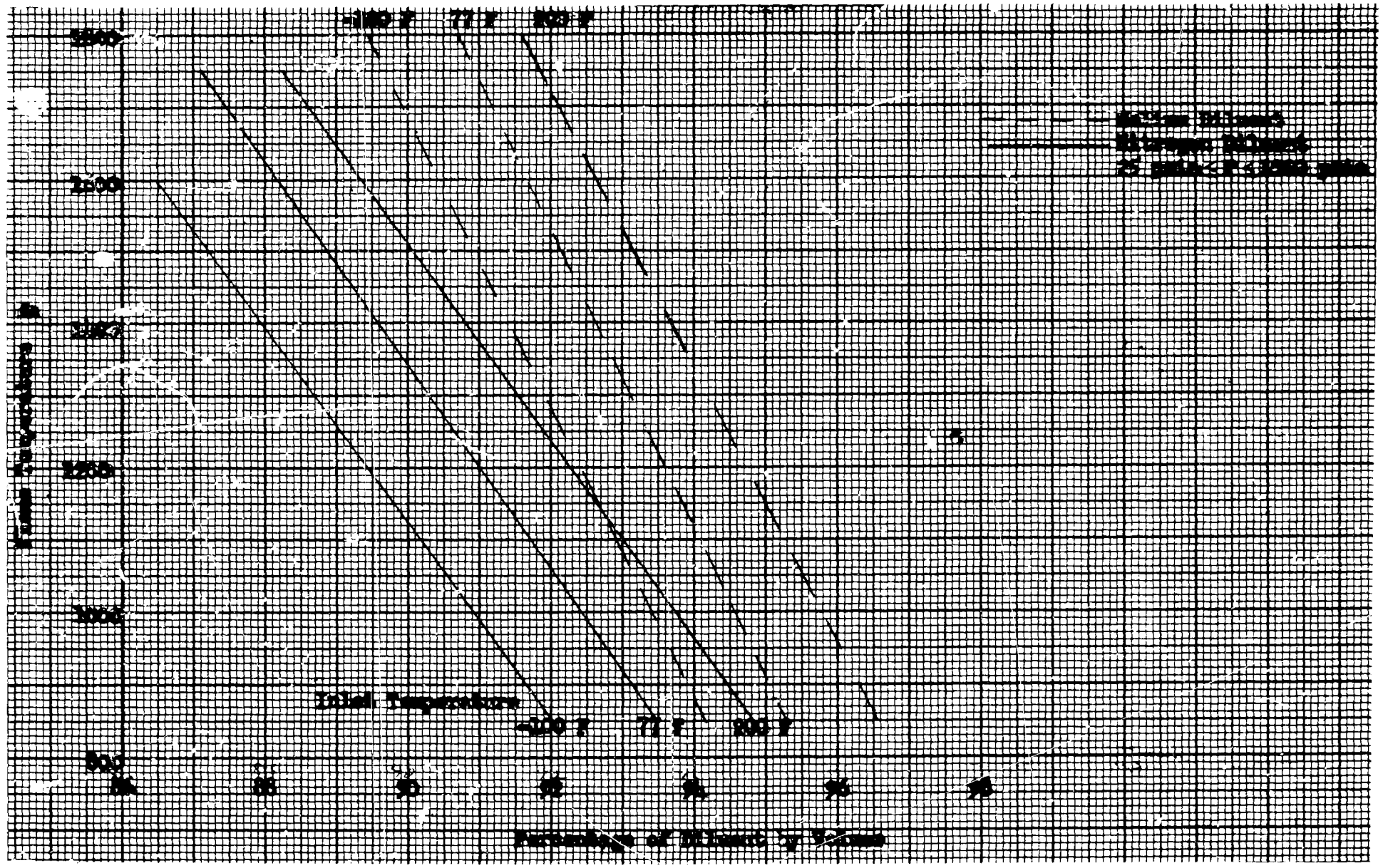

Figure 58. Effect of Inlet Temperature on Flame Temperature for He and N_2 Diluents with $O_2/H_2/CH_4$

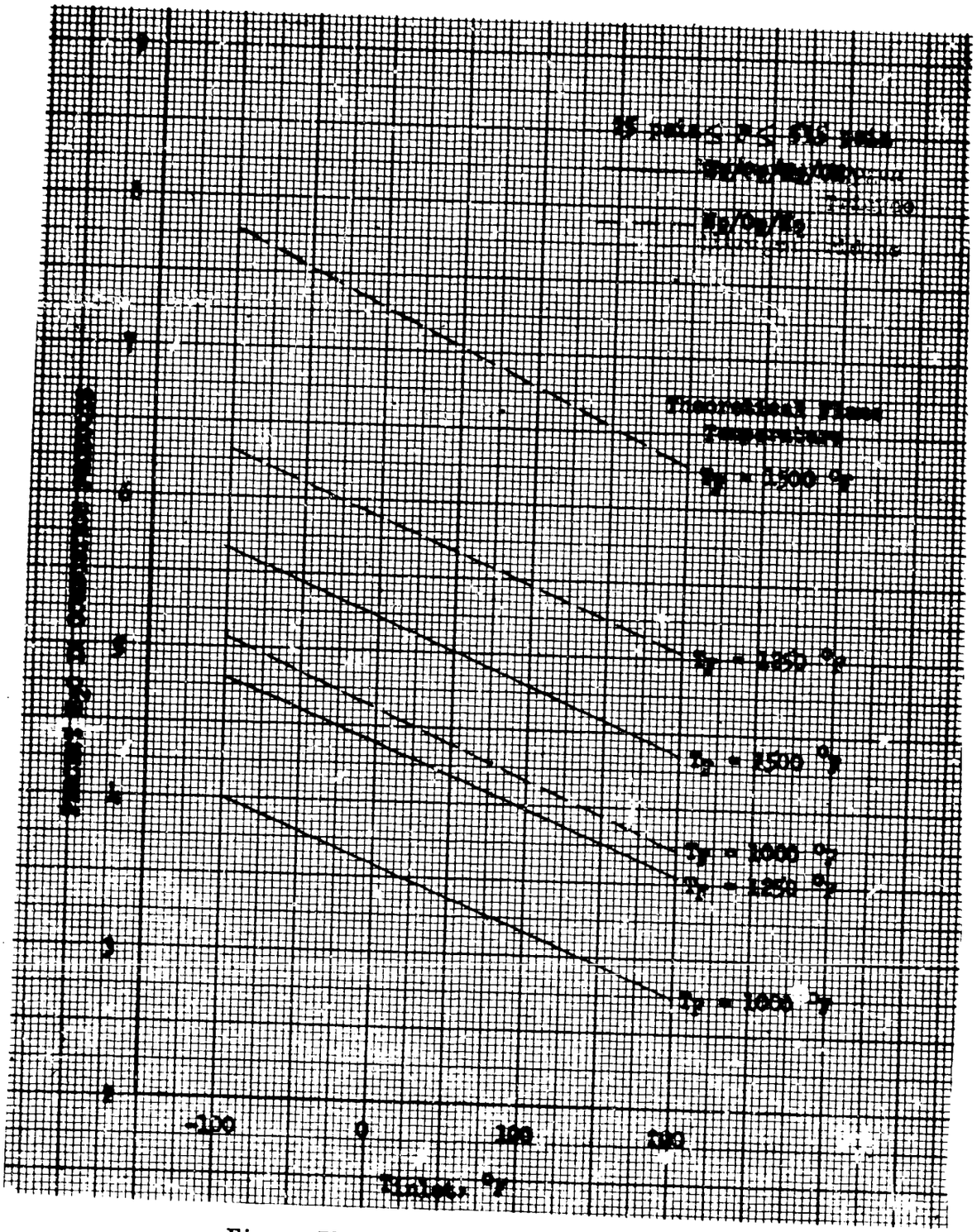

Figure 59. Water Content of $N_2/O_2/H_2$ and $N_2/O_2/H_2/CH_4$ Mixtures

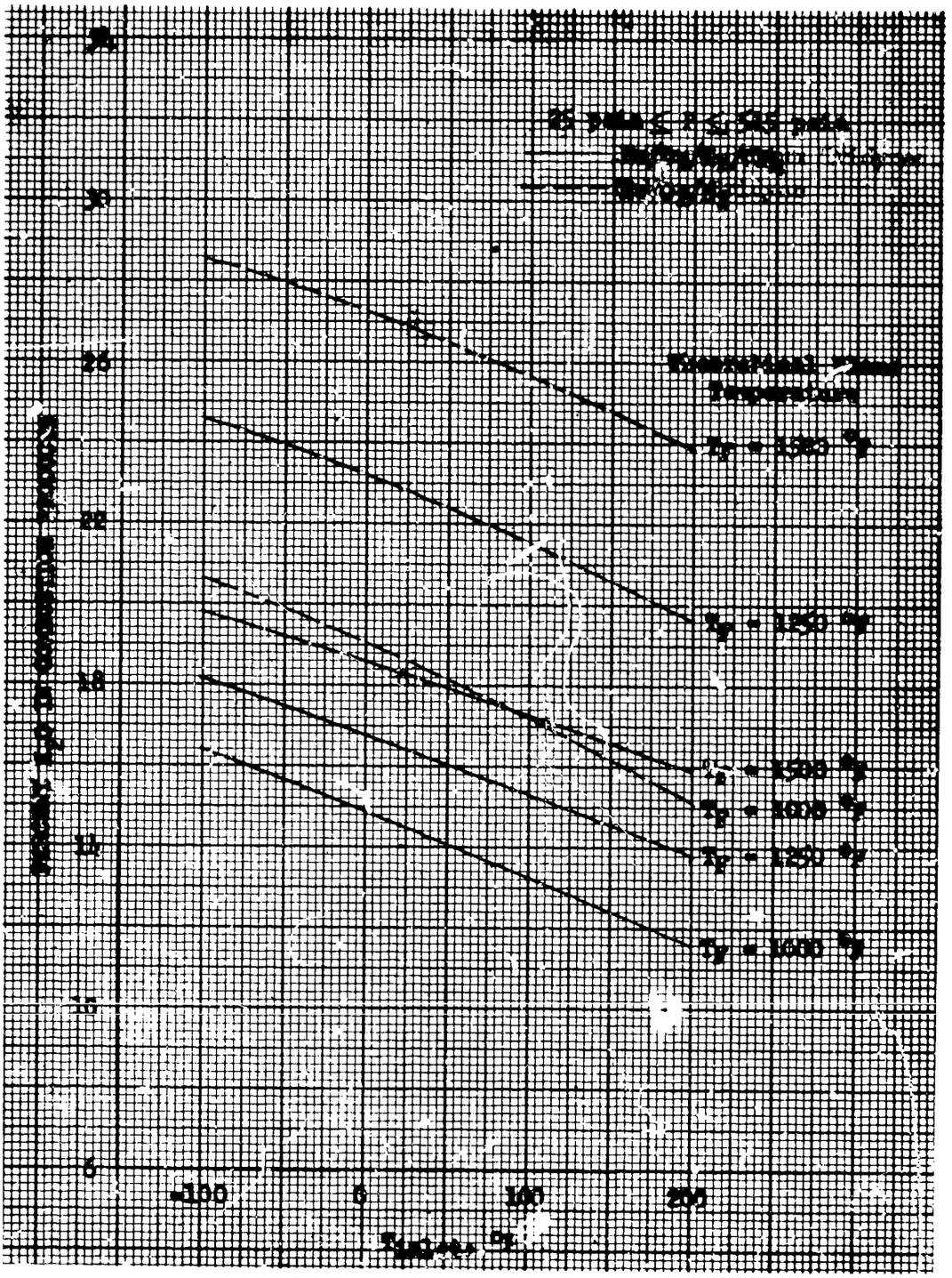

Figure 60. Water Content of $He/O_2/H_2$ and $He/O_2/H_2/CH_4$ Mixtures

(U) Table 12 shows that a significant weight advantage can be obtained using the helium diluent systems rather than the nitrogen diluent systems. This is primarily because of the large difference in molecular weight that exists between the two diluents. The addition of methane as one of the reactants increases the amount of required pressurant by about 3 percent. The water content of the combustion products, however, is reduced to about 68 percent of the $He/O_2/H_2$ value in the high-temperature case, and to about 80 percent of the $He/O_2/H_2$ value in the low-temperature case by using the methane additive in the reactant.

(U) The effects of combustion product water content were determined using the Rocketdyne digital computer pressurization program. This program computes the system pressurant requirements including the effects of heat transfer, water condensation, and duty-cycle variations. Appendix A details the equations utilized in this computer program.

(U) The digital computer pressurization program was used to size a 150,000 lb-sec total impulse attitude control system which utilizes an N_2O_4/MMH propellant combination. Calculations were performed defining the effects of combustion flame temperature on the pressurant weight requirements for the $He/O_2/H_2$ and $N_2/O_2/H_2$ mixtures at propellant tank pressures of 25 and 500 psia. Expulsion durations, assuming a linear continuous propellant depletion rate, of 400, 900, 1800, and 2400 seconds are compared in Fig. 61 through 64, respectively. The pressurant weights are relatively insensitive to flame temperature at pressures near 25 psia. This suggests the pressurant weight is not seriously affected by changes in flame temperature resulting from changes in inlet temperature caused by polytropic expansion. A more significant decrease in pressurant weight with increasing flame temperature is noted at the 500-psia pressures. The $N_2/O_2/H_2$ system displays a variance of up to 28 percent at the 500-psia pressure. The increase of water condensation with increasing combustion temperature results in a slight increase in pressurant weight for the $He/O_2/H_2$ system at 25 psia as more water is formed at the higher temperature. At higher pressures the heat losses and the resulting condensation are less, producing lower pressurant weight as flame temperature increases.

TABLE 12

PRELIMINARY RELATIVE WEIGHT COMPARISON

1500 F Combustion Temperature	$N_2/O_2/H_2$	$He/O_2/H_2$	$N_2/O_2/H_2/CH_4$	$He/O_2/H_2/CH_4$
Pressurant Weight, pounds	68	12.5	69.9	13.62
Tank Weight, pounds	85.5	84.3	82.7	86.5
Regulator, Fill Valve, Isolation Valve, and Check Valve, pounds	13.5	13.5	13.5	13.5
TOTAL, pounds	167.0	110.5	166.1	113.6
Water in Combustion Products, percent	6.92	25.85	4.84	17.65
900 F Combustion Temperature				
Pressurant Weight, pounds	98.9	16.60	102.1	17.15
Tank Weight, pounds	119.0	119.2	120.5	122.0
Regulator, Fill Valve, Isolation Valve, and Check Valves, pounds	13.5	13.5	13.5	13.5
TOTAL, pounds	231.4	149.3	236.1	152.7
Water in Combustion Products, percent	3.80	14.9	3.00	12.54

T_{inlet} = 77 F

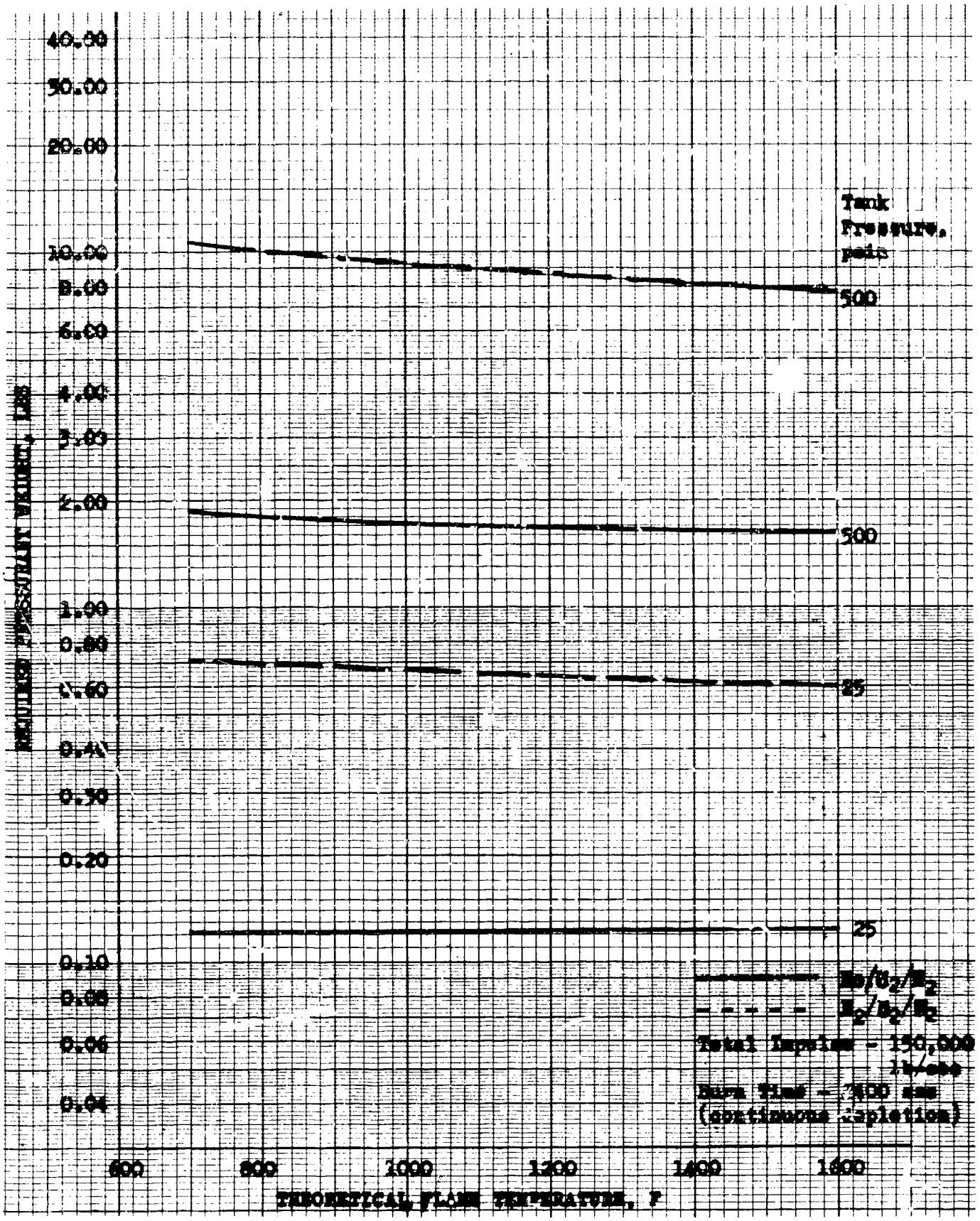

Figure 61. Effect of Flame Temperature on Pressurant Weight (a)

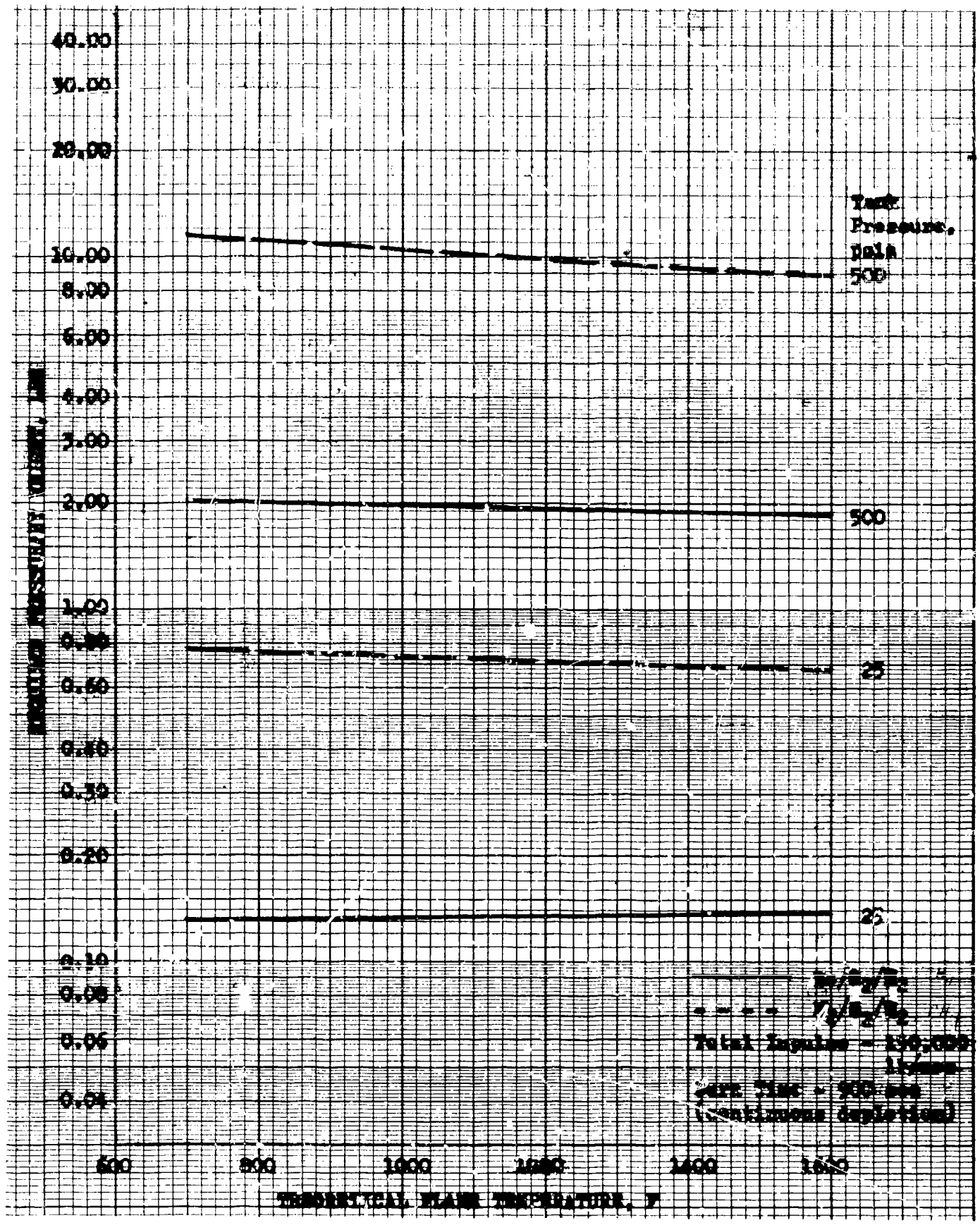

Figure 62. Effect of Flame Temperature on Pressurant Weight (b)

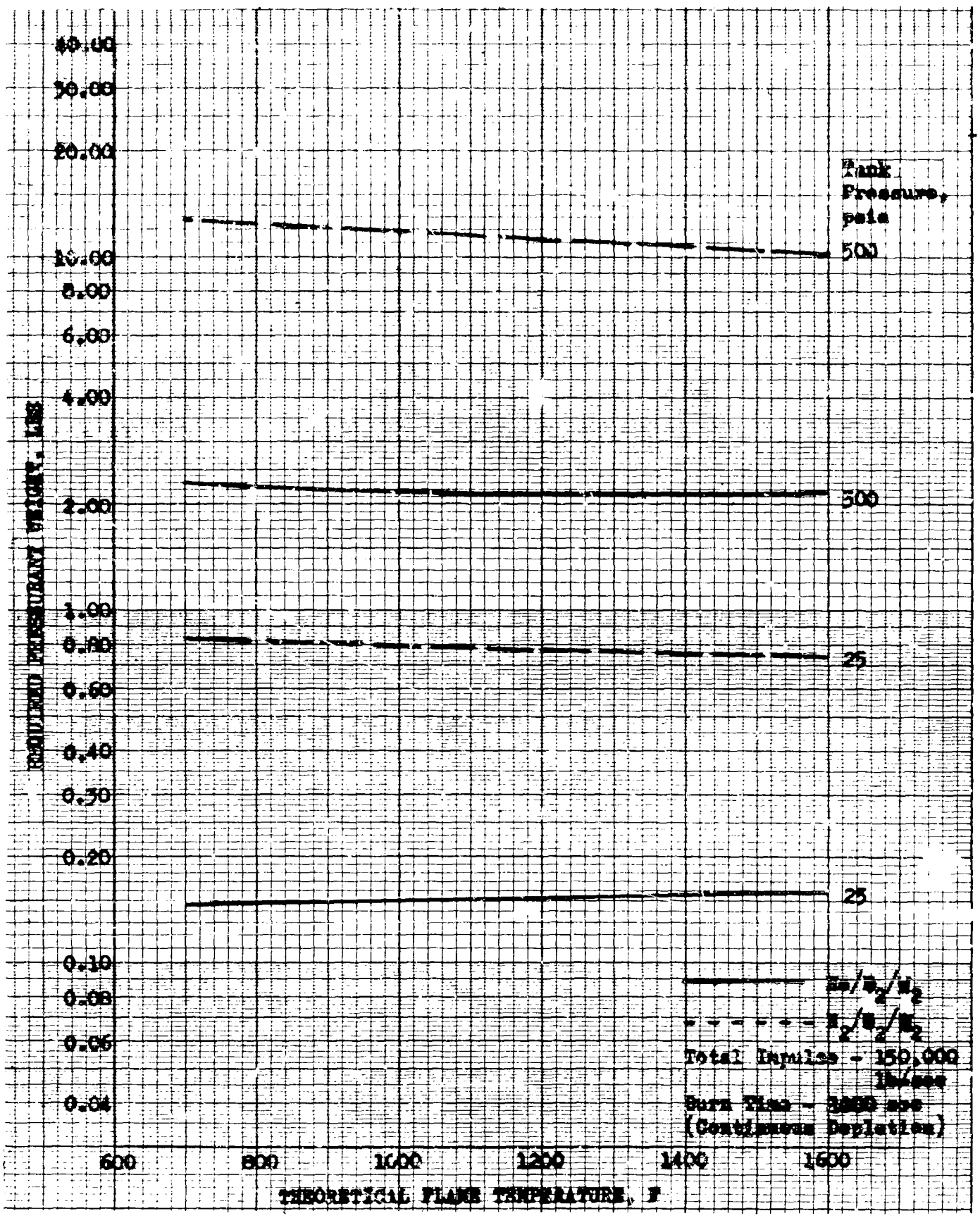

Figure 63. Effect of Flame Temperature on Pressurant Weight (c)

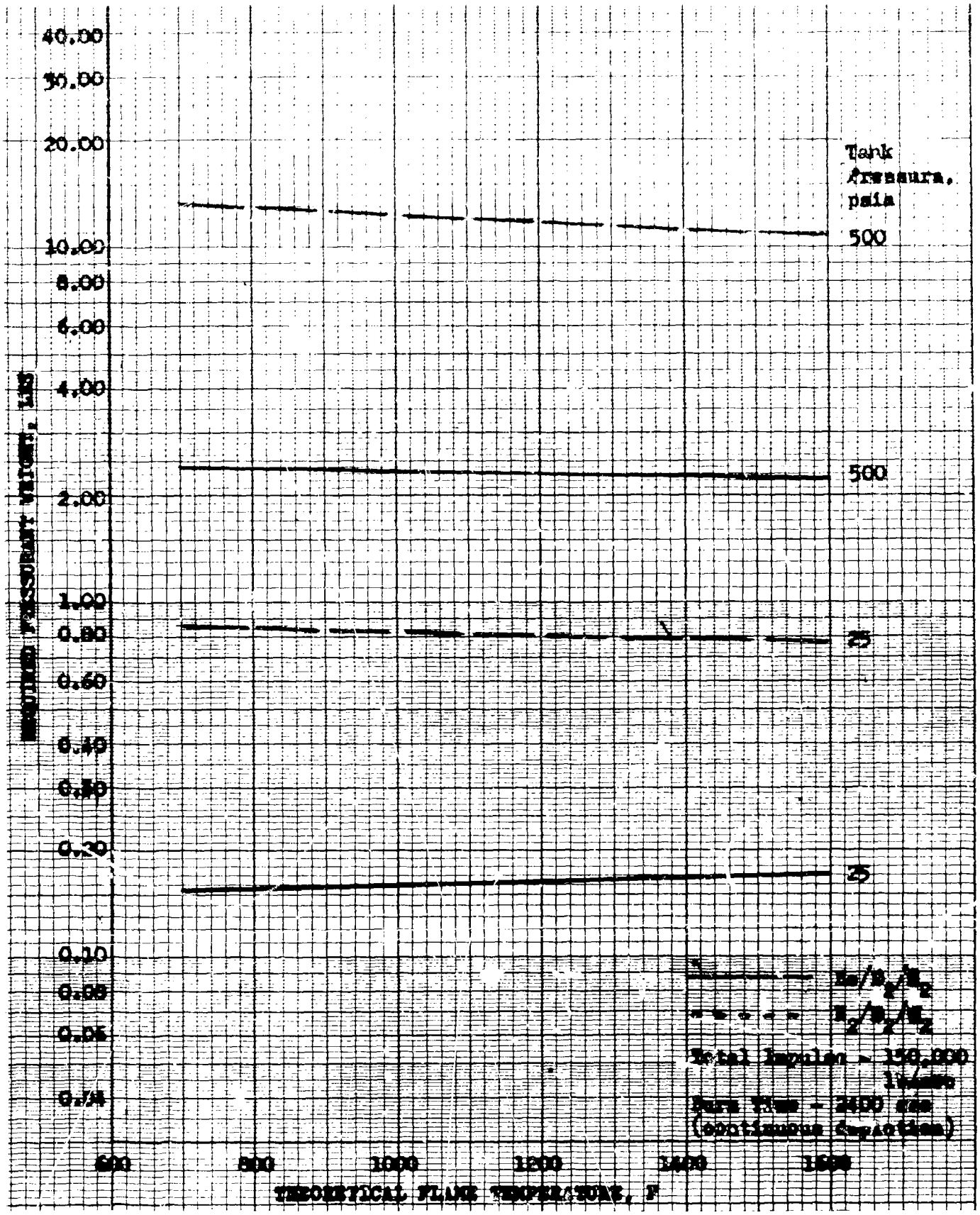

Figure 64. Effect of Flame Temperature on Pressurant Weight (d)

(U) Figures 67 through 68 present comparable parametric values for $He/O_2/H_2/CH_4$ and $N_2/O_2/H_2/CH_4$. The helium mixtures at 25 psia show a weight decrease at increasing flame temperatures as a result of a lower water content in the combustion products. Here, also, a pressurant weight [illegible] of up to 27 percent is shown at 500 psia for the nitrogen mixture. Comparison of the pressurant weights for mixtures containing methane and without methane, considering equivalent displacement volumes and [illegible] diluent gas, shows a slight weight increase results from the methane addition. This result is caused by the higher effective molecular weight of the combustion products which contain carbon dioxide. However, any defined propulsion system and mission duty cycle would require a separate evaluation because of heat transfer effects and water condensation variations with time.

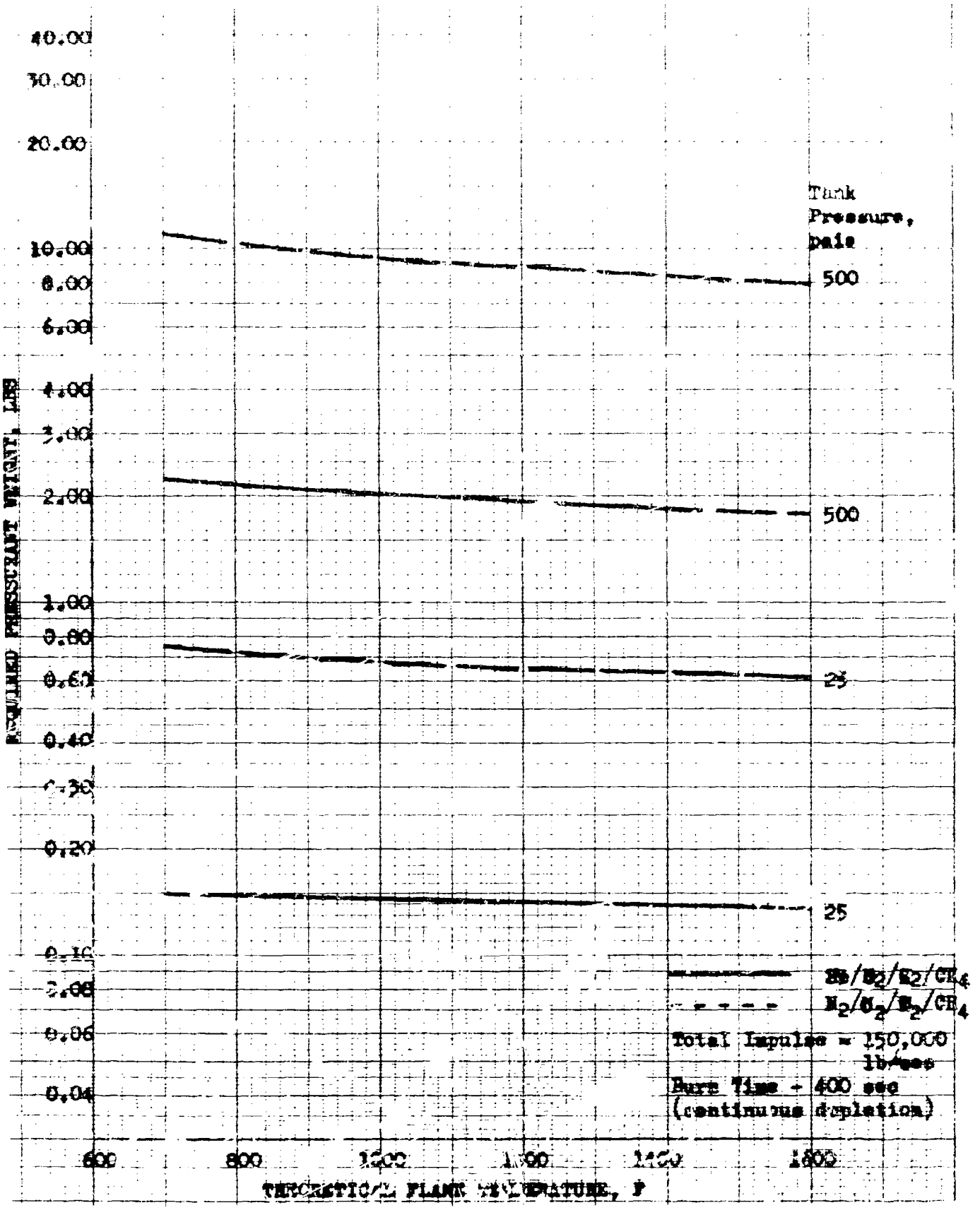

Figure 6j. Effect of Flame Temperature on Pressurant Weight (e)

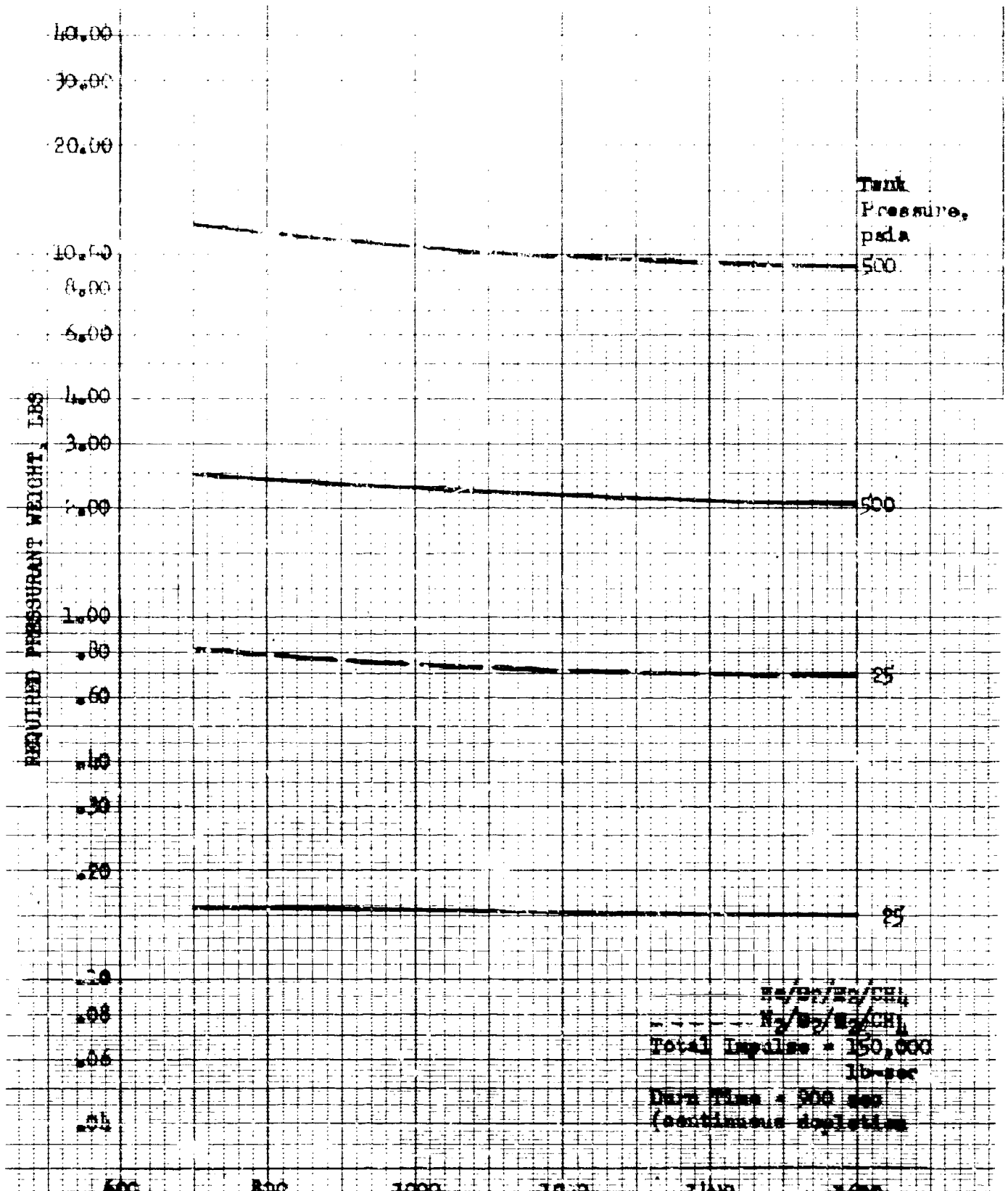

Figure 66. Effect of Flame Temperature on Pressurant Weight (f)

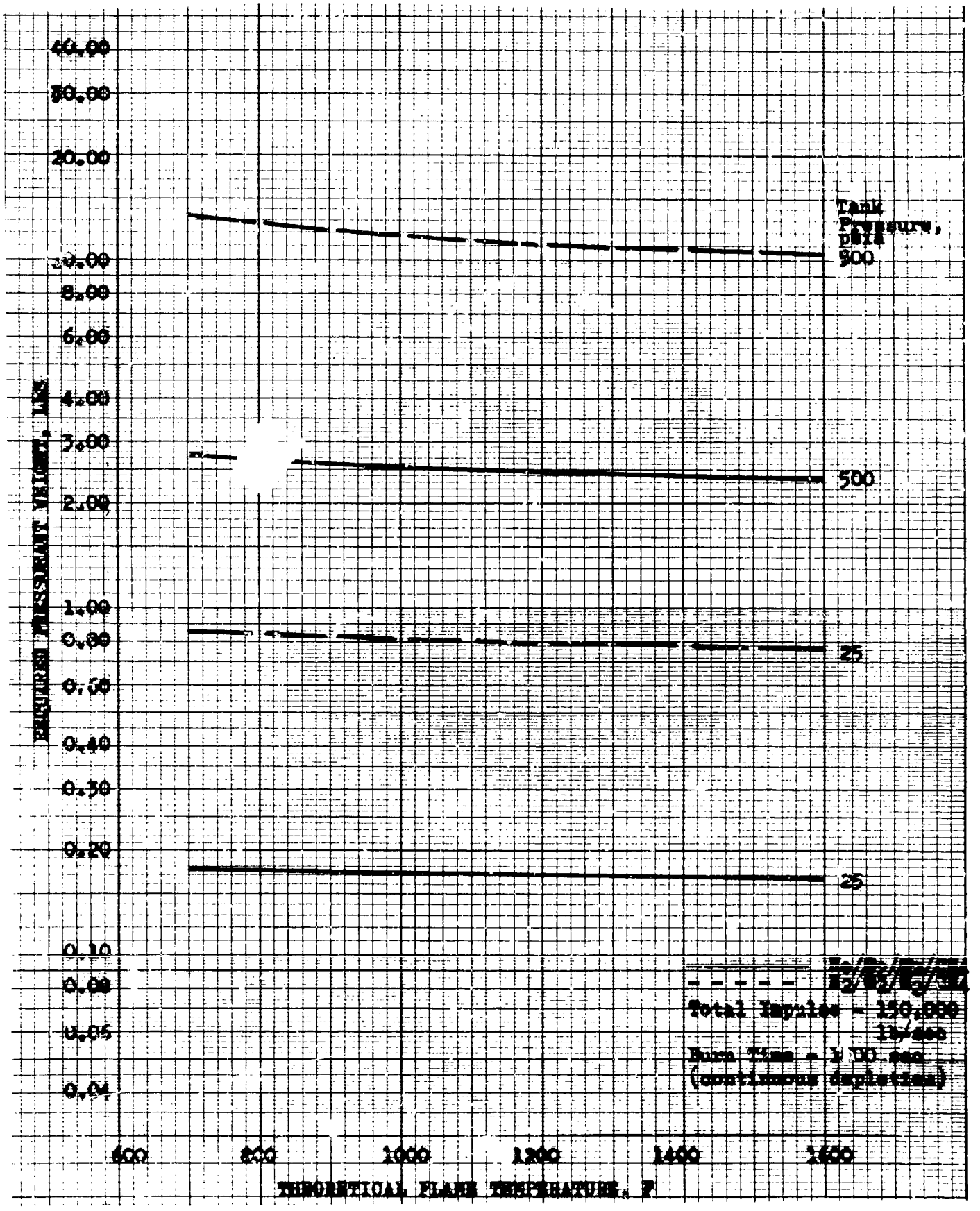

Figure 67. Effect of Flame Temperature on Pressurant Weight (g)

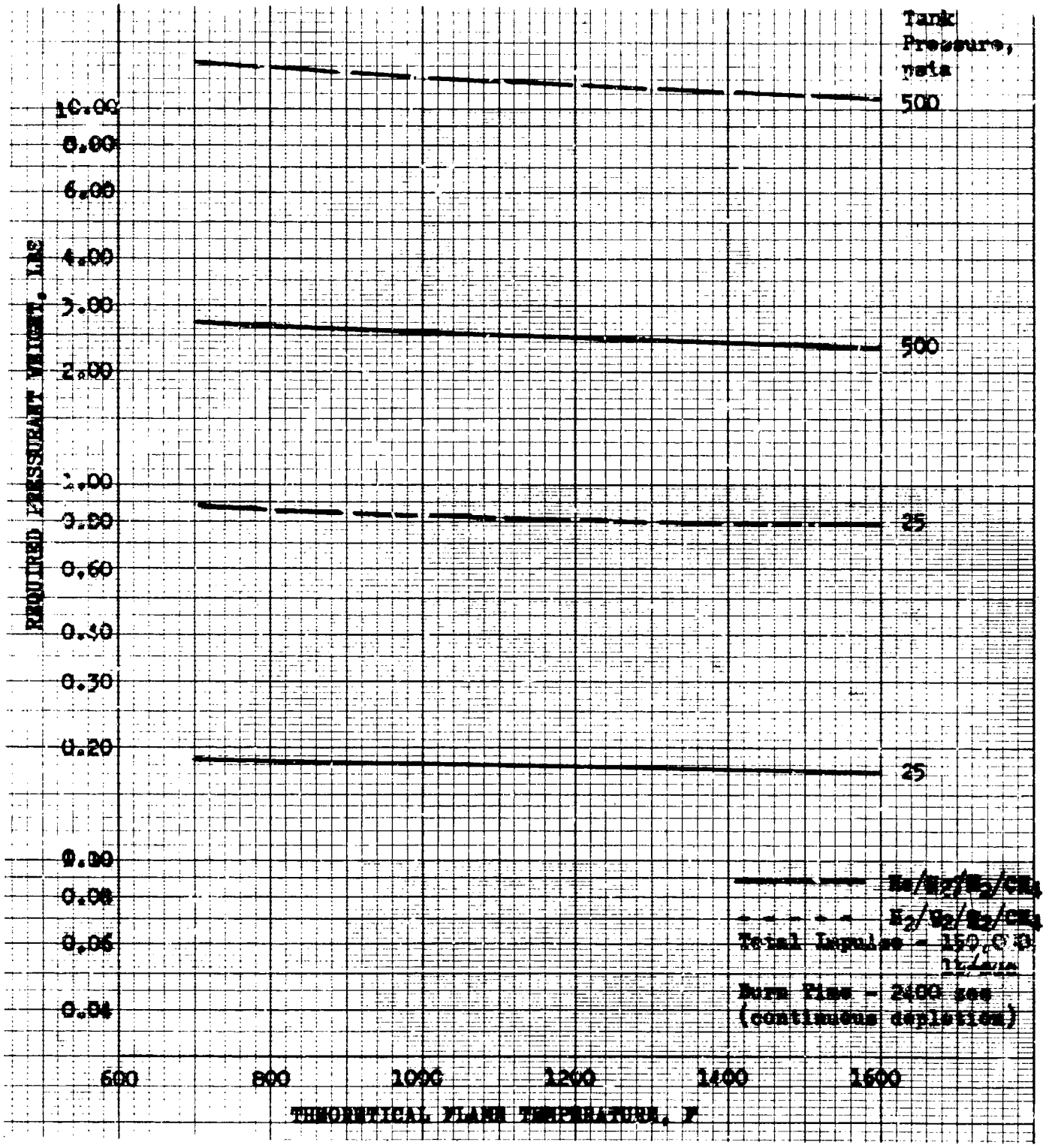

Figure 68. Effect of Flame Temperature on Pressurant Weight (h)

COMPARISON OF EXPERIMENT WITH THEORY

(U) A summary of the data obtained from the program experiments and predicted values is presented in Table 13. The experimental pressurant quantities were obtained by using two independent methods. The first method integrated the pressurant flowrate with respect to time, while the second method used the initial and final pressurant tank pressures and temperature, which were corrected for compressibility effects. Reasonable agreement was obtained between the two methods which showed differences of less than 4 percent for the alcohol expulsion tests and less than 8 percent for the LN_2 expulsion tests. Later comparisons with predicted values are based on the integrated flowrates.

(U) The analytical predictions for both the helium pressurant and the catalytically reacted pressurant were obtained from the digital computer program described in Appendix A. Although the computer model includes the effects of expellant vapor, the analytical quantities shown in Table 13 are for the weights of pressurant only.

(U) Very good agreement between the analytical predictions and the experimental data is noted for both of the alcohol expulsion tests. The predicted values of required pressurants are within 15 percent of the experimental quantity for the helium pressurant tests and within 4.5 percent for the catalytically reacted pressurant tests. Additionally, the analytical computer model predicts an average propellant tank wall temperature of 573 R for the blended pressurant expulsion tests, while the average experimentally measured temperature is approximately 550 R. Close agreement between the analytical and experimental tank wall temperature is also shown for the helium expulsion tests. However, a large discrepancy is shown between the average pressurant temperature predicted by the computer program and those obtained experimentally. The measured temperatures were found to agree closely to the boiling temperature of alcohol at the expellant pressure. The pressurant thermocouple installations apparently retained expellant fluid which vaporized during the expulsions and resulted in the recording of fluid vaporization temperatures rather than those of the pressurant. The same effect influenced the pressurant temperature recordings during the LN_2 expulsion tests.

TABLE 13

COMPARISON OF ANALYTICAL PREDICTIONS AND EXPERIMENTAL DATA

		Helium Expelling Isopropyl Alcohol	$He/O_2/H_2$ Expelling Isopropyl Alcohol	Helium Expelling LN_2	$He/O_2/H_2$ Expelling LN_2
Pressurant Weight Analytically Obtained, pounds		0.502	0.339	0.601	0.253
Pressurant Weight Experimentally Obtained Using Pressurant Tank Pressures and Temperatures, pounds		0.562	0.331	0.882	Unavailable
Pressurant Weight Experimentally Obtained by Integrating Pressurant Flowrate, pounds		0.585	0.324	0.781	0.246
Average Pressurant Temperature After Run (Analytical), R		537	947	409	1075
Propellant Tank Pressurant Temperature (Experimental), R	Top Position	532.6	765.9	350	514
	Middle Position	537.9	774.4	200	268
	Bottom Position	535.2	768.1	151	146
Average Propellant Tank Wall Temperature (Analytical), R		537	573	146	162
Propellant Tank Wall Temperature (Experimental), R	Top Position	532.3	571.1	149	166
	Middle Position	529.2	544.2	167	142
	Bottom Position	535.7	535.5	142	142
Final Propellant Tank Pressure (Experimental), psia		191	179	186	169

(U) The LN_2 expulsion experiments presented some problems analytically as the nitrogen vaporization rate was difficult to estimate. However, the analytically predicted quantity of helium was within 23 percent of the measured value, and the quantity of $He/O_2/H_2$ predicted was within 3 percent of that measured. The computed tank wall temperatures agreed closely with the recorded values.

ESTIMATE OF SYSTEM WEIGHTS

(U) The weights of catalytically reacted pressurization system can be closely approximated if careful attention is applied in estimating the weight of each component. Figure 69 is a schematic representation of a typical catalytically reacted pressurization system showing the major components. The weights of most of the components (such as regulators, check valves, fill valves, etc.) can be obtained by reference to detailed weight lists of systems similar in size to the one being considered. Three components, however, require weight calculations to be made specifically for each selected system. These are the pressurant weight, pressurant tank weight, and catalyst bed weight.

(U) The weight of pressurant needed to expel the propellants, as well as the final mixture temperature and average propellant tank wall temperature, can be determined by using the equations of the computer program detailed in Appendix A. This computer program has been developed utilizing a constant combustion temperature. Correcting to the operation conditions of an actual system involves some provision for the polytropic expansion of the pressurant. Figures 61 through 68 show that the quantity of catalytically heated pressurant calculated using the computer model should be increased by about 5 percent at the 25-psia tank pressure level and by approximately 7 percent at the 500-psia level to provide for these effects. The residual pressurant left in the pressurant bottle can be estimated by assuming a polytropic exponent for the expanding gases and computing the final pressurant bottle temperature. The pressurant tank volume is then:

$$V_t = \frac{W_t R T_i Z_i}{P_i \left[1 - \frac{Z_i P_f T_i}{P_i T_f} \right]} \qquad (8)$$

and the weight of the residual gas is:

$$W_r = \frac{P_f V_t}{R T_f} \qquad (9)$$

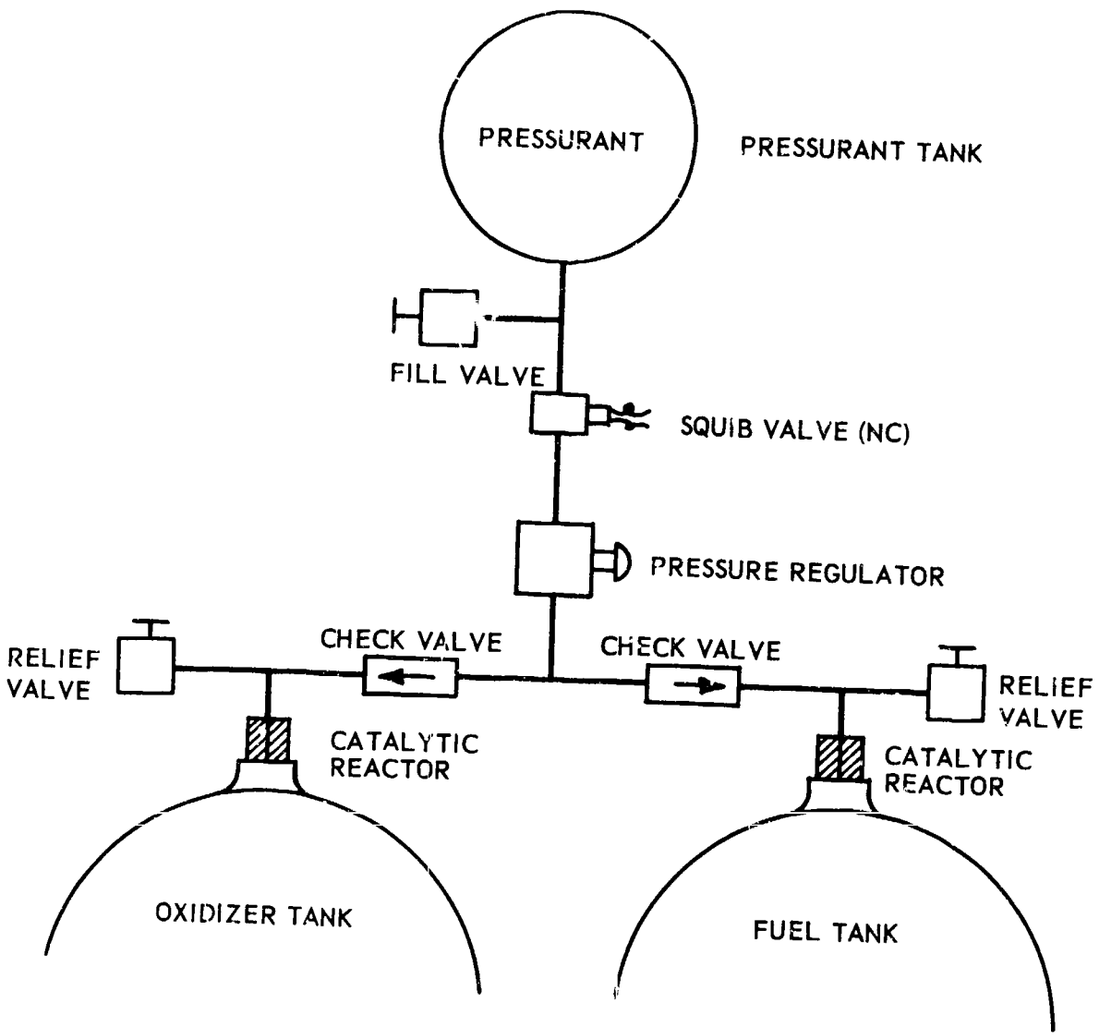

Figure 69. Schematic Representation of a Typical Catalytically Ignited Pressurization System

(U) The weight of a spherical pressurant tank can be closely estimated by:

$$W_t = \frac{1.5}{S} (W_r + W_a) R T \rho_m Z_i = 9.5 (W_r + W_a) \qquad (10)$$

using titanium as the tank material.

(U) The volume of catalyst required to promote virtually complete reactions may be estimated using the following equation which was derived from the reactor bed experiments.

$$V_c = \frac{52.7 \dot{w}}{A} \qquad (11)$$

where V_c is the net volume of the catalyst bed and $\dot{w}/A$ is the pressurant flowrate-per-unit cross-sectional area of the catalyst bed in lb/sec-in.^{2}.

MINUTEMAN PBCS PRESSURIZATION SYSTEM ANALYSIS

(U) The pressurization requirements for use on the Minuteman PBCS module were analyzed by use of the Rocketdyne pressurization computer program. The design characteristics of the system analyzed are detailed in Table 14. Cylindrical propellant tanks with bellows for expulsion devices were considered in the study.

(C) Two duty cycles were used in the system analysis. The first consisted of a constant rate propellant depletion over a 235-second interval, at a 1.06 lb/sec propellant flowrate. The second duty cycle assumed two equal duration expulsion periods of 117.5 seconds at the 1.06 lb/sec flowrate, separated by a coast interval of 125 seconds with the total operational duration equalling 360 seconds. This was considered to be one of the more severe pressurization requirements of the various mission duty cycles as the pressurant would be exposed to a maximum heat loss during the coast interval.

(C) The computations for the amount of catalytically heated pressurant, $He/O_2/H_2$, assumed a polytropic expansion coefficient of 1.33 for the pressurant remaining in the pressurant tank. A nominal reactor temperature of 1500 F was used. The results show the $He/O_2/H_2$ system to be 37 percent less in weight than a cold-gas helium system. Additionally the two different duty cycles considered in the analysis yielded almost identical pressurant weights. The comparative results are shown in Table 15.

PRESSURIZATION SYSTEM FOR THE MANEUVERING SATELLITE VEHICLE

(C) Analyses were performed to determine the applicability of a catalytically reacted pressurant subsystem to an advanced propulsion system employing

TABLE 14

DESIGN CRITERIA FOR THE MINUTEMAN
PBCS PROPULSION SYSTEM

Propellants	
Oxidizer	N_2O_4
Fuel	MMH
Mixture Ratio, o/f	1.6:1
Propellant Weight, pounds	250
Operating Temperature, F	80 ±20
Storage Temperature Maximum, F	150
Mission Duration, seconds	360
Pressurant	Helium
Pressurant Storage Pressure, psia	3200
Pressurant Bottle Safety Factor	2.0
Duty cycle, A	Continuous depletion of propellant at 1.06 lb/sec
Duty cycle, B	Depletion of propellant at 1.06 lb/sec for 117.5 seconds; no depletion for 125 seconds; and depletion at 1.06 lb/sec to termination
Pressurization System Weight, pounds	
Pressurant Tank	14.86
Tank Bracket	2.7
Isolation Valve	0.54
Regulator and Filter	1.2
Pressure Switch	0.8
Relief Valve	0.9

TABLE 14
(Concluded)

Burst Disk	0.4
Manifold	1.0
Fill Valve	0.1
Helium	1.0
TOTAL	23.5
Propellant Tank	
Configuration	Cylindrical
Inside Diameter, inches	13.75
Length, inches	22.3
Wall Thickness	0.060
Tank Material Density, lb/cu in.	0.283
Tank Wall Specific Heat, Btu/lb-F	0.11

TABLE 15

PRESSURIZATION SYSTEM COMPARISON

	Helium Cold Gas Pressurization System	Reactive Gas** Pressurization System	
		Duty Cycle "A" (235-Second Duration)	Duty Cycle "B" (360-Second Duration)
Quantity of Pressurant Required, Pounds	1.00	.67	.70
Pressurant Tank Weight, Pounds	14.86	6.19	6.45
Regulator, Squib Valve, Fill Valve, Filter, Brackets	7.64	7.64	7.64
Total, Pounds	23.50	14.50	14.79

*Duty cycle "A" consists of continuous depletion of propellant at 1.06 lb/sec. Duty cycle "B" consists of use of propellant at a 1.06 lb/sec rate for 117.5 seconds, an off period of 125 seconds, and then depletion at a 1.06 lb/sec flowrate.

Initial pressure in pressurant tank, psia	3,200
Final pressure in pressurant tank, psia	300

cryogenic propellants. Principal design parameters for the vehicle were abstracted from the Maneuvering Satellite Optimization Study (Ref. 7). These are listed in Table 16. Some slight changes were incorporated in the system components and operation to simplify the analytical study. Emphasis is maintained on the elements concerned with the use of a heated gas pressurant, and no effort is made to influence the overall system designs or functions.

Pressurization Operation

(C) A mixture of $He/O_2/H_2$, catalytic reaction temperature of 1500 R, is tanked in a titanium pressure vessel at vehicle equilibrium temperature, 400 R, for use as a prepressurant for the LF_2 tank. Prior to injection into the LF_2 tank, the gas is catalyzed to 1500 R, passed through a heat exchanger and cooled to 550 R where the majority of the water formed by reaction (85 percent) is condensed and removed. The collected water is vented overboard periodically, as required.

(C) Helium is stored in the LH_2 tank at LH_2 temperatures, 35 to 47 R. It is passed through the heat exchanger used for the $He/O_2/H_2$ gases, heated to 550 R, and then injected as a prepressurant for the LH_2. After pump operation has been started, gaseous hydrogen (200 R) from the thrust chamber cooling jackets is used to maintain the LH_2 tank pressure at 70 psia.

(C) The LF_2 tank pressure is maintained at 70 psia during thrusting operation by continuing the flow of the prepressurant gas, $He/O_2/H_2$, and by redirecting the heated helium, no longer required for LH_2 pressurization, into the LF_2 tank to augment the $He/O_2/H_2$. After thrusting operation has terminated, the propellant pressurant gases are assumed to reach equilibrium temperatures with the respective propellants.

Study Results

(C) The study scope was limited to a comparison of a prepressurization and pressurization subsystem concept employing a reactive gas, $He/0_2/H_2$, as an energy source with an equivalent system in which unheated helium is used. A comparison of the pressurant and tank weights for the systems is shown in Table 17. The $He/0_2/H_2$ system weight total is 46.9 percent of the unheated helium system.

TABLE 16

MANEUVERING SATELLITE DESIGN PAPAMETERS

Propellants	
Oxidizer	LF_2
Fuel	LH_2
Propellant Weight, pounds	
LF_2	14,616
LH_2	1,124
Mixture Ratio, o/f	13:1
Propellant Volume, Initial, cubic feet	
LF_2	150.5
LH_2	250.0
Ullage, Initial, cubic feet	
LF_2	6.6
LH_2	17.8
Propellant Temperature, Initial, R	
LF_2	140
LH_2	35
Propellant Tank Pressure, Operational, psia	70

TABLE 16
(Concluded)

Heat Transfer to Propellant	
Launch Operation, Btu	
LF_2	5,200
LH_2	11,200
Orbital Operation, ^{n}tu/day	
LF_2	240
LH_2	240

System Operation

A duty cycle is selected of nine system operations within a 24-hour period. Each operation is assumed to last 900 seconds at varying thrust levels with equal increments of propellants being consumed each period.

Prepressurization at Launch

At launch, the LF_2 tank is pressurized to 47 psia with helium at 140 R. Heating during launch results in a 50-psia ullage pressure and 4-percent ullage volume.

The LH_2 tank is pressurized to 30 psia with helium at 35 R which also results in a 4-percent ullage at 50 psia at end of boost.

TABLE 17

COMPARISON OF MANEUVERING SATELLITE
PRESSURANT AND TANK WEIGHT

	Cold Helium System	Heated $He/O_2/H_2$ and Helium System
Storage Temperature, R		
Helium	400	37
$He/O_2/H_2$		400
Pressurant Weight, pounds		
Helium	53.3	25.6
$He/O_2/H_2$	---	13.2
Pressurant Tank Weight, pounds		
Helium	336.0	41.7
$He/O_2/H_2$		92.8
Pressurant and Tank Weight, pounds	389.3	178.3

GENERAL NOMENCLATURE

A	=	cross-sectional area of catalyst bed
c_b	=	specific heat of catalyst
c_p	=	specific heat of combusted pressurant
D_p	=	catalyst pellet diameter
D_t	=	diameter of catalyst bed
F	=	ratio of total tank weight to shell weight (taken as 1.10)
g	=	gravitational constant
G_o	=	pressurant mass flow per unit area
h_p	=	heat transfer coefficient from pressurant to catalyst
h_w	=	heat transfer coefficient from pressurant to catalyst liner
k	=	constant defined by Eq. 3a
K	=	thermal conductivity of pressurant
L	=	catalyst bed length
M_B	=	mass of catalyst bed
P	=	pressure
ΔP	=	catalyst bed pressure drop
Pr	=	pressurant Prandtl number
R	=	universal gas constant divided by molecular weight
Re	=	Reynolds number based on pellet diameter
S	=	design stress
SF	=	safety factor
t	=	time

T = temperature

T_o = initial temperature

T^* = flame temperature

V_c = volume of catalyst bed

V_t = volume of pressurant tank

W_a = weight of usable pressurant

W_t = weight of pressurant tank

W_r = weight of residual gases

Z = compressibility factor

$\dot{w}$ = pressurant flowrate

ϵ = catalyst bed void volume

ρ = average density of reacted pressurant

ρ_m = density of pressurant tank material

μ = average viscosity of reacted pressurant

Subscripts

i = initial

in = inlet

f = final

REFERENCES

1. Wilkins, M. E. and R. J. Carros: Combustion Tests of Oxygen-Hydrogen-Helium Mixtures at Loading Pressures up to 8000 Pounds per Square Inch, NASA TN-D-1892.

2. Roberts, R., H. Burge, and M. Ludacki: Investigation of Catalytic Ignition of Oxygen/Hydrogen Systems, (NASA CR-54657), Rocketdyne Report R-6303, Rocketdyne, a Division of North American Aviation, Inc., Canoga Park, California, December 1965.

3. Bendersky, C.: Hydrogen/Oxygen Catalytic Ignition, Rocketdyne, a Division of North American Aviation, Inc., Canoga Park, California, January 1963.

4. Roberts, R.: Hydrogen/Oxygen Catalytic Ignition for Application to the J-2 Engine, RR 64-2, Rocketdyne, a Division of North American Aviation, Inc., Canoga Park, California, January 1964.

5. Prono, E., R. Roberts, G. Falkenstein, and H. Burge: Feasibility Investigation of Catalytic Ignition of Premixed Oxygen, Nitrogen, and Hydrogen Propellants, RR 65-8, Rocketdyne, a Division of North American Aviation, Inc., Canoga Park, California, March 1965.

6. McAdams, William H.: Heat Transmission, Third Edition, McGraw-Hill, New York, 1954.

7. Technical Report AFRPL-TR-65-252, Maneuvering Satellite Propulsion System Optimization Study, Air Force Rocket Propulsion Laboratory, Edwards, California, April 1966.

APPENDIX A

DERIVATION OF EQUATIONS DESCRIBING PRESSURANT HEAT TRANSFER AND CONDENSATION

(U) The pressurization of a liquid by a hot gas is an extremely complex process which requires a number of simplifying assumptions be introduced to obtain a set of equations suitable for solution. The assumptions indigenous to this analysis are listed below:

1. Complete mixing occurs in both gas and liquid phases.
2. Heat transfer from the gas to the tank walls and liquid is determined by natural convection.
3. Gas properties can be estimated by simplified relationships.
4. The boundary conditions are liquid flowrate ($\dot{W}_p$), tank wall area (A_w), and propellant surface area (A_p), and are known functions of time.
5. Tank pressure is constant and no vaporization of liquid occurs.

(U) With these assumptions, a mass balance on the gas phase of the tank gives:

$$\dot{W}_g - \dot{W}_c = \frac{d}{dt}\left(\frac{mPV_g}{RT_g}\right) = \frac{mP}{RT_g}\frac{\dot{W}_p}{\rho_p} - \frac{\dot{W}_g}{T_g}\frac{dT_g}{dt} \qquad (1)$$

(U) If the gas contains a weight fraction, F, of a condensible gas, the rate of condensation is given by:

$$\dot{W}_c = \dot{W}_g (F_{in} - F) - W_g \frac{dF}{dt} \qquad (2)$$

(U) The fraction of condensible gas present in a saturated carrier

$$F = \frac{P_{vp}}{P_T} = \frac{e^{\left(a - \frac{\Delta H_m}{RT_g}\right)}}{P_T} \qquad (3)$$

(U) The rate of change of the fraction condensible is given by:

$$\frac{dF}{dt} = \left(\frac{\Delta Hm}{RT_g^2}\right) \frac{dT_g}{dt} \; F \tag{4}$$

(U) The rate of condensation is, therefore:

$$\dot{W}_c = - \frac{\dot{W}_g}{T_g} \; F \left(\frac{\Delta Hm}{RT_g}\right) \frac{dT_g}{dt} + (F_{in} - F) \dot{W}_g \tag{5}$$

(U) Substitution of Eq. 5 into Eq. 1 gives the total pressurization gas flow-rate required to maintain a constant tank pressure.

$$\dot{W}_g = \frac{\frac{Pm}{RT_g} \frac{\dot{W}_p}{\rho_p} - \frac{\dot{W}_g}{T_g} \left[1 + F \frac{\Delta Hm}{RT_g}\right] \frac{dT_g}{dt}}{1 + F - F_{in}} \tag{6}$$

(U) An energy balance can now be made for (1) the gas volume, (2) the tank wall, and (3) the liquid volume. The gas volume contains an amount of suspended liquid so that the energy balance is written as:

$$\frac{d}{dt} \left[W_g H_g + W_c H_c\right] = \dot{W}_g H_{in} - q_w - q_p \tag{7}$$

(U) The gas enthalpy is approximated by:

$$H_g = C_{P_g} T_g + F \Delta H \tag{8}$$

which assumes equal specific heats for both constituents of the gas. In a like manner, the enthalpy of the condensed phase is assumed to be:

$$H_c = C_{P_g} T_g \tag{9}$$

(U) The energy balance for the gas volume therefore has the form:

$$(\dot{W}_g - \dot{W}_c) H_g + W_g C_{P_g} \frac{dT_g}{dt} + W_g \Delta H \frac{dF}{dt} +$$

$$\dot{W}_c H_c + W_c C_{P_g} \frac{dt_g}{dt} = \dot{W}_g H_{in} - q_w - q_p \tag{10}$$

(U) Rearranging gives:

$$\left[W_g C_{P_g} + W_c C_{P_g} + \frac{W_g}{T_g} \Delta HF \frac{\Delta Hm}{RT_g} \right] \frac{dT_g}{dt} = \dot{W}_g \left[H_{in} - H_g \right] + \dot{W}_c \Delta HF - q_w - q_p \tag{11}$$

(U) Using Eq. 5 and 6 to eliminate $\dot{W}_g$ and $\dot{W}_c$ gives:

$$\left\{ W_g C_{P_g} + W_c C_{P_g} + \frac{W_g}{T_g} \left[F \Delta H \frac{\Delta Hm}{RT_g} (1+F) + \left(1 + \frac{F \Delta Hm}{RT_g} \frac{H_{in} - H_g + F \Delta H (F_{in} - F)}{1 - F_{in} + F} \right) \right] \right\} \frac{dT_g}{dt}$$

$$= \frac{Pm \dot{W}_p C_{P_g} (T_{in} - T_g)}{(1 - F_{in} = F)} + \frac{Pm \dot{W}_p}{RT_g \rho_p} \frac{(F_{in} - F) \Delta H (1+F)}{(1 - F_{in} + F)} -$$

$$h A_w (T_g - T_w) - h A_p (T_g - T_p) \tag{12}$$

(U) Equation 12 is a first-order differential equation with variable coefficients and can be solved readily by the TAP-3 computer program. The energy balances for the wall and propellant can be written as:

<u>Wall</u>

$$A_w \rho_w C_{P_w} b \frac{dT_w}{dt} = h A_w (T_g - T_w) + A_w h_a (T_{aw} - T_w) \tag{13}$$

<u>Propellant</u>

$$W_p C_{P_p} \frac{dT_p}{dt} = h S_p (T_g - T_p) + (A_T - W_w) \frac{(T_{aw} - T_p)}{1/h + d/k} \tag{14}$$

(U) The heat transfer coefficients are computed by the program using simplified property values for the gas (and air) as follows:

$$\mu = 5 \times 10^{-9} \, m^{1/2} \, T^{0.6} \quad \text{lb/in.-sec} \tag{15}$$

$$C_p = \frac{2\ \gamma/m}{\gamma-1} \quad \text{Btu/lb-R} \tag{16}$$

$$Pr = \frac{4\ \gamma}{9\ \gamma-5} \tag{17}$$

$$\rho = \frac{P}{RT} \quad \text{lb/ft}^3 \tag{18}$$

(U) For the pressurization gas, the heat transfer coefficient is estimated from the equation:

$$h = 0.5\ \frac{k}{D}\ (Pr\ Gr)^{1/4} \tag{19}$$

(U) For aerodynamic heating, the Colburn "j" equation for a flat plate is used:

$$h_{aero} = 0.0295\ \left(\frac{\mu}{L}\right)^{1/5}\ (\rho\ V)^{4/5}\left(\frac{C_p}{Pr}\right)^{2/3} \tag{20}$$

(U) The adiabatic wall temperature is estimated using a recovery factor of 0.9. The film temperature is assumed to be the average of the wall and adiabatic wall temperature.

(U) This computer model has been modified using the film penetration theory developed by Huang and Kuo (Ref. A-1) to account for diffusion. This theory suggests that when a thin layer of stagnant fluid exists on the boundary of two fluid phases which are brought in contact with each other, the molecular species move across the film by steady-state molecular diffusion, and there is no mass accumulation at any point within the film. The additional equations utilized to improve the mathematical model are presented below:

Concentration Gradient

$$\frac{d^2\ C_A}{d\ X^2} = 0 \tag{21}$$

Diffusion Flux

$$G_W = \rho_g\ D_A \left(\frac{C_{A_W}}{\delta_W}\right) \tag{22a}$$

$$G_P = \rho_g\ D_A \left(\frac{C_{A_P}}{\delta_P}\right) \tag{22b}$$

APPENDIX A NOMENCLATURE

A = surface area

C_A = concentration gradient

C_p = specific heat

D = tank diameter

D_A = molecular diffusivity of component A

F = fraction of condensible in gas in vapor form by weight

G_w = diffusion flux

H = specific enthalpy

L = distance from missile nose

P = pressure

R = universal gas constant

T = temperature

V = missile velocity

W = weight

a = constant in vapor pressure equation

b = tank wall thickness

d = tank wall insulation thickness

h = convective heat transfer coefficient

k = thermal conductivity

m = molecular weight

q = heat transfer rate

t = time

δ = boundary layer thickness

γ = specific heat ratio of gas (frozen)

μ = viscosity

ρ = density

Subscripts

a = refers to aerodynamic conditions

g = refers to pressurization gas

in = refers to inlet conditions of pressurization gas

p = refers to liquid propellant

w = refers to tank wall

Reference A-1

Huang, C. J., and C. H. Kuo: "Mathematical Models for Mass Transfer Accompanied by Reversable Chemical Reaction," A. I. Ch. E. Journal, Vol. 11, No. 5, p. 901

APPENDIX B

COMPOSITIONS FOR THE MIXTURE REACTOR BED EXPERIMENTS

(U) The proportions of reactant gases used in the helium diluent for the catalytic reactor experiments were determined by use of a Rocketdyne free-energy digital computer program. The basic ternary mixture, $He/O_2/H_2$, was selected to yield a 1500 F combustion temperature with a gas inlet temperature of 77 F, and at a combustion efficiency of 96 percent. The resulting mixture consists of 89.2 volume percent helium, 3.6 volume percent oxygen, and 7.2 volume percent hydrogen. Variations in reactant concentrations and flame temperatures with reactor inlet temperatures are shown in Fig. B-1. The flame temperatures shown in Fig. B-1 are based on 100-percent combustion efficiency.

(U) The reactant concentrations of the $He/O_2/H_2/CH_4$ blends used in the reactor experiments were derived from the following considerations:

1. Sufficient amounts of hydrogen are used to result in a combustion temperature of 500 F with an initial gas temperature of -100 F, assuming a complete stoichiometric reaction of oxygen and hydrogen. This amount of hydrogen was established at a hydrogen mass fraction of 0.0111 to react with an oxygen mass fraction of 0.0888.

2. Stoichiometric proportions of oxygen/methane are added as a function of inlet temperature to produce a maximum catalyst temperature of 1500 F. As an example, with an initial gas temperature of 200 F, the oxygen/hydrogen reaction will produce a temperature rise increment of 600 F, resulting in a gas temperature of 800 F, assuming no reaction from the oxygen/methane constituents. Sufficient quantities of oxygen/methane are used to produce a temperature rise increment from 800 to 1500 F. While the above approach

assumes a step-type reaction, the actual process is closely approximated by the Rocketdyne free-energy computer program. Very close agreement is shown between the two methods. The ideal temperature rise resulting from the oxygen/methane reaction is shown in Fig. B-2 as a function of the methane mass fraction.

(U) The mixture proportions selected for the experimental evaluations of the program are shown in Table B-1 as a function of inlet temperature.

TABLE B-1

MIXTURE PROPORTIONS

Inlet Temperature, F	-100	77	200
Mass Fraction, He	0.6736	0.7032	0.7246
O_2	0.2711	0.2464	0.2292
CH_4	0.0453	0.0393	0.0351
H_2	0.0111	0.0111	0.0111

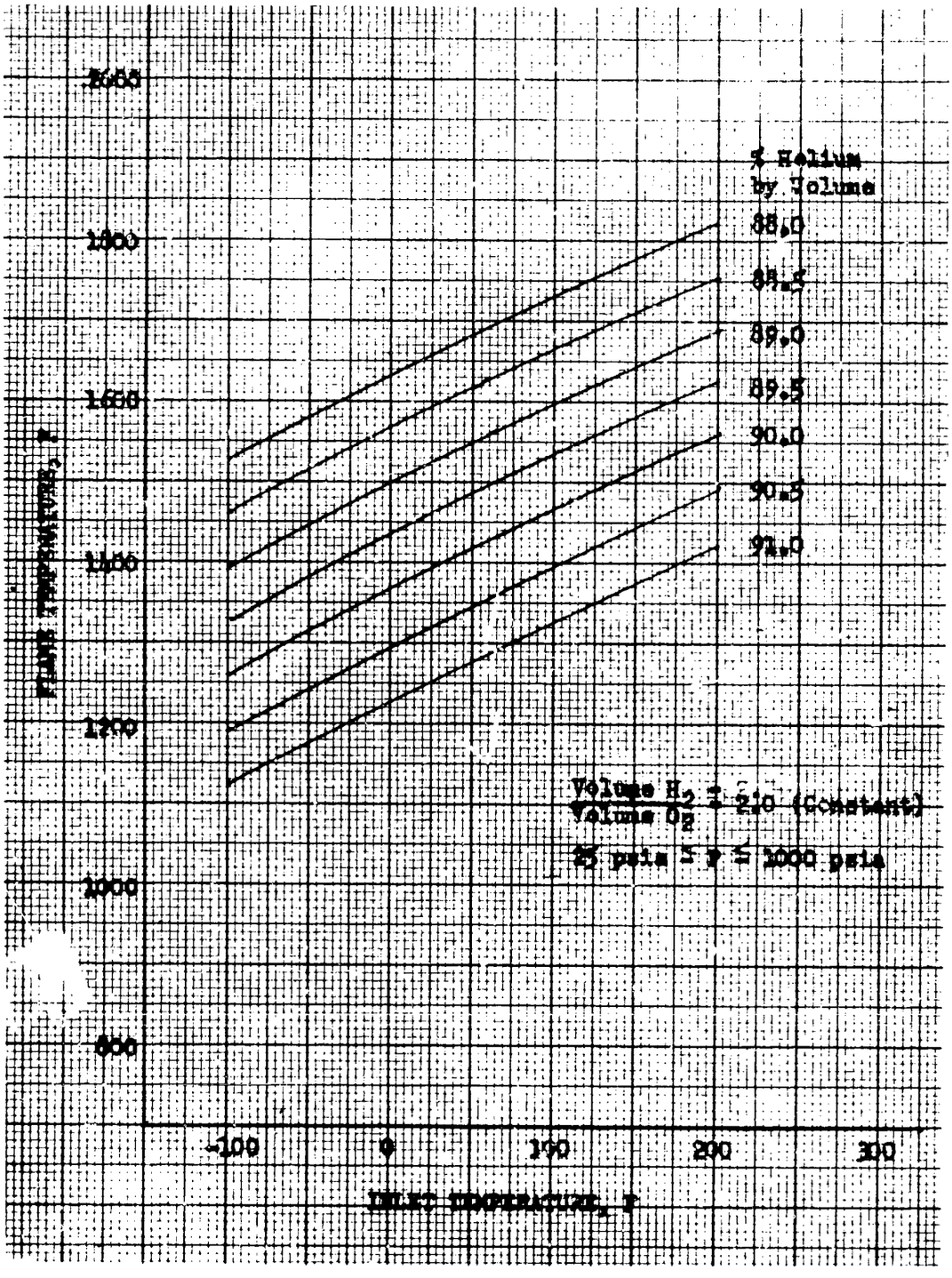

Figure B-1 Effect of Inlet Temperature on Flame Temperature for $He/O_2/H_2$ Mixtures

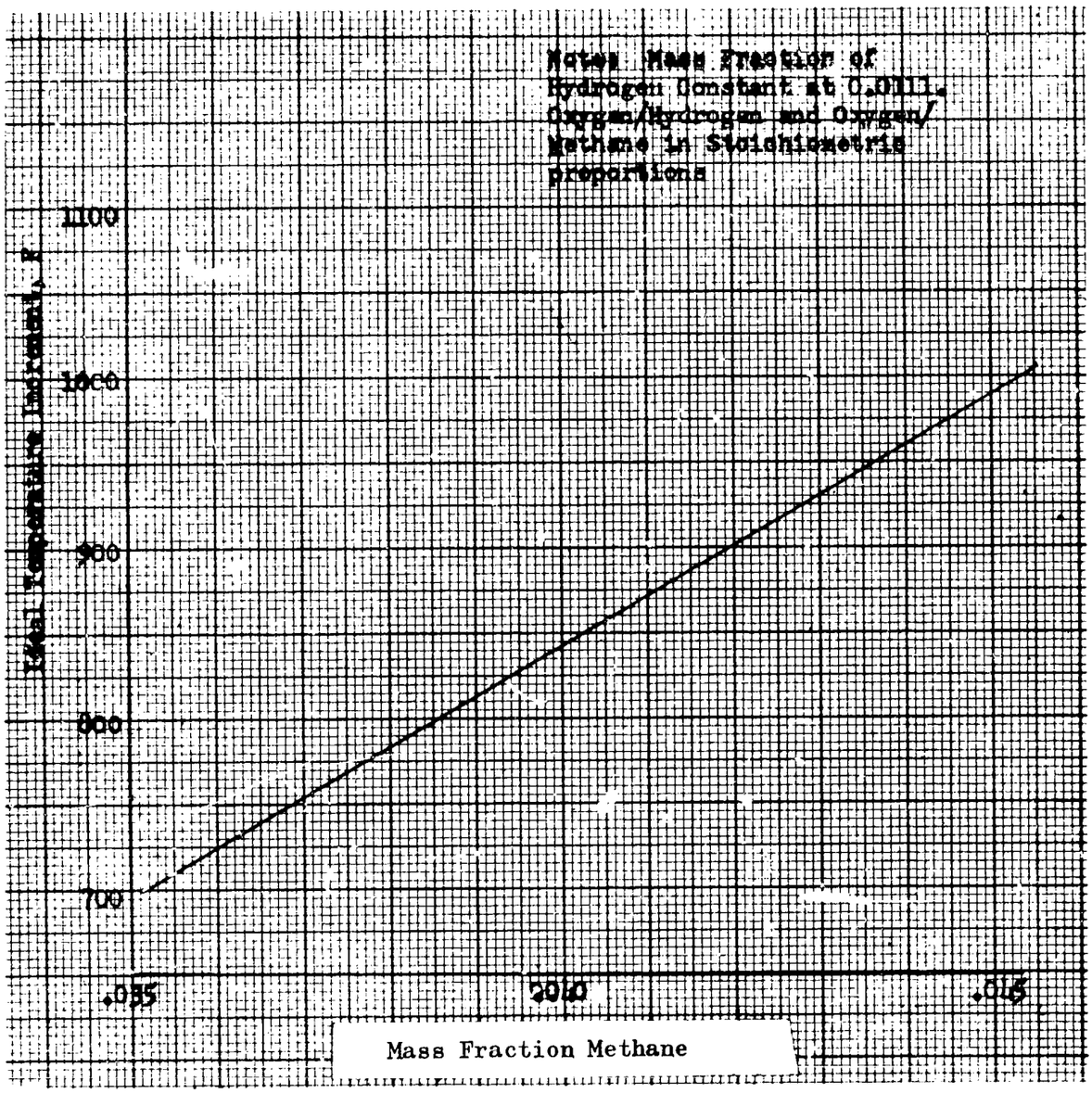

Figure B-2 Ideal Temperature Increment for $He/O_2/H_2/CH_4$ Mixtures

UNCLASSIFIED

Security Classification

DOCUMENT CONTROL DATA - R&D

(Security classification of title, body of abstract and indexing annotation must be entered when the overall report is classified)

1. ORIGINATING ACTIVITY *(Corporate author)*

Rocketdyne, a Division of North American Aviation, Inc., 6633 Canoga Avenue, Canoga Park, California

2a. REPORT SECURITY CLASSIFICATION

CONFIDENTIAL

2b. GROUP

4

3. REPORT TITLE

Advanced Pressurization Systems Technology Program (U)

4. DESCRIPTIVE NOTES *(Type of report and inclusive dates)*

Final

5. AUTHOR(S) *(Last name, first name, initial)*

Barber, Hartley E.

6. REPORT DATE	7a. TOTAL NO. OF PAGES	7b. NO. OF REFS
15 November 1966	167	None

8a. CONTRACT OR GRANT NO.	9a. ORIGINATOR'S REPORT NUMBER(S)
AF04(611)-11383	
b. PROJECT NO.	R-6745
c.	9b. OTHER REPORT NO(S) *(Any other numbers that may be assigned this report)*
d.	AFRPL-TR-66-278

10. AVAILABILITY/LIMITATION NOTICES

In addition to security requirements which must be met, this document is subject to special export controls and each transmittal to foreign governments or foreign nationals may be made only with prior approval of AFRPL, Edwards, California 93523.

11. SUPPLEMENTARY NOTES	12. SPONSORING MILITARY ACTIVITY
	AFRPL, Research and Technology Division, Edwards, California, Air Force Systems Command, United States Air Force

13. ABSTRACT

The results of catalytic reactor experiments using mixtures of oxygen/hydrogen and oxygen/hydrogen/methane in the inert diluents, helium and nitrogen, are reported. Analyses are included showing the basis for the selection of the better gaseous mixtures as pressurants for use in propellant pressurization systems. The experiments include the areas of detonability, elevated temperature storage, catalytic reactor response and performance, and expulsion demonstrations (U).

DD FORM 1 JAN 64 1473

UNCLASSIFIED

Security Classification

14. KEY WORDS	LINK A		LINK B		LINK C	
	ROLE	WT	ROLE	WT	ROLE	WT
CATALYTIC REACTOR GASEOUS MIXTURES PRESSURANTS PRESSURIZATION SYSTEMS DETONABILITY TEMPERATURE STORAGE RESPONSE PERFORMANCE EXPULSION						

INSTRUCTIONS

1. **ORIGINATING ACTIVITY:** Enter the name and address of the contractor, subcontractor, grantee, Department of Defense activity or other organization *(corporate author)* issuing the report.

2a. **REPORT SECURITY CLASSIFICATION:** Enter the overall security classification of the report. Indicate whether "Restricted Data" is included. Marking is to be in accordance with appropriate security regulations.

2b. **GROUP:** Automatic downgrading is specified in DoD Directive 5200.10 and Armed Forces Industrial Manual. Enter the group number. Also, when applicable, show that optional markings have been used for Group 3 and Group 4 as authorized.

3. **REPORT TITLE:** Enter the complete report title in all capital letters. Titles in all cases should be unclassified. If a meaningful title cannot be selected without classification, show title classification in all capitals in parenthesis immediately following the title.

4. **DESCRIPTIVE NOTES:** If appropriate, enter the type of report, e.g., interim, progress, summary, annual, or final. Give the inclusive dates when a specific reporting period is covered.

5. **AUTHOR(S):** Enter the name(s) of author(s) as shown on or in the report. Enter last name, first name, middle initial. If military, show rank and branch of service. The name of the principal author is an absolute minimum requirement.

6. **REPORT DATE:** Enter the date of the report as day, month, year; or month, year. If more than one date appears on the report, use date of publication.

7a. **TOTAL NUMBER OF PAGES:** The total page count should follow normal pagination procedures, i.e., enter the number of pages containing information.

7b. **NUMBER OF REFERENCES:** Enter the total number of references cited in the report.

8a. **CONTRACT OR GRANT NUMBER:** If appropriate, enter the applicable number of the contract or grant under which the report was written.

8b, 8c, & 8d. **PROJECT NUMBER:** Enter the appropriate military department identification, such as project number, subproject number, system numbers, task number, etc.

9a. **ORIGINATOR'S REPORT NUMBER(S):** Enter the official report number by which the document will be identified and controlled by the originating activity. This number must be unique to this report.

9b. **OTHER REPORT NUMBER(S):** If the report has been assigned any other report numbers *(either by the originator or by the sponsor)*, also enter this number(s).

10. **AVAILABILITY/LIMITATION NOTICES:** Enter any limitations on further dissemination of the report, other than those imposed by security classification, using standard statements such as:

(1) "Qualified requesters may obtain copies of this report from DDC."

(2) "Foreign announcement and dissemination of this report by DDC is not authorized."

(3) "U. S. Government agencies may obtain copies of this report directly from DDC. Other qualified DDC users shall request through _____."

(4) "U. S. military agencies may obtain copies of this report directly from DDC. Other qualified users shall request through _____."

(5) "All distribution of this report is controlled. Qualified DDC users shall request through _____."

If the report has been furnished to the Office of Technical Services, Department of Commerce, for sale to the public, indicate this fact and enter the price, if known.

11. **SUPPLEMENTARY NOTES:** Use for additional explanatory notes.

12. **SPONSORING MILITARY ACTIVITY:** Enter the name of the departmental project office or laboratory sponsoring *(paying for)* the research and development. Include address.

13. **ABSTRACT:** Enter an abstract giving a brief and factual summary of the document indicative of the report, even though it may also appear elsewhere in the body of the technical report. If additional space is required, a continuation sheet shall be attached.

It is highly desirable that the abstract of classified reports be unclassified. Each paragraph of the abstract shall end with an indication of the military security classification of the information in the paragraph, represented as *(TS)*, *(S)*, *(C)*, or *(U)*.

There is no limitation on the length of the abstract. However, the suggested length is from 150 to 225 words.

14. **KEY WORDS:** Key words are technically meaningful terms or short phrases that characterize a report and may be used as index entries for cataloging the report. Key words must be selected so that no security classification is required. Identifiers, such as equipment model designation, trade name, military project code name, geographic location, may be used as key words but will be followed by an indication of technical context. The assignment of links, rules, and weights is optional.